Title page:

Oxana Sachenkova*%, CORE-RIKEN-AUTHORS# and Lukasz Huminiecki*&%

* Department of Biochemistry and Biophysics, Stockholm University, Stockholm, Sweden
& Department of Cell and Molecular Biology, Karolinska Institutet, Sweden
% Science for Life Laboratory, SciLifeLab, Sweden
# RIKEN Omics Centre, Yokohama, Japan

Corresponding author: Lukasz.Huminiecki@scilifelab.se

Keywords: gene expression, CAGE, evolution, cancer

Title:

Patterns of expression space change in the F5-CAGE encyclopedia of vertebrate gene expression

Abstract:

The F5-CAGE encyclopedia of expression patterns is an arguably the most comprehensive and technologically uniform functional genomics dataset generated to date. F5-CAGE includes 952 human and 396 mouse tissues, primary cell and cancer cell-line samples. The unifying theme of this work is application of F5-CAGE to investigate expression space change between tissues, in gene families, between different TSSes of a gene, and under the influence of enhancers and insulators.

In the context of tissue expression space, brain tissues repeatedly exhibit many unique transcriptional features, including clustering into fetal, newborn, and aged adult samples, and differential phyloexpression signature. All samples group into three distinct categories with respect to their rates of expression pattern evolution (static, dynamic, and intermediate).

In the context of expression change in gene families, there is trend for young genes to be tissue-specific, with the exception of taxon Eutheria. Paralog expression pattern divergence suggests global disregulation and devolution of expression in caner cell-lines. As a focused example, we discuss the cdc42 gene family which includes many tissue-specific genes and dramatic expression pattern shifts, correlated with promoter structure revealed by ENCODE.

Most genes have multiple TSSes, with up to 87 in the case of tintin, contributing to multiple isoforms which were previously attributed only to alternative splicing. Number of TSSes correlates between human and mouse orthologs, and there is a trend for older genes to have more TSSes than young genes. Genes with multiple TSSes may be associated with carcinogenesis.

Finally, we test the hypothesis of CTCF acting as isolator between paralogs, and instead show its function is more likely in bringing duplicates under the control of the same enhancer.

(278 words)

Introduction:

Animals are primarily characterized by multicellularity, and existence of distinct tissue- and cell-types. Characterization of the animal expression space in terms of its tissue-specificity, multiple TSSes, roles of insulators and enhancers, promoter structure, differences between normal tissues, primary cells in culture, and cancer cell lines, as well as the timing of emergence of specific cell- and tissue-unique expression programs, is of general interest to broad readership.

The major strength and novelty of the F5-CAGE expression encyclopedia is it's comprehensive and technologically uniform nature, as well as unbiased coverage of the entire genome space, allowing for comparison between tissue samples, primary cell-lines, and cancer cell-lines. F5-CAGE is arguably the most complete functional genomics dataset generated to date. Table 1 briefly summarizes the first release of the F5 CAGE resource. CAGE is less susceptible to cross-hybridization between related paralog sequences, as these tags target very fast diverging promoter regions, instead of conserved transcribed sequences targeted by ESTs of microarrays. CAGE also enables investigation of the genome in a unbiased way, not being limited to a pre-selected protein-coding genes chosen for a given microarray chip platform by the manufacturer.

Expression datasets available to date, have been limited in scope to a narrow and biased set of somatic tissues, and not allowing for parallel examination of coding and non-coding transcripts (Su, Cooke et al. 2002). Meta-analysis of expression datasets is associated with enormous problems due to technological differences between platforms and analysis pipelines. Due to these limitations, many controversies with regards to animal expression pattern evolution remained unresolved. For example, several authors argued for (Khaitovich, Weiss et al. 2004) and against (Jordan, Marino-Ramirez et al. 2005) the hypothesis of neutral rate of expression pattern evolution, and it still remains controversial what is the appropriate method of calculating expression distances (Pereira, Waxman et al. 2009; Piasecka, Robinson-Rechavi et al. 2012) and clustering expression profiles (Eisen, Spellman et al. 1998; Quackenbush 2001). However fairly early in this debate, we signaled that Person R works best for tissue-specific genes, and that conservation of expression profiles is a complex phenomenon, most likely dependent on tissues and functional classes of genes of interest (Huminiecki and Wolfe 2004). Data presented here strengthen these early conclusions. We hope that F5-CAGE will settle most debates with reference to animal expression pattern evolution.

Here, we apply F5-CAGE to investigate expression space change between tissues, in gene families, between different TSSes of a gene, and under the influence of enhancers and insulators. Henceforth, we refer to different F5-CAGE samples groups using shorts: normal tissues (T), primary cells in culture (PC), and cancer cell lines (CCL); and hs for human and mm for mouse. For example, hs-CCL refers to all human cancer cell line samples in F5-CAGE, while mm-T refers to all murine tissue samples (see also Table 1).

Results:

Principal component analysis (PCA) exploration of the F5 CAGE encyclopedia
The initial exploration of expression pattern diversity in the F5 CAGE encyclopedia using PCA revealed no global clustering pattern for either PC1/PC2, or PC2/PC3 comparisons (data not shown). Significantly, no clustering into tissue groups corresponding to ectoderm, mesoderm and endoderm could be observed. However, a PCA focused on human brain revealed unexpected clustering into fetal, newborn and aged adult samples.

Unique expression features of brain samples
In the F5-CAGE encyclopedia, brain samples stand out in many respects, suggesting unique features associated with expression pattern evolution in the CNS. Previously, when comparing expression profiles derived from dbEST, SAGEmap and Affymetrix microarrays, we noted that brain has uniquely complex transcriptional program (Huminiecki, Lloyd et al. 2003), and that brain-expressed genes mostly derive from the 2R-WGD event (Huminiecki and Heldin 2010) with few novel brain-specific genes forming during diversification of mammals. The results presented here, both strengthen and clarify these hypotheses. Brain samples clustered together (Figure 1), and were clear outliers in many different analyses. For example, unlike all other tissues, brain samples exhibited unique clustering by age of donor, forming three clusters which can be attributed to developmental stage: (a) fetal, (b) newborn, and (c) aged adult (Figure 2). No other tissue type demonstrated this type of clustering, despite availability of multiple donors and developmental stages for both human and mouse samples, precluding the possibility that the observed effect was due to post-mortem delay, or differential pre-processing of embryonic samples during RNA isolation.

Phylogenetic timing of gene duplications using TreeFam8 database
We have previously used TreeFam database (Li, Coghlan et al. 2006) to phylogenetically time gene duplication events (Huminiecki and Heldin 2010). New and much larger release of the database, TreeFam8, was used here. This new database strongly confirmed previous work, linking taxa Vertebrata and Bilateria with two greatest waves of gene duplications in the history of animal kingdom (---).

Phylogenetic data from TreeFam database was linked with F5-CAGE WP4 gene expression tables (linking RefSeq transcripts with all CAGE tags +/- 500 bps from RefSeq TSS), and most later stages of analysis were performed in R/Bioconductor (2.11), using among others, packages Biodist (correlations), gplot and ggplot (graphics), rtracklayer, TxDb.Hsapiens.UCSC.hg19.knownGene, and GOstats.

Hierarchical clustering of human tissue samples
When F5-CAGE WP4 expression data are clustered (Spearman correlation used as expression distance measure), samples cluster primarily depending on cell/tissue type of origin, not sample donor or developmental stage (see heatmaps in Figure 1 for hs-T, FigS1a for hs-PC, FigS1b for hs-CCL; and FigureS1c for mm-T). This indicates that tissue-of-origin differences are much more important than individual variability, as multiple donors are available for a high proportion of samples. Significantly, hs-CCL clustering shows a major divide between leukemias and solid tumors (FigS1b).

Assignment of ortholog tissues

We compared ortholog human-mouse tissue clusters obtained by simple name matching (NM-clusters), with those inferred using inter-species hierarchical clustering of samples (ISHC). Table 2 is a summary table, comparing orthology inferences made from the Pearson R based ISHC-clusters (Fig4a) and the NM-clusters. The full F5 CAGE NM-dataset is shown in TableS2. 8 NM-clusters are recovered by the ISHC, while 19 are not (Table 2). The name clusters which are recovered include: skin, liver, tongue, heart, pancreas, pituitary gland, thymus and “total RNA control”.

Gene duplication timing and spatial expression domain of progeny genes

We defined phyloexpression profiles as strong associations between individual F5-CAGE samples, and gene duplicates derived from certain taxa, and searched for associations between phyloexpression profiles and taxa-specific evolutionary novelties. F5-CAGE contains many rare tissues, and phyloexpression profiles of these samples are of particular interest.

This analysis revealed several exceptionally strong tissue/taxon associations (TableS7). TableS7 lists top three samples of expression associated with each taxon of duplication. For example, genes derived from human specific duplications, tend to be expressed in thymus, liver and adipose tissue. Parotid gland is associated with strong expression of gene duplicates dating to taxa Homo/Pan/Gorilla and Catarrhini. Genes expressed in thymus appear associated with many taxa, suggesting that immune system innovation was a persistent theme throughout most animal evolution.

TableS8 lists genes “behind” several top phyloexpression signatures from TableS7 and Figure 6. For example, chosen sample+taxon associations include: seminal vesicle +Catarrhini, testis+Eutheria, uterus+Eutheria, adipose+human, vagina+human, salivary glad+Catarrhini. Some associations could have been inferred from published literature, while others are novel and provide rich material for formulation of interesting hypothesis about animal evolution. For example, cystatins (Baron, DeCarlo et al. 1999) and proline-rich salivary proteins (Amado, Lobo et al. 2010) are known to be present in saliva, and here we show that these proteins are very strongly associated with Catarrhini specific gene duplications and strongly expressed in salivary gland samples. Semenogelin I and II are two top proteins associated with the seminal vesicle+Catarrhini phyloexpression signature.

Young duplicates are tissue-specific in their expression domain, while old duplicates are broadly expressed

We observe two broad evolutionary trends related to animal expression patterns: trend for gradual paralog expression pattern divergence, and trend for young genes to be more tissue-specific in their expression domain, than old genes. FigureS2 shows the trend for gradual expression pattern divergence between paralogs in human tissues over evolutionary time. In addition, we observe a very strong trend for young duplicates to be more specific in their spatial expression domain (Figure 5). Taxon Eutheria (FigureS2) is a strong outlier to the gradual divergence trend, raising the possibility of unique functional characteristics of genes derived from this taxon. Bilateria is also an outlier, although to a lesser extent. Overall, paralog expression divergence is fast, reaching overall plateau as soon as Amniota. In contrast, the trend for older genes becoming more and more housekeeping, doesn't really reach a plateau until the base of the animal tree of life (taxon Metazoa). When this analysis is extended into human normal and cancer cell lines, it becomes apparent that similar trends can be observed in normal cells, but cancer cell lines differ, as there is no strong signature for young duplicates to be co-expressed (Fig 6c).

Histogram in Fig 6b illustrates the size of the dataset (number of paralog pairs) available for each taxon (with Vertebrates and Bilateria being most numerous).

We then asked what are the functional characteristics of genes lying at the extremes of these two trends. Supplementary tables TableS6a and TableS6b summarize the results of GO term and PFAM domain enrichment, for all taxa. TableS6a and TableS6b relate to the fast expression divergence rate, and high breadth of expression extremes of the distribution, respectively. The number of pairs available for some taxa may too low to reach definite conclusions, but several observations at the strict p=0.00001 cut-off are worth mentioning:
(a) Eutheria, highly significant association of top correlated (0.75 quantile: TableS6a) genes with cellular macromolecular complex assembly (GO:0034622; p=3.43e-06), chromatin assembly or disassembly (GO:0006333; p=4.65e-06), nucleosome assembly (GO:0006334; p=4.65e-06), and DNA packaging (GO:0006323; 8.38e-06) terms; (b) association of PF00125 (Histone; p=1.13e-10) domain with human-specific highly housekeeping genes (top 0.75 quantile: TableS6b); (c) associations of the following cellular location (CC) GO terms with broadly expressed (top 0.75 quantile: TableS6b) duplicates mapping to Homo/Pan/Gorilla and Catarrhini: extracellular region (GO:0005576; 1.8e-07), extracellular space (GO:0005615; 5.79e-08); (d) under-representation of intracellular (GO:0005622; 4.21e-07), cell (GO:0005623; p=2.54e-06), cytoplasm (GO: 0005737; p=7.84e-06), organelle (GO:0043226; 1.05e-05) among broadly expressed duplicates mapping to Catarrhini.

Taken together, GO and PFAM enrichment analysis suggests that histones and secreted proteins, i.e. genes annotated with terms related to extracellular space, are outliers to the general trend for recently emerging genes (i.e. genes emerging in hominids and monkeys) to be narrowly expressed. On the other hand, the emergence of placental mammals (taxon Eutheria), was associated with a burst of duplications or unusual characteristics in terms their expression patterns, being comparatively widely expressed (Figure 5) and well-correlated in their expression patterns (FigureS2), with genes involved in chromatin assembly and potentially epigenetic control driving the trend.

Evolutionary history of mammalian tissues.
To illustrate to the potential of phylogenetically-aware expression pattern profiling, we focus here on two examples. Figure 6 focuses on the reproductive track, while FigureS3 focuses on brain samples. Few new brain genes have been created since 2R-WGD, but many genes specific to the reproductive track have emerged in mammals. In addition, TableS7 and TableS8 describe strongest associations between taxa of gene duplications, and expression patterns in F5 CAGE.

Example gene family with dynamic pattern of expression pattern evolution
TreeFam family TF101109 is a family of small signaling G proteins (more specifically GTPases), and members of the Rac subfamily of the family Rho family of GTPases. Rho family of GTPases appear to regulate a diverse array of cellular events, including the control of cell growth, cytoskeletal reorganization, and the activation of protein kinases. The cdc42 gene family includes many tissue-specific genes and dramatic expression pattern shifts Figure 7.

Expression of cdc42 family in human tissues illustrate a novel phenomenon of mutually exclusive expression, where Ras–related C3 botulinum toxin substrate 3 (Rac3: GeneID 5881) is very highly expressed in five fetal tissues from which RHOG (GeneID 391), and ras–related C3 botulinum toxin substrate 2 (RAC2: GeneId 5880) are excluded. The five tissue in question include: fetal parietal lobe, fetal temporal lobe, fetal duodenum, fetal occipital lobe, and fetal brain pool, indicating that following 2R-WGD Rac3 neofuncionalized to play a role embryonic CNS. In contrast, RHOG is highly expressed in adult corpus callosum, where the other two genes are not detectable. Furthermore, a cluster of tissues associated with the immune and circulatory systems (thymus adult, blood

adult, tonsil adult, appendix adult, thymus fetal, vein adult, spleen adult, lymph node adult, spleen fetal), express RHOG and RAC2, but not RAC3. An examination of the cdc42 TreeFam family tree (http://www.treefam.org/cgi-bin/TFinfo.pl?ac=TF101109), suggests that Rac2 and Rac3 are 2R-ohnologs, while divergence between Rac2/3 ancestral gene and RHOG predates the origin of animals (taxon of duplication = Eukaryota). This suggests a very clear example of expression pattern neofunctionalization following Rac2/3 gene duplication, where RAC2 retained most of the ancestral expression characteristics (shared by RHOG), while RAC3 acquired new expression sites in fetal brain, while loosing expression in most other adult and fetal tissues.

For clarity, it should be mentioned that RHOJ and RHOQ are very divergent unrelated members of the family which appear to show little evidence for expression in human tissues. Rac1 and cdc42 are also highly divergent genes (taxon of duplication Eukaryota), which appear nevertheless similar in their expression characteristics in human tissues.

It is also interesting to compare expression features of the cdc42 family across human tissues with those observed in normal cell lines and cancer cell lines. Here RAC3 appears weakly expressed in unrelated cancer cell-lines, in congruence with it's emerging characteristics as a tightly regulated tissue-specific gene, restricted in its expression mostly to embryonic brain tissues. In contrast, RHOG and RAC2 are widely expressed in most cancer cell lines, and no clear pattern of mutually exclusive expression can be seen. In normal cell lines, RHOG and RAC2 are also widely expressed, while RAC3 is limited in its expression.

Examples of loci with multiple alternative transcription start sites (TSSes):
F5 Decomposition-based Peak Identification (DPI) procedure identifies separate transcription start sites (TTSes), associated with either protein-coding genes, non-coding genes, or novel transcribed loci in the genome. In total, the DPI procedure identified 184,827 robust peaks in human, and 116,277 in mouse. The numbers of robust DPI peaks located within 500bp of annotated 5'-end transcript were 93,614 and 61,072 respectively ---ref_main, and those peaks were used to infer transcription patters of protein-coding genes in F5-CAGE protein-coding gene expression tables (so-called WP4 tables). Unlike the TSSes themselves, WP4 tables are conceptually similar to microarray datasets.

Histogram in Figure 9a shows the distribution of frequencies of protein coding genes with respect to the number of associated TSSes. There are 24677 known human genes in total in this dataset, with 91671 TSSes mapped in total. 8181 genes are associated with exactly one TSS, 4617 with two, and 3275 with three. There is a long tail of genes associated with high number of TSSes (up to 87 for the titin gene: Figure 8). At the extreme end of this distribution lie 19 human loci associated with more than 40 TSSes: MAP1B 45, IGF2 64, COL1A1 58, DST 51, IGFBP5 43, APOB 64, AKAP13 46, ARPP21 44, TCF4 51, ALB 48, FN1 81, LEF1 42, TTN 87, SORBS2 47, XIRP2 49, CALD1 49, NTRK2 43, GFAP 46, PDE4D 60. Many of these genes extremely rich in TSSes are structural proteins involved in cells cytoskeleton or extracellular matrix, for example: collagen, type I, alpha 1 (COL1A1), fibronectin 1 (FN1), caldesmon 1 (CALD1), dystonin (DST), albumin (ALB), titin (TTN), glial fibrillary acidic protein (GFAP), and apolipoprotein B (APOB), and were known to produce multiple isoforms, but these were attributed to alternative-splicing, or RNA editing (APOB), not alternative TSSes.

Titin is a giant muscle protein, very abundant in muscles. An average adult human is said to contain as much as half a kilogram of titin (reviewed in 22105831---). Titin / MIR548N

locus (Figure 8) is associated with the highest number of alternative TSSes in the human genome, in the F5-CAGE dataset (namely 87 TSSes). It was known that titin, a striated muscle protein, was associated with extreme variability in the I-band, the M-line and the Z-disc regions, contributing to differences in elasticity of different titin isoforms and, therefore, to the differences in elasticity of different muscle types. However, to date, this variability was associated with alternative splicing (--- 22105831, 20339475). Here, we suggest that alternative isoforms of titin are also results of alternative TSSes.

Interestingly, there is also a miRNA gene (MIR548N), and two long non-coding RNAs in the titin locus (NR_038272.1, and NR_038271.1).

We have also examined the structure of a number of high-TSS loci in the human genome:

a) septin 9 (SEPT9, chr17: 75,222,695-75,551,472) shown in FigureS12.
b) ubiquitin-conjugating enzyme E2D 3 (UBE2D3, chr4: 103,746,336-103,751,072, TF101108) shown in FigureS13.
c) suppression of tumorigenicity 1 (NBL1, chr1:19,969,473-19,971,376), shown in FigureS14. NM_005380.6, transcript variant 2 is associated with p1@NBL1 and p3@NBL1, while NM_001204084.2, transcript variant 3 is associated with p5@NBL1 and p6@NBL1.
d) endothelin converting enzyme 1 (ECE1, chr1: 21,595,010-21,704,874), shown in FigureS15. The ECE1 locus spans very large region of over 100kb of genomic space, with four known endothelin-converting enzyme 1 (NM_001397), 2 (NM_001113349), 3 (NM_001113347), and 4 (NM_001113348).
e) apolipoprotein B, (APOB, chr2:21,213,641-21,277,606) associated with 64 TSSes, and described in FigureS16.
f) Insulin-like growth factor 2 locus (IGF2, chr11:2,148,248-2,175,234) associated with 64 TSSes and shown in FigureS17.
g) fibronectin 1 (FN1, chr2:216,237,783-216,288,189) locus associated with 81 TSSes, shown in FigureS18. FN1 was known to be associated with at least 20 different transcript variants, and associated with disease (PMID: 9870923).
h) caldesmon 1 (CALD1, chr7:134,483,301-134,674,600), a calmodulin- and actin-binding protein, known to produce many alternative isoforms. The locus structure is shown in FigureS19.
i) xin actin-binding repeat containing 2, (XIRP2, chr2:167,670,903-168,205,330), or cardiomyopathy-associated protein 3 (OMIM: 609778). The locus structure is shown in FigureS20.
j) A kinase (PRKA) anchor protein 13 (AKAP13, chr15:85,555,155-86,661,302), shown in FigureS21. AKAP12 alternative isoforms were known to function as alternative scaffolds to coordinate Rho and PKA signalling.

Finally, gene set enrichment analysis with the MSigDB database for genes with most TSSes: 58 genes with more than 30 TSSes (set A), and 19 genes with more than 40 TSSes (set B). Set A if, of course, a superset of B. GSEA-MSigDB analysis reveals strong associations for both sets.

Set A consists of MAP1B, CFLAR, IGF2, COL1A1, KIAA1217, DST, IGFBP3, IGFBP5, FOXP1, APOB, AKAP13, PRRX1, PDE4DIP, RABGAP1L, ARPP21, LMO7, TCF4, RTN4, MUC6, ZEB2, ALB, NDRG2, ANK3, FN1, LEF1, MTUS1, THBS1, TTN, SORBS3, SORBS2, XIRP2, TG, MAP2, COL6A2, GNAS, SERPINA1, SYNE1, H19, ZBTB38, LPAR1, PAPPA, CTNND2, DLG2, CALD1, CD36, CCDC80, ANK2, MYLK, NRXN1, CLU, SEPT9, MBP, NTRK2, GFAP, TYRP1, MYH11, GPM6A, PDE4D; and includes 2 growth factors (IGF2 and TG), two homeodomain proteins (PRRX1 and ZEB2), 1 cell differentiation marker (CD36), 3 kinases (MYLK, NTRK2, and TTN), 7 TFs (FOXP1,

LEF1, LMO7, PRRX1, TCF4, ZBTB38, ZEB2), as well as 7 known oncogenes (COL1A1, FOXP1, GNAS, MYH11, PDE4DIP, PRRX1, SEPT9)

Set B consists of MAP1B, IGF2, COL1A1, DST, IGFBP5, APOB, AKAP13, ARPP21, TCF4, ALB, FN1, LEF1, TTN, SORBS2, XIRP2, CALD1, NTRK2, GFAP, PDE4D; and includes one growth factor (IGF2), two TFs (LEF1 and TCF4), two protein kinases (NTRK2 and TTN), and one known oncogene (COL1A1).

Top ten MSigDB sets associated with test Set A are (FigureS7 and FigureS8): genes in cancer modules 66, 12, 100, 137, 11, 47, and 2; TSSes containing the motifs TTGTTT and SMTTTTGT, and genes upregulated in angioimmunoblastic lymphoma (AILT).

Top ten MSigDB sets associated with the test Set B are (FigureS9 and FigureS10): genes in cancer modules 12, 23 and 47, genes associated with TSS motifs TTGTTT, TGCCAAR, as well as as genes up- or down regulated in a number of experimental conditions involving retroviral transduction, RNAi knock-out (PDEF) or growth factor stimulation (e.g. progesterone, PDEF).

Pairs of paralogs overlapping CTCF sites and F5 enhancers

CTCF is a chromatin binding factor that was proposed to function in transcriptional regulation as insulator, by binding and looping chromatin, and preventing interaction between promoter and nearby enhancers or silencers (Phillips and Corces 2009). Our goal was to test the hypothesis of CTCF insulator effect using pairs of paralogs, as co-expression probes uniquely calibrated by nature to measure the effects of overlapping enhancers and CTCF sites.

Out of the total number of 71,716 duplication pairs linked to expression data, 1788 pairs were located closer than 10 kb from each other (10kb-SCPPes). Among 10kb-SCPPes the ratio of the pairs overlapping a CTCF binding site, versus those which didn't, was 48% to 51% (864 pairs against 924). For the paralogs in the distance of 10-100kbps (Figure 10b), 87% overlapped a CTCF. For pairs located further than 100kb, 99% overlapped a CTCF. We focused on 10kb-SCPPes as these pairs were balanced between overlapping and non-overlapping, and were in the right distances for which CTCF effects might be expected.

10kb-SCPPes overlapping a CTCF (Figure 10a) have clearly a bimodal distribution, with the majority of paralogs strongly correlated in expression (0.5-1 PC), or anti-correlated (-0.5-0 PC). On the other hand, the majority 10kb-SCPPes not overlapping a CTCF have PC in the interval between 0 and 0.5.

Tissue-specific paralogs can appear more strongly co-expressed when PC is used as expression distance measure. To control for the possible bias resulting from tissue-specific expression, we analyzed expression breadth (EB) of 10kb-SCPP+CTCF (0.444) and 10kb-SCPP-CTCF (0.13). Since EB(10kb-SCPP+CTCF) > EB(10kb-SCPP-CTCF), differences in tissue-specificity cannot account for the observed effects.

Next, we examined the overlap between 10kb-SCPPes and F5-enhancers(Sandelin). Figure 11 shows PC density plots for three subsets of 10kb-SCPPes: 10kb-SCPP+CTCF+F5en (red); 10kb-SCPP+CTCF-F5en (green); 10kb-SCPP-CTCF-F5en (blue). Interestingly, out of 50 identified 10kb-SCPP+F5en pairs, 46 were also overlapping CTCF. Only 4 pairs had only overlap with F5en, suggesting that CTCF sites and enhancers colocalize and cooperate in regulation of expression of paralog pairs.

Discussion:

Hierarchical clustering of F5-CAGE samples according to their protein-coding gene expression profiles provides overview of the comprehensive encyclopedia of vertebrate gene expression, which we present here (Figure 1 and FigureS1).

In addition to hierarchical clustering, to examine overall variability of expression between different tissues in the Fantom5 dataset, we used principal component analysis (PCA). However, no clear overall pattern of clustering was revealed using PCA. This underlines intrinsic variability of expression patterns in different lineages, and argues against well controlled global blocks of transcriptional regulation common to sets of tissues, for example for those derived from the three distinct embryonic layers (ectoderm, endoderm, and mesoderm).

PCA, however, proved more interesting when applied to brain samples separately (Figure 2). Brain has many unique expression features, such as high number of genes specific to this tissue (Huminiecki, Lloyd et al. 2003) most of which originated from the 2R-WGD event (Huminiecki and Heldin 2010), which prompted us to examine brain samples separately by PCA (Figure 2). Interestingly, Brawand et al. (Brawand, Soumillon et al. 2011) reported lack of clear separation of brain tissue by PCA, in a limited sample of six organs. However, our dataset is vastly more complete than that used by Brawand et al., and includes samples from multiple donors and developmental stages.

The most striking feature of our brain-focused PCA analysis (Figure 2) is that brain libraries appear to form three distinct clusters (a) fetal, (b) neonatal, and (c) somewhat dispersed adult cluster. Intuitively, this makes sense if one considers lengthy brain development and maturation: brains of newborns are arguably the most immature of all babies organs. No similar clustering by developmental stage could be observed for two other human tissues examined in detail: lung, or liver, where samples from multiple donors and developmental stages were available in the F5 dataset (data not shown).

This initial PCA analysis was followed by hierarchical clustering of human brain samples (dendrogram shown in FigureS1d), which confirmed the existence of age-related clusters, described in detail in TableS1.

FigureS1e shows subsequent comparative-expression-PCA (CE-PCA) analysis performed jointly for both human and mouse brain samples (where human and mouse data were linked using ortholog genes, following the same principle applied to the ISHC). In the CE-PCA, human and mouse samples form two strongly demarcated clusters. Insufficient mouse data are available at this stage to draw firm conclusions (for example, there are no mouse fetal F5-CAGE samples, and mouse data are somewhat biased towards cerebellum and visual cortex samples). However, given available data, no developmental stage related clustering can be observed in mouse (Figure S1e), suggesting that murine brain development is different in that respect from hominid.

Previous studies comparing evolutionary profiles between species assumed a very simple model for assignment of ortholog tissues: automatically assuming that samples with matching names in different species are ortholog tissues. Here, we suggest that this is over-simplification of a complex problem. Firstly, expression pattern evolution is fast: lineage-specific expression pattern shifts and tissue-specific evolutionary novelties put into question the very assumption of the existence of ortholog tissues. Conceptually it may simply be wrong to assume that human brain corresponds to mouse brain, or that human stomach corresponds to mouse stomach, as the behavioral and ecological differences between these two species are very substantial. Secondly, differences in pre-processing of samples and anatomical differences between species may make it difficult to isolate RNAs in a reproducible fashion from species with dramatically different body size, and different

anatomy (especially in case of tissues with complex anatomy, such as the CNS, or reproductive system).

To investigate the problem of ortholog tissue assignment more systematically, we compared ortholog clusters derived through (a) simple name matching procedure (NM-clusters), and the ortholog-based ISHC procedure. Conceptually, NM-clustering procedure may be regarded as equivalent to a data-mining approach utilizing supervised learning. On the other hand, the ISHC procedure, just like hierarchical clustering on which it is based, is an unsupervised learning approach (TableS2).

The NM-clusters which are recovered through the ISHC include: skin, liver, tongue, heart, pancreas, pituitary gland, thymus and "total RNA control". However, twice as many NM-clusters (namely 19) were not recovered. This effect seems robust to alterations of the ISHC procedure. We have experimented with other expression distance measures, and ISHC based on whole family-averaging rather than ortholog genes, but not higher rates of NM-cluster recovery could be achieved (data not shown).

Histogram in Fig3b contains stack histogram with Pearson R distributions, obtained during the course of the ISHC procedure, for the two intra-species comparisons (hs, mm), and the inter-species comparison (hs-mm). Inter-species distances (hs-mm) are somewhat higher than intra-species distances (hs and mm): 0.78, 0.68 and 0.72 are the respective means.

A number of observations followed on comparison of several sample types (tissues, primary cells, and cancer cell-lines) available for human in the F5-CAGE dataset. For example, one of the most broadly relevant conclusions of this work, is that closely related paralogs are not correlated in their expression in cancer-cell lines, in contrast to tissues and primary cell-lines. In other words, while recent closely related paralogs tend to be expressed in the same tissue, they are not co-expressed in the same cancer cell lines. Assuming that co-expression of closely related paralogs is conditioned by the structure of their promoter regions, this suggest that normal conditions of promoter regulation do not exist in cancer cell lines. The effect cannot be attributed to cell culture conditions alone, as paralog co-expression signature is seen in primary cell culture samples.

It has been proposed previously that primary mutations and expression pattern changes in cancers are accompanied by a wide range of secondary changes, however, the findings presented here are perhaps the most comprehensive demonstration of this expression pattern disregulation in cancer. We propose a novel term: devolution of expression patterns, to suggest that normal evolutionary constraints on expression patterns do not exist in cancer.

In a more detailed follow up analysis focused on expression patterns of entire gene families, we have compared two expression characteristics of TreeFam families in tissues, primary cells, and cancer cell-lines: average expression, and preferential expression measure (supplementary tables S3, S4, and S5). Data in TableS5 can be queried in multiple additional ways, depending on the biological question that is of most interest to the reader. For example, one can identify families preferentially expressed in both tissues, and primary cells, versus cancer cell-lines; preferentially expressed in tissues versus primary cells and cancer cell-lines; tissue-specific in tissues but not in cancer; tissue-specific in tissues and primary cells but not cancer cell-lines, etc, etc.

To examine overall differences in average gene family expression characteristics between F5-CAGE tissues, primary cells, and cancer cell-lines, we performed multivariate analysis of seven variables associated with TreeFam families in the F5-CAGE dataset (FigureS5): number of human family members (family_size), average expression in human tissues (AVG_tissues), average expression in cells (AVG_cells), average expression in cancer (AVG_cancer), preferential expression measure in tissues (PEM_tissues), preferential expression measure in cells (PEM_cells), and preferential expression measure

in cancer (PEM_cancer). While average expression values correlate strongly between the three sample types, preferential expression measure in tissues does not correlate with those calculated for cells and cancer cell lines. This makes sense if one considers that tissues are mixtures of different cell-types, and suggests that fundamentally different regulatory phenomena are responsible for tissue-specific expression versus cell-line specific expression.

Finally, we have used self-organizing map (SOM) as a multivariate data-mining approach to cluster gene families into groups of similar expression characteristics in human tissues, primary cells, and cancer cell lines (FigureS6a and FigureS6b, TableS9a and TableS9b). The rectangular 6 by 6 SOM proved efficient in clustering TreeFam familyA families into groups with similar expression characteristics in the three human sample types. Several, clusters (i.e. prototypes) warrant particular attention (**prototype No**: *size*): (**1**: *2*) high average expression in all three sample types (SH3 domain-binding glutamic acid-rich-like protein, tumor rejection antigen); (**4**: *3*) high expression in tissues but low in cells and cancer cell lines (natriuretic peptide precursor A/B, quinoid dihydropteridine reductase, kinesin family member 5); (**30**: *5*) high PEM in cells and cancer cell lines, all other variables low (superoxide dismutase 2, RAB7, ATP synthase, RAN, protein disulfide isomerase family A); (**35**: *4*) high PEM in tissues, lower in cells and cancer cell lines, all other variables low (damage-specific DNA binding protein, replication factor C, cleavage and polyadenylation specific factor 3, replication protein A1); (**36**: *2*) very high PEM in cells and cancer cell-lines, all other variables low (heat shock 27kDa protein, and superoxide dismutase families).

It is interesting to ask if changes in expression patterns, in particular dramatic shifts in expression patters, and mutually exclusive expression are correlated with promoter structure and transcription binding patterns. We have therefore, examined promoters of the three cdc42 family genes (RAC2, RAC3, and RHOG) using pooled ENCODE data for transcription factor binding sites (Tfbs) from ENCODE cell lines (see methods). Table 3 lists all Tfbs linked to these promoters, and a subset of the the dataset with the strongest signal (score > 750, overall score varies between 0-1000). Table 4 shows Jaccard index values for pairwise comparisons between all family members. We have also examined promoter regions of these three genes manually with the UCSC genome browser featuring ENCODE data. Narrowly expressed, RAC3 (promoter region at chr17: 79988532 - 79990531) features one strong binding site for TF ZBTB7A (ZBTB7A_(SC-34508); cluster score (out of 1000): 1000; K562 cell line; chr17:79989226-79989435), a weak and narrow DNASEI site (score 24), and a weak H3K27AC signal. In contrast, liberally expressed RAC2 (Promoter = chr22: 37639306-37641305) and RHOG (Promoter = chr11:3861214-3863213) have broad and high-scoring DNASEI sites (DNASEI scores of 121 and 136 respectively), and very strong H3k27AC signals. RAC2 and RHOG have many Tfbs within narrow 500 bps window of their TSSes, with strong NFKB signature for both RAC2 (cluster score (out of 1000): 852; chr22:37640075-37640448; cell line GM12891), and RHOG (cluster score (out of 1000): 716; chr11:3862446-3862758; cell line GM12891). This suggests a scenario where ancestral NFKB binding site was replaced by ZBTB7A in RAC3.

Indeed, published literature and genomics data available for NFKB and ZBTB7A, give further credence to the evolutionary scenario correlating replacement of these two Tfbs, with expression pattern shift from broad expression pattern preferentially associated with immune and circulatory systems (RAC2 and RHOG), to narrow expression associated with fetal brain (RAC3):

(a) ZBTB7A (http://www.factorbook.org/mediawiki/index.php/ZBTB7A) stands for Homo sapiens zinc finger and BTB domain containing 7A (a gene originally called Pokemon, a name which was withdrawn for obvious reasons under a threat of legal

action), with highest expression in GNF Expression Atlas 1 associated with “whole brain”. Interestingly, ZBTB7A promoter region itself (chr19:4,066,216-4,068,615) features three ENCODE ZBTB7A_(SC-34508) binding sites, in addition to Egr-1, SUZ12, and a CTCF binding site. ZBTB7A had been shown to be an oncogenic transcription factor (Maeda, Hobbs et al. 2005; Maeda, Hobbs et al. 2005), and has been implicated in glioma (Rovin and Winn 2005). ZBTB7A can act as a transcriptional repressor or activator depending on the promoter context.

(b) NFKB (http://www.factorbook.org/mediawiki/index.php/NFKB) is very widely expressed in animal cells and well-known to play a role in immune and stress responses 16724054.

An interesting sideline to the examination of cdc42 family, is that the gene tree derived from F5-CAGE expression clustering, bears little similarity to the TreeFam phylogenetic tree for this family, suggesting that expression patterns cannot be readily used as phenotypic markers for phylogenetic inference. This conclusion of limited phylogenetic signal contained in expression pattern data, is also in some ways a logical extension of FigureS2, which shows little differentiation in paralog expression patterns can be seen for taxa older than Amniota, and high variability in expression distances seen for younger taxa.

To examine the structure the landscape of alternative TTSes at these loci in more detail, we have manually examined a number of them, using the FANTOM5-UCSC genome browser (FigureS12-21). Several of these loci are muscle protein, and some were known to generate alternative isoforms. However, these alternative isoforms were presumed to result from alternative splicing; here we show they derive from alternative TSSes and alternative promoters. In many cases, these TSSes align well with Tfbs from the ENCODE dataset.

To verify biological significance of multiple mapping TSSes, we compared the correlation between the number of mapped TSSes for human and mouse, for 1:1 ortholog genes (using matching gene symbol names). R value of 0.5023387 for Pearson R was obtained for this correlation (Figure 9b).

Future work: we are currently using the ENCODE dataset in conjunction with F5-CAGE to examine the over-all correlation between promoter structure as defined by ENCODE Tfbs and DNASEI footprints and expression patterns, in particular in gene duplicates. However, this analysis will be finalized when full ENCODE dataset, including mouse data, is released in the future.

We are also currently investigating the relationship between TSS divergence between paralogs and their expression pattern divergence. Previous published work suggested that sharing TSS increases expression correlation (Park and Makova 2009), however that study used out-dated methodology for gene family identification and alignment (CLUSTALW), out-dated gene expression datasource, and was limited only to the ENCODE pilot regions (Birney, Stamatoyannopoulos et al. 2007).

Finally, as the assignment of ortholog tissues in an unsupervised approach is based on matching expression patterns of gene orthologs, this question is closely related to the broader issue of ortholog conjecture (Studer and Robinson-Rechavi 2009). Recently, there has been a heated debate with reference to the ortholog conjecture, in particular with reference to the use of gene ontology data for tests of the hypothesis (Nehrt, Clark et al. 2011; Altenhoff, Studer et al. 2012; Thomas, Wood et al. 2012). We are currently testing ortholog conjecture using F5-CAGE expression data, hoping that our expression encyclopedia will be a much better proxy of gene function between species.

Data access:

--- consortium provides details

Methods:

F5-CAGE WP4 expression tables

TreeFam8 database
The release 8 of the TreeFam database (2012.02.10) includes 79 species (based on Ensembl v.54). There are 1,539,621 genes in total in 16,064 different TreeFam families.

Expression distances and hierarchical clustering
Expression distances were calculated using Bioconductor package bioDist Release (2.11).

Supercomputer resources
The Swedish National Infrastructure for Computing (SNIC) coordinates and develops high end computing capacity for Swedish research. The computations were performed on resources provided by SNIC through Uppsala Multidisciplinary Center for Advanced Computational Science (UPPMAX).

ENCODE data
Multi-cell-line clustered Tfbs data (file wgEncodeRegTfbsClusteredV2.bed), called from henceforth TfbsClusteredV2, published by the ENCODE consortium in 2012 (ENCODE), were used to analyze promoter regions of gene of interest within 500 bps window (-/+ 250 bps from the TSS). TfbsClusteredV2 includes 2.7 million peaks, which combine data from the Myers Lab at the HudsonAlpha Institute for Biotechnology and by the labs of Michael Snyder, Mark Gerstein and Sherman Weissman at Yale University; Peggy Farnham at UC Davis; and Kevin Struhl at Harvard, Kevin White at The University of Chicago, and Vishy Iyer at The University of Texas Austin. TfbsClusteredV2 includes data for 148 TFs including CTCF and PolII.

Promoter regions of several genes were also inspected manually using the UCSC Genome Browser on Human Feb. 2009 (GRCh37/hg19) Assembly, which included tracks with the identical subset of ENCODE data.

Gene Set Enrichment
To investigate functional enrichment among genes with most TSSes, we have used the Gene Set Enrichment algorithm and the online MSigDB database (MSigDB database v3.1, GSEA/MSigDB web site v3.85), available as JavaScript-based webportal to the database**(MSigDB)**.

Correlation between the number of mapped TSSes for human and mouse
13844 ortholog pairs for human and mouse were identified by matching gene symbol names (out of total of 24677 human and 20320 mouse genes), with 67932 TSSes in human, and 46420 in mouse. For this dataset, the median was 4 TSSes linked to one human protein-coding gene, and 75% quantile was 6 TSSes. Maximum was 87. For mouse genes, the median was 3, 75% quantile was 4, and maximum 41. Lower values observed for mouse, could be explained either as the properties of the dataset (CAGE coverage for mouse is lower than for human), or as reflecting genuine biological differences in transcription initiation between these two species.

It should be noted that there were statistically significant differences between TSS coverage for 1:1 orthologs, and whole human and mouse sets. For example, the average number of TSSes for all human genes was 3.714836, while for human genes with a 1:1 mouse ortholog, it was 4.906963 (p-value < 2.2e-16 in Welch Two Sample t-test). Similarly, the average number of TSSes for all mouse genes was 2.900492 , while for mouse genes

with a 1:1 mouse ortholog, it was 3.353077 (p-value < 2.2e-16 in Welch Two Sample t-test). These differences cannot affect the conclusion about overall conservation of TSS numbers between human and mouse, but significantly higher numbers of TSSes associated with 1:1 orthologs in both human and mouse, suggest that genes which underwent duplication in any these lineages have a lower number of TSSes associated with them. This possible link between TSS coverage and duplicability warrants further investigation, however, other sources of skew, such as gene length must be controlled for.

CTCF overlap

For performing the analysis on CTCFs location and it's relationship with the expression levels of the paralogs we used the CTCF data provided by the ENCODE project. First, CTCF binding sites were extracted from wgEncodeRegTfbsClusteredV2.bed. This file combines data from many different cell lines and transcription-factor targeting antibodies. The paralogous genes were mapped to their locations using Refseq ids and the known gene promoters data set from the package FunciSNP.data (Coetzee, Rhie et al. 2012). Only the pairs that are located on the same chromosome were considered and the Genomic Range for each pair was constructed from the position of the promoter of the first gene to the position of the promoter of it's duplicate partner. Same chromosome duplicate TreeFam pairs of all ages were considered.

Data access:

Acknowledgments:

Disclosure declaration:

The authors declare no competing interests.

FIGURE LEGENDS:

Fig1. Hierarchical clustering of human tissue samples (Spearman correlation).
CNS samples cluster together, forming two distinct sub-clusters: (a) medulla oblongata, spinal cord, brain glands, and eye cluster; (b) other brain tissues. The single outlying substantia nigra sample may be a technical problem since other substantia nigra samples cluster more closely with the CNS tissues. Several additional clusters are clearly visible in human tissues, and have been annotated at the dendrogram level.

Fig2. Brain samples group into age-related clusters.
Human brain samples cluster in a PCA analysis (PC1 versus PC2) into three age related clusters. Samples are shown using colored marks (adult - red, fetal - green, newborn - blue). These clusters are illustrated using oval shapes with boundaries hued in respective colors. Few samples are outliers to the overall PCA clustering pattern, for example: putamen, cerebellum, spinal cord, medulla oblongata. Interestingly, most outlying samples correspond to the brain stem, suggesting different developmental patterns for forebrain, midbrain and hindbrain.

Fig3. Inter-species hierarchical clustering of samples (ISHC).
Panel (**a**) shows the tree for inter-species hierarchical clustering of samples (ISHC). Panel (**b**) shows histogram with Pearson R distribution (all-against-all sample comparisons) for hs (human), mm (mouse), and hs-mm (human-mouse).

Fig4. Paralog expression divergence in normal versus cancer cells.
Paralog expression divergence offers unexpected evidence for global transcriptional disregulation in cancer cell lines. Panel (a) human tissues, panel (b) cancer cell lines. Expression distances are calculated using Pearson R.

Fig5. Young genes are tissue-specific, old genes are housekeeping.
As organisms grew in complexity and new tissues formed, new genes became more and more tissue-specific in their epression patterns. However, there are exceptions to this trend: in particular, taxa Eutheria and Deuterostomia, suggesting unique evolutionary features of genes associated with these taxa.

Fig6. Evolutionary history of mammalian tissues: reproductive system.

Fig7. Evolution of expression patterns in the cdc42 family
Panel (a) shows heatmap of expression patterns for the cdc42 family in human tissues. Panel (b) shows heatmap of the values for Jaccard-index for ENCODE Tfbs in pairwise comparisons. Table in panel (c) shows actual values of the Jaccard-index.

Figure 8. 87 TSSes in the TTN locus.

Figure 9. Most genes have multiple TSSes, and tendency to be associated with high number of TSSes is conserved between human and mouse.
Panel (a) shows the histogram of the number of TSSes per gene in human, and panel (b) shows the scatterplot of the number of TSSes in human and mouse for pairs of orthologs.

Figure 10. Close paralog pairs overlapping a CTCF site are more similar in expression profile. Density plots of Pearson expression correlations between pairs of same chromosome paralogs, depending on distances: (a) distance less than 10kb; (b)

distance between 10kb-100kb; (c) more than 100kb. Panel (d) shows histograms of the distances between the paralogs, with (green) or without CTCF overlap (red).

Figure 11. Close paralogs which overlap both an enhancer and a CTCF site are highly correlated in expression. Density plots of Pearson correlation between expression levels in pairs of same chromosome paralogs (distance less than 10kb) which overlap both an enhancer and a CTCF (red line); overlap only a CTCF (green line); overlap none of those (turquoise line). Number of pairs divided only by the enhancer is very low, and insufficient to draw a density plot.

Supplementary figures:

FigS1a. Hierarchical clustering of hs-PC samples (Spearman correlation).

FigS1b. Hierarchical clustering of hs-CCL samples (Spearman correlation).

FigS1c. Hierarchical clustering of mm-T samples (Spearman correlation).

FigS1d. Dendrogram of human brain samples.

FigS1e. PCA of human and mouse brain samples.

FigS2. Expression pattern divergence bar-plot between paralogs.

FigS3. Evolutionary history of mammalian tissues: brain samples.

FigS4. Expression pattern evolution rates vary widely between tissues
Tissues can be subdivided into three groups of differing expression pattern evolution rates, as calculated by Eucledian distance between paralog pairs. The three groups are: (a) dynamic (for example, consistently including thumus, adipose, liver, pancreas and blood), (b) intermediate and (c) static. Brain samples are split between clusters (b) and (c).

FigS5. Comparative multivariate analysis of gene family expression patterns
To examine overall differences in average gene family expression characteristics between F5-CAGE tissues, primary cells, and cancer cell-lines, we performed multivariate analysis of the following 7 variables associated with TreeFam families in the F5-CAGE dataset (Figure 12a): number of human family members (family_size), average expression in human tissues (AVG_tissues), average expression in cells (AVG_cells), average expression in cancer (AVG_cancer), preferential expression measure in tissues (PEM_tissues), preferential expression measure in cells (PEM_cells), and preferential expression measure in cancer (PEM_cancer).

FigS6. Self-organizing map (SOMs) identifies clusters of families with similar characteristic expression characteristics in the three human sample types
6 by 6 rectangular SOM (R package Kohonen) was used to classify 682 TreeFam manually-annotated familyA families into groups with similar size, average expression and preferential expression in the three human sample types. Classification of all families into a prototype number is given in TableS9a (prototypes are numbered/ordered left to right first, and bottom to top second). “Counts plot” in panel (a) illustrates final prototype sizes, while panel (b) illustrates average variable values for all TreeFam families clustering into a given prototype. Exact prototype sizes are as follows (in ascending numerical order): 2, 7, 8, 3, 3, 5, 7, 12, 16, 7, 10, 6, 13, 9, 28, 9, 23, 16, 12, 37, 55, 4, 19, 22, 28, 26, 56, 38, 8, 5, 57, 78, 32, 14, 4, 2. Prototype 32 is the most populated one, with 78 TreeFam families (top row, 2nd from the left). Exact average variable values in each prototype are given in TableS9b.

FigS7. Functional enrichment. GSEA in top TSS genes.

FigS8. Functional enrichment. GSEA in top TSS genes.

FigS9. Functional enrichment. GSEA in top TSS genes.

FigS10. Functional enrichment. GSEA in top TSS genes.

FigS11. Number of TSSes and gene taxon of origin.

FigS12. TTSes in the septin 9 locus.

FigS13. TTSes in the ubiquitin-conjugating enzyme E2D 3 locus.

FigS14.TTSes in the suppression of tumorigenicity 1 locus.

FigS15. TTSes in the endothelin converting enzyme 1 locus.

FigS16. TTSes in the apolipoprotein B locus.

FigS17. TTSes in the Insulin-like growth factor 2 locus.

FigS18. TTSes in the fibronectin 1 locus.

FigS19. TTSes in the caldesmon 1 locus: (a) detailed view; (b) overview.

FigS20. TTSes in the xin actin-binding repeat containing 2 locus.

FigS21. TTSes in the A kinase (PRKA) anchor protein 13 locus.

FIGURES:

TABLES:

Table 1. The structure of the F5 encyclopedia of expression patterns.

Table 2. Two strategies for ortholog tissue assignment.
Comparison of two different approaches for ortholog tissue identification: “name matching” (NM) and inter-species hierarchical clustering. Eight name clusters are also simple inter-species hierarchical clusters (signified by “YES” in the last column and green color in the first). However, many name clusters are not recovered as inter-species hierarchical clusters (Fig4) (signified by “NO” in the last column), while two are split and difficult to classify (signified by “Not certain” in the last column).

Table 3. cdc42 family ENCODE Tfbs in a 500 bp window (-/+ 250 bps from the TSS).

Table 4. Tfbs Jaccard index for the cdc42 family ENCODE Tfbs

Supplementary tables:

TableS1. Brain samples in human cluster according to developmental stage.

TableS2. The full F5 CAGE NM-dataset is shown.

TableS3 Gene families with differential tissue-specific expression in tissues versus primary cells and cancer cell lines.

TableS4. Families with differential average expression in tissues versus primary cells and cancer cell lines.

TableS5. Gene family expression status in tissues, primary cells and cancer cell lines.

TableS6a. GO term and PFAM domain enrichment, for all taxa, in genes with unusually fast expression divergence rate.

TableS6b. GO term and PFAM domain enrichment, for all taxa, in genes with unusually high breadth of expression.

TableS7. Strongest associations between timing of gene duplication and expression site in F5 CAGE.

TableS8. Example genes behind strongest associations between timing of gene duplication and expression site in F5 CAGE.

TableS9a. SOM analysis of gene families: family size, average expression in T, PC and CCL samples; average PEM in T, PC and CCL samples. Assignment to one of 36 SOM clusters/prototypes.

TableS9b. Characterization of 36 SOM clusters/prototypes: SOM prototype number; average family size for all families assigned to the prototype; average expression in T, PC and CCL samples; average PEM in T, PC and CCL samples.

Table 1. Number of samples in distinct F5-CAGE categories for human and mouse: tissues, primary cells, cancer cell lines.

	human	mouse
total	952	396
tissues	179	280
primary cells	513	116
cancer cell lines	260	-
brain tissues	60	51
reproductive tissues	14	21

Table 2. Comparison of ortholog human-mouse tissue clusters obtained by simple name matching (NM-clusters), with those inferred using inter-species hierarchical clustering of samples (ISHC).

Name matching (NM) cluster	No. of human samples in the NM cluster	No. of mouse samples in the name cluster	NM cluster recovered by the ISHC procedure
lung	3	14	NO
colon	3	1	Not certain
diencephalon	1	2	NO
skin	3	5	YES
kidney	2	10	NO
liver	2	16	YES
uterus	2	2	NO
tongue	3	1	YES
stomach	1	10	NO
ovary	1	3	NO
aorta	1	1	NO
heart	3	15	YES
prostate	1	1	NO
vagina	1	1	NO
spleen	2	6	NO
placenta	1	2	NO
pancreas	1	12	YES
testis	2	11	NO
small intestine	2	1	Not certain
medulla oblongata	3	2	NO
adrenal gland	1	7	NO
spinal cord	4	1	NO
pituitary gland	1	8	YES
thymus	2	14	YES
hippocampus	3	2	NO
cerebellum	3	38	NO
RNA	2	2	YES
eye	6	9	NO
epididymis	1	3	NO
Total: 29 clusters	Total: 58 samples	Total: 186 samples	Total: 8-YES, 19-NO

Table 3. cdc42 family ENCODE Tfbs in a 500 bp window (-/+ 250 bps from the TSS).

No	EntrezID	Name, TSS location	All Tfbs	Strong Tfbs
1	23433	ras homolog family member Q,RHOQ, 46769867,chr2	Promoter=chr2:46769617-46770116, includes: HA-E2F1, Pol2, ELF1_(SC-631), ZNF263, ZEB1_(SC-25388), Sin3Ak-20, CCNT2, Nrf1, E2F1, c-Myc, E2F6_(H-50), E2F6, Egr-1, **ZBTB7A**_(SC-34508), TAF1, EBF	Promoter=chr2:46769617-46770116, includes (at 0.75 quantile cut-off): HA-E2F1, ZNF263,
2	391	ras homolog family member G,RHOG, -3848208,chr11	Promoter=chr11:3861964-3862463, includes: HA-E2F1, CCNT2, Pol2, HEY1, ELF1_(SC-631), Pol2-4H8, GABP, PU.1, Egr-1, HA-E2F1, **NFKB**	Promoter=chr11:3861964-3862463, includes (at 0.75 quantile cut-off): ,
3	57381	ras homolog family member J,RHOJ, 63671145,chr14	Promoter=chr14:63670852-63671351, includes: KAP1, c-Jun, c-Fos, JunD, GATA-2, CTCF, HDAC2_(SC-6296), Rad21, p300, ELF1_(SC-631), Pol2(b), SRF, Pol2	Promoter=chr14:63670852-63671351, includes (at 0.75 quantile cut-off): c-Jun, Pol2(b),
4	5879	ras-related C3 botulinum toxin substrate 1 (rho family, small GTP binding protein Rac1),RAC1, 6414126,chr7	Promoter=chr7:6413876-6414375, includes: TFIIIC-110, TBP, Pol2, RPC155, BDP1, HA-E2F1, YY1, YY1_(C-20), HMGN3, E2F4, p300, E2F1, TAF1, c-Myc, GABP, Egr-1, ELF1_(SC-631), NANOG_(SC-33759), CCNT2, Pol2, Pol2-4H8, HEY1, YY1_(C-20)	Promoter=chr7:6413876-6414375, includes (at 0.75 quantile cut-off): TBP, HA-E2F1, YY1, YY1_(C-20), E2F1, GABP,
5	5880	ras-related C3 botulinum toxin substrate 2 (rho family, small GTP binding protein Rac2),RAC2,-37621312,chr22	Promoter=chr22:37640056-37640555, includes: Pol2-4H8, TAF1, HEY1, **NFKB**, Pol2, POU2F2, Oct-2, Sin3Ak-20, c-Fos, TBP, GABP, ELF1_(SC-631), ETS1, E2F6_(H-50), PU.1, c-Myc, Max, Egr-1, IRF1, PAX5-C20, Pbx3, EBF1_(C-8), **ZBTB7A**_(SC-34508), TCF12	Promoter=chr22:37640056-37640555, includes (at 0.75 quantile cut-off): **NFKB**, Pol2,
6	5881	ras-related C3 botulinum toxin substrate 3 (rho family, small GTP binding protein Rac3),RAC3, 79989532,chr17	Promoter=chr17:79989282-79989781, includes: ETS1, Sin3Ak-20, **ZBTB7A**_(SC-34508), Egr-1, SRF	Promoter=chr17:79989282-79989781, includes (at 0.75 quantile cut-off): **ZBTB7A**_(SC-34508),
7	998	cell division cycle 42 (GTP binding protein, 25kDa),CDC42, 22379120,chr1	Promoter=chr1:22378870-22379369, includes: TFIIIC-110, Nrf1, Pol2, E2F6_(H-50), IRF1, RFX5_(N-494), ELF1_(SC-631), SP1, GABP, p300, PU.1, JunD, TBP, **NFKB**, HMGN3, E2F4, PAX5-C20, CCNT2, USF-1, USF1_(SC-8983), Egr-1, c-Myc, GTF2F1_(RAP-74), YY1_(C-20), YY1, c-Jun, PAX5-N19, Sin3Ak-20, Pol2(b), eGFP-JunD, **ZBTB7A**_(SC-34508), NRSF, Pol2-4H8, TAF1, SIX5, ZEB1_(SC-25388), Pol2(phosphoS2), HEY1, EBF1_(C-8), TCF12, POU2F2, Oct-2	Promoter=chr1:22378870-22379369, includes (at 0.75 quantile cut-off): Nrf1, Pol2, ELF1_(SC-631), PU.1, HMGN3, eGFP-JunD, Pol2-4H8, TAF1, HEY1,

	RHOQ	RHOG	RHOJ	RAC1	RAC2	RAC3	CDC42
RHOQ	1.00	0.24	0.07	0.28	0.25	0.17	0.23
RHOG	0.24	1.00	0.10	0.35	0.31	0.07	0.21
RHOJ	0.07	0.10	1.00	0.10	0.09	0.06	0.12
RAC1	0.28	0.35	0.10	1.00	0.25	0.04	0.34
RAC2	0.25	0.31	0.09	0.25	1.00	0.16	0.43
RAC3	0.17	0.07	0.06	0.04	0.16	1.00	0.07
CDC42	0.23	0.21	0.12	0.34	0.43	0.07	1.00

Table 4. Jaccard index for the cdc42 family

TableS1. Brain samples in human cluster according to developmental stage.

fetal	newborn	adult
temporal lobe, fetal, donor1, tech_rep1.CNhs11772.10063.101H9.hg19 occipital lobe, fetal, donor1.CNhs11784.10073.102A1.hg19 parietal lobe, fetal, donor1.CNhs11782.10072.101I9.hg19 brain, fetal, pool1.CNhs11797.10085.102B4.hg19	**1st Cluster:** parietal lobe, newborn, donor10223.CNhs14074.10356.105E5.hg19 medial temporal gyrus, newborn, donor10223.CNhs14070.10353.105E2.hg19 occipital cortex, newborn, donor10223.CNhs14073.10355.105E4.hg19 amygdala, newborn, donor10223.CNhs14078.10360.105E9.hg19 hippocampus, newborn, donor10223.CNhs14081.10363.105F3.hg19 thalamus, newborn, donor10223.CNhs14084.10366.105F6.hg19 medial frontal gyrus, newborn, donor10223.CNhs14069.10352.105E1.hg19 putamen, newborn, donor10223.CNhs14083.10365.105F5.hg19 caudate nucleus, newborn, donor10223.CNhs14071.10354.105E3.hg19 putamen, adult, donor10258.CNhs14225.10372.105G3.hg19 **2nd Cluster:** medulla oblongata, newborn, donor10223.CNhs14079.10361.105F1.hg19 locus coeruleus, newborn, donor10223.CNhs14080.10362.105F2.hg19 substantia nigra, newborn, donor10223.CNhs14076.10358.105E7.hg19 spinal cord, newborn, donor10223.CNhs14077.10359.105E8.hg19 substantia nigra,adult, donor10196.CNhs13803.10178.103C7.hg19 spinal cord, fetal, donor1.CNhs11764.10056.101H2.hg19	**1st Cluster:** medial temporal gyrus,adult, donor10196.CNhs13809.10183.103D3.hg19 medial frontal gyrus,adult, donor10196.CNhs13796.10170.103B8.hg19 occipital cortex,adult, donor10196.CNhs13798.10172.103C1.hg19 parietal lobe,adult, donor10196.CNhs13797.10171.103B9.hg19 medial frontal gyrus, adult, donor10258.CNhs14221.10368.105F8.hg19 hippocampus,adult, donor10196.CNhs13795.10169.103B7.hg19 amygdala,adult, donor10196.CNhs13793.10167.103B5.hg19 hippocampus, adult, donor10258.CNhs14227.10374.105G5.hg19 parietal cortex, adult, donor10258.CNhs14226.10373.105G4.hg19 parietal lobe, adult, donor10252.CNhs12317.10157.103A4.hg19 medial temporal gyrus, adult, donor10252.CNhs12310.10150.102I6.hg19 middle temporal gyrus, donor10252.CNhs12316.10156.103A3.hg19 amygdala, adult, donor10252.CNhs12311.10151.102I7.hg19 olfactory region, adult.CNhs12611.10195.103E6.hg19 occipital cortex, adult, donor10252.CNhs12 . 10163.103B1.hg19 occipital lobe, adult, donor1.CNhs11787.10076.102A4.hg19 brain, adult, donor1.CNhs11796.10084.102B3.hg19 postcentral gyrus, adult, pool1.CNhs10638.10032.101E5.hg19 occipital pole, adult, pool1.CNhs10643.10036.101E9.hg19 parietal lobe, adult, pool1.CNhs10641.10034.101E7.hg19 paracentral gyrus, adult, pool1.CNhs10642.10035.101E8.hg19 insula, adult, pool1.CNhs10646.10039.101F3.hg19 frontal lobe, adult, pool1.CNhs10647.10040.101F4.hg19 nucleus accumbens, adult, pool1.CNhs10644.10037.101F1.hg19 temporal lobe, adult, pool1.CNhs10637.10031.101E4.hg19 brain, adult, pool1.CNhs10617.10012.101C3.hg19 putamen, adult, donor10196.CNhs12324.10176.103C5.hg19 caudate nucleus, adult, donor10252.CNhs12321.10164.103B2.hg19 caudate nucleus,adult, donor10196.CNhs13802.10177.103C6.hg19 thalamus, adult, donor10258.CNhs14223.10370.105G1.hg19 substantia nigra, adult, donor10258.CNhs14224.10371.105G2.hg19 hippocampus, adult, donor10252.CNhs12312.10153.102I9.hg19 medial temporal gyrus, adult, donor10258.CNhs14229.10376.105G7.hg19 cerebellum, adult, donor10252.CNhs12323.10166.103B4.hg19 cerebellum,adult, donor10196.CNhs13799.10173.103C2.hg19 cerebellum, adult, pool1.CNhs11795.10083.102B2.hg19 cerebellum, newborn, donor10223.CNhs14075.10357.105E6.hg19

fetal	newborn	adult
		2nd Cluster: spinal cord,adult, donor10196.CNhs13807.10181.103D1.hg19 locus coeruleus,adult, donor10196.CNhs13808.10182.103D2.hg19 thalamus,adult, donor10196.CNhs13794.10168.103B6.hg19 globus pallidus,adult, donor10196.CNhs13801.10175.103C4.hg19 diencephalon, adult.CNhs12610.10193.103E4.hg19 spinal cord, adult, donor10252.CNhs12227.10159.103A6.hg19 locus coeruleus, adult, donor10252.CNhs12322.10165.103B3.hg19 thalamus, adult, donor10252.CNhs12314.10154.103A1.hg19 substantia nigra, adult, donor10252.CNhs12318.10158.103A5.hg19 globus pallidus, adult, donor10252.CNhs12319.10161.103A8.hg19 medulla oblongata, adult, pool1.CNhs10645.10038.101F2.hg19 globus pallidus, newborn, donor10223.CNhs14082.10364.105F4.hg19 spinal cord, adult, donor10258.CNhs14222.10369.105F9.hg19 Outliers dura mater, adult, donor1.CNhs10648.10041.101F5.hg19 pineal gland, adult, donor10252.CNhs12228.10160.103A7.hg19 pineal gland,adult, donor10196.CNhs13804.10179.103C8.hg19 medulla oblongata, adult, donor10252.CNhs12315.10155.103A2.hg19 medulla oblongata,adult, donor10196.CNhs13800.10174.103C3.hg19

TableS3. Gene families with differential tissue-specific expression in tissues versus primary cells and cancer cell lines.
Average PEM values, across all genes in a given family and all samples in a given category, are given in: T - tissues, PC - primary cells, CCL - cancer cell lines. Top ten families, with at least ten members, for each of the four differentially expressed categories are given.

top 10 PEM high in cancer				
TF101527	Eukaryotic translation initiation factor 4 gamma	1.0	16.2	24.0
TF106303	translocation protein isoform 1	9.6	18.5	18.5
TF105310	wingless-type MMTV integration site family	7.4	12.9	12.9
TF105321	glutathione S-transferase A/M/P1	8.3	12.1	12.1
TF106495	Rho guanine nucleotide exchange factor (GEF) 1	11	9.8	10.3
TF105128	dual specificity phosphatase 3/14/18/19/21/26	7.4	10.0	10.0
TF105122	dual specificity phosphatase 1/2/4-7/9/10	9.7	8.9	8.9
TF106481	Trinucleotide repeat containing 9 (TNRC9)/Langerhans cell protein (LCP1)/ Granulosa cell HMG box protein 1 (GCX1)/Thymocyte sele	5.6	8.8	8.8
TF105351	p21 (CDKN1A)-activated kinase 1-3	5.8	8.8	8.8
TF106499	gonadotropin-releasing hormone receptor/arginine vasopressin receptor	5.1	8.5	8.5
top 10 PEM high in tissues				
TF106108	fucosyltransferase 8 (alpha (1	6.0	0.0	0.0
TF106311	N-acetyltransferase 1/2 (arylamine N-acetyltransferase)	2.7	1.5	1.5
TF105318	glutathione peroxidase	6.0	3.8	3.8
TF101524	Eukaryotic translation initiation factor 4A	2.8	1.8	1.8
TF106173	histone deacetylase 6/histone deacetylase 10	2.0	1.4	1.4
TF101007	Cyclin G/I	4.2	3.2	3.2
TF101031	Cyclin-dependent kinase-like 1/2/3	3.0	2.4	2.4
TF101069	Cell division cycle associated protein 4	3.5	2.9	2.9
TF101128	RAD6 homolog	2.0	1.6	1.6
TF101155	cytoplasmic linker associated protein	2.7	2.3	2.3
top 10 PEM high in cancer, low in tissues				
TF101527	Eukaryotic translation initiation factor 4 gamma	1.0	16.2	24.0
TF105042	heat shock 70kDa protein 2/6/7	2.2	5.1	5.1
TF106303	translocation protein isoform 1	9.6	18.5	18.5
TF105750	stomatin (EPB72)-like 2	3.2	6.2	6.2
TF105310	wingless-type MMTV integration site family	7.4	12.9	12.9

TF106002	epidermal growth factor receptor / v-erb-b2 erythroblastic leukemia viral oncogene	2.7	4.7	4.7
TF106450	REST corepressor 12/3	2.1	3.5	3.5
TF106499	gonadotropin-releasing hormone receptor/arginine vasopressin receptor	5.1	8.5	8.5
TF101080	Septin 6/8/10/11	4.1	6.6	6.6
TF105317	glypican family	3.8	6.1	6.1
top 10 PEM high in tissues, low in cancer				
TF106108	fucosyltransferase 8 (alpha (1	6.0	0.0	0.0
TF106311	N-acetyltransferase 1/2 (arylamine N-acetyltransferase)	2.7	1.5	1.5
TF105318	glutathione peroxidase	6.0	3.8	3.8
TF101524	Eukaryotic translation initiation factor 4A	2.8	1.8	1.8
TF106173	histone deacetylase 6/histone deacetylase 10	2.0	1.4	1.4
TF101007	Cyclin G/I	4.2	3.2	3.2
TF101031	Cyclin-dependent kinase-like 1/2/3	3.0	2.4	2.4
TF101069	Cell division cycle associated protein 4	3.5	2.9	2.9
TF101128	RAD6 homolog	2.0	1.6	1.6
TF101155	cytoplasmic linker associated protein	2.7	2.3	2.3

TableS4. Families with differential average expression in tissues versus primary cells and cancer cell lines.
Fold difference given in the “fold” column. Average TPM values, across all genes in a given family and all samples in a given category, are given in: T - tissues, PC - primary cells, CCL - cancer cell lines. Top ten families, with more than two human members, for each of the four differentially expressed categories are given.

high in CCL, low in T		**fold**	**T**	**PC**	**CCL**
TF106434	Ubiquitin-like	18.8	1.0	10.9	18.8
TF101116	Ubiquitin-conjugating enzyme E2 C	13.7	3.3	18.5	45.2
TF105231	kinesin family member 18A	11.9	1.5	6.3	17.5
TF105232	kinesin family member 20A/23 (MKLP1)	11.0	2.8	12.7	30.9
TF101001	Cyclin B	10.3	6.7	30.1	69.5
TF105331	aurora kinase	9.6	0.7	2.6	6.9
TF101002	Cyclin A	9.4	2.4	9.5	22.6
TF101021	Cyclin-dependent kinase 1/2/3	9.0	2.8	9.4	25.1
TF101170	F-box only protein 5	8.1	2.1	5.5	17.3
TF101076	Cell division cycle associated 7	7.5	3.3	6.9	24.9
high in T, low in PC and CCL		**fold**	**T**	**PC**	**CCL**
TF105403	A kinase (PRKA) anchor protein 3/4	63.4	1.4	0.0	0.0
TF105451	retinol dehydrogenase 8 (all-trans)	9.4	0.2	0.0	0.0
TF101036	Cyclin-dependent kinase 5 activator	5.6	36.6	2.5	4.1
TF101074	F-box/WD-repeat protein 7	4.9	17.0	1.6	1.9
TF105225	kinesin family member 5 (KHC)	3.3	131	15.6	24.2
TF106489	Patched	3.0	2.9	0.3	0.7
TF106496	Adenomatous polyposis coli	2.7	21.9	3.7	4.5
TF105285	flavin containing monooxygenase	2.4	4.1	1.0	0.7
TF105395	integrin beta 1 binding protein 3	2.3	21.4	4.5	4.7
TF105424	dual oxidase	2.3	4.5	1.3	0.7
high in PC and CCL, low in T		**fold**	**T**	**PC**	**CCL**
TF106434	Ubiquitin-like	29.7	1.0	10.9	18.8
TF101116	Ubiquitin-conjugating enzyme E2 C	19.3	3.3	18.5	45.2
TF105231	kinesin family member 18A	16.2	1.5	6.3	17.5
TF105232	kinesin family member 20A/23 (MKLP1)	15.5	2.8	12.7	30.9

TF101001	Cyclin B	14.8	6.7	30.1	69.5
TF101002	Cyclin A	13.4	2.4	9.5	22.6
TF105331	aurora kinase	13.3	0.7	2.6	6.9
TF101021	Cyclin-dependent kinase 1/2/3	12.3	2.8	9.4	25.1
TF101142	Cyclin-dependent kinases regulatory subunit	10.7	16.6	55.1	123
TF101170	F-box only protein 5	10.7	2.1	5.5	17.3
high in T, low in CCL		**fold**	**T**	**PC**	**CCL**
TF105403	A kinase (PRKA) anchor protein 3/4	98.9	1.4	0.0	0.0
TF105451	retinol dehydrogenase 8 (all-trans)	13.6	0.2	0.0	0.0
TF101036	Cyclin-dependent kinase 5 activator	9.0	36.6	2.5	4.1
TF101074	F-box/WD-repeat protein 7	8.9	17.0	1.6	1.9
TF105424	dual oxidase	6.7	4.5	1.3	0.7
TF105569	Zinc finger protein 106 homolog	6.2	36.7	12.2	5.9
TF105285	flavin containing monooxygenase	6.0	4.1	1.0	0.7
TF105225	kinesin family member 5 (KHC)	5.4	131	15.6	24.2
TF106496	Adenomatous polyposis coli	4.9	21.9	3.7	4.5
TF105395	integrin beta 1 binding protein 3	4.5	21.4	4.5	4.7

TableS6. See accompanying files TableS6a.txt and TableS6b.txt

TableS7. Strongest associations between timing of gene duplication and expression site in F5 CAGE.

Taxon	Short name	Full name	value
HUMAN	thymus liver adipose	thymus, adult, pool1.CNhs10633.10027.101D9.hg19 liver, fetal, pool1.CNhs11798.10086.102B5.hg19 adipose, donor1.CNhs13972.10184.103D4.hg19	245.550373474054, 113.830800845426, 108.231343517192
Homo/Pan/ Gorilla	parotid gland salivary gland blood	parotid gland, adult.CNhs12849.10199.103F1.hg19 salivary gland, adult, pool1.CNhs11677.10093.102C3.hg19 blood, adult, pool1.CNhs11761.10053.101G8.hg19	334.943127801149, 324.458197889213, 320.092508641026
Catarrhini	parotid gland liver trachea	parotid gland, adult.CNhs12849.10199.103F1.hg19 liver, fetal, pool1.CNhs11798.10086.102B5.hg19 trachea, adult, pool1.CNhs10635.10029.101E2.hg19	243.468270217443, 124.307182830041, 70.8639227847559
Eutheria	thymus liver thymus	thymus, adult, pool1.CNhs10633.10027.101D9.hg19 liver, fetal, pool1.CNhs11798.10086.102B5.hg19 thymus, fetal, pool1.CNhs10650.10043.101F7.hg19	566.323654743391, 225.788115451309, 208.247650380362
Theria	blood liver thymus	blood, adult, pool1.CNhs11761.10053.101G8.hg19 liver, fetal, pool1.CNhs11798.10086.102B5.hg19 thymus, adult, pool1.CNhs10633.10027.101D9.hg19	139.028270874016, 134.020715393351, 104.065647888749
Amniota	thymus thymus breast	thymus, adult, pool1.CNhs10633.10027.101D9.hg19 thymus, fetal, pool1.CNhs10650.10043.101F7.hg19 breast, adult, donor1.CNhs11792.10080.102A8.hg19	116.93878540317, 50.2908907452444, 45.6543158685601

Tetrapoda	thymus esophagus pancreas	thymus, adult, pool1.CNhs10633.10027.101D9.hg19 esophagus, adult, pool1.CNhs10620.10015.101C6.hg19 pancreas, adult, donor1.CNhs11756.10049.101G4.hg19	185.17845759193, 149.778206000194, 139.671894228099
Euteleostomi	thymus adipose thymus	thymus, adult, pool1.CNhs10633.10027.101D9.hg19 adipose, donor1.CNhs13972.10184.103D4.hg19 thymus, fetal, pool1.CNhs10650.10043.101F7.hg19	78.6409808377661, 48.7050213293096, 42.7078793767614
Chordata	pancreas skeletal muscle artery	pancreas, adult, donor1.CNhs11756.10049.101G4.hg19 skeletal muscle, adult, pool1.CNhs10629.10023.101D5.hg19 artery, adult.CNhs12843.10190.103E1.hg19	114.337614853883, 74.9230098351664, 58.7017523063515
Deuterostomia	pancreas placenta dura mater	pancreas, adult, donor1.CNhs11756.10049.101G4.hg19 placenta, adult, pool1.CNhs10627.10021.101D3.hg19 dura mater, adult, donor1.CNhs10648.10041.101F5.hg19	50.0273404519974, 31.0416435172888, 28.2508159948265
Bilateria	thymus adipose pancreas	thymus, adult, pool1.CNhs10633.10027.101D9.hg19 adipose, donor1.CNhs13972.10184.103D4.hg19 pancreas, adult, donor1.CNhs11756.10049.101G4.hg19	108.48916971048, 73.8207660128358, 56.0027402697822
Eumetazoa	thymus thymus liver	thymus, adult, pool1.CNhs10633.10027.101D9.hg19 thymus, fetal, pool1.CNhs10650.10043.101F7.hg19 liver, fetal, pool1.CNhs11798.10086.102B5.hg19	117.867716198574, 51.5054249037973, 50.8844737140422
Fungi/ Metazoa	thymus adipose adipose	thymus, adult, pool1.CNhs10633.10027.101D9.hg19 adipose, donor1.CNhs13972.10184.103D4.hg19 adipose, donor3.CNhs13974.10186.103D6.hg19	450.200187073667, 232.438498377191, 177.112712684284

Metazoa	skeletal muscle artery pancreas	skeletal muscle, adult, pool1.CNhs10629.10023.101D5.hg19 artery, adult.CNhs12843.10190.103E1.hg19 pancreas, adult, donor1.CNhs11756.10049.101G4.hg19	42.7661408222488, 40.9127053558847, 37.0478158146202
Eukaryota	thymus skeletal muscle vagina	thymus, adult, pool1.CNhs10633.10027.101D9.hg19 skeletal muscle, adult, pool1.CNhs10629.10023.101D5.hg19 vagina, adult.CNhs12854.10204.103F6.hg19	100.769739509574, 75.1287161094575, 72.4926635448796

TableS8. See accompanying file TableS8.pdf.
TableS9a. See accompanying file TableS9a.txt.
TableS9b. See accompanying file TableS9a.txt.

Bibliography

Altenhoff, A. M., R. A. Studer, et al. (2012). "Resolving the ortholog conjecture: orthologs tend to be weakly, but significantly, more similar in function than paralogs." PLoS computational biology **8**(5): e1002514.

Amado, F., M. J. Lobo, et al. (2010). "Salivary peptidomics." Expert review of proteomics **7**(5): 709-721.

Baron, A., A. DeCarlo, et al. (1999). "Functional aspects of the human salivary cystatins in the oral environment." Oral diseases **5**(3): 234-240.

Birney, E., J. A. Stamatoyannopoulos, et al. (2007). "Identification and analysis of functional elements in 1% of the human genome by the ENCODE pilot project." Nature **447**(7146): 799-816.

Brawand, D., M. Soumillon, et al. (2011). "The evolution of gene expression levels in mammalian organs." Nature **478**(7369): 343-348.

Coetzee, S. G., S. K. Rhie, et al. (2012). "FunciSNP: an R/bioconductor tool integrating functional non-coding data sets with genetic association studies to identify candidate regulatory SNPs." Nucleic acids research **40**(18): e139.

Eisen, M. B., P. T. Spellman, et al. (1998). "Cluster analysis and display of genome-wide expression patterns." Proceedings of the National Academy of Sciences of the United States of America **95**(25): 14863-14868.

ENCODE. "TfbsClusteredV2." from http://genome.ucsc.edu/cgi-bin/hgTrackUi?db=hg19&g=wgEncodeRegTfbsClusteredV2.

Huminiecki, L. and C. H. Heldin (2010). "2R and remodeling of vertebrate signal transduction engine." BMC Biol **8**: 146.

Huminiecki, L., A. T. Lloyd, et al. (2003). "Congruence of tissue expression profiles from Gene Expression Atlas, SAGEmap and TissueInfo databases." BMC Genomics **4**(1): 31.

Huminiecki, L. and K. H. Wolfe (2004). "Divergence of spatial gene expression profiles following species-specific gene duplications in human and mouse." Genome Res **14**(10A): 1870-1879.

Jordan, I. K., L. Marino-Ramirez, et al. (2005). "Evolutionary significance of gene expression divergence." Gene **345**(1): 119-126.

Khaitovich, P., G. Weiss, et al. (2004). "A neutral model of transcriptome evolution." PLoS Biol **2**(5): E132.

Li, H., A. Coghlan, et al. (2006). "TreeFam: a curated database of phylogenetic trees of animal gene families." Nucleic Acids Research **34**(Database issue): D572-580.

MSigDB MSigDB database.

Nehrt, N. L., W. T. Clark, et al. (2011). "Testing the ortholog conjecture with comparative functional genomic data from mammals." PLoS computational biology **7**(6): e1002073.

Park, C. and K. D. Makova (2009). "Coding region structural heterogeneity and turnover of transcription start sites contribute to divergence in expression between duplicate genes." Genome Biology **10**(1): R10.

Pereira, V., D. Waxman, et al. (2009). "A problem with the correlation coefficient as a measure of gene expression divergence." Genetics **183**(4): 1597-1600.

Phillips, J. E. and V. G. Corces (2009). "CTCF: master weaver of the genome." Cell **137**(7): 1194-1211.

Piasecka, B., M. Robinson-Rechavi, et al. (2012). "Correcting for the bias due to expression specificity improves the estimation of constrained evolution of expression between mouse and human." Bioinformatics **28**(14): 1865-1872.

Quackenbush, J. (2001). "Computational analysis of microarray data." Nature reviews. Genetics **2**(6): 418-427.

Sandelin, A. e. a. Systematic in-vivo characterization of active enhancers across the human body.

Studer, R. A. and M. Robinson-Rechavi (2009). "How confident can we be that orthologs are similar, but paralogs differ?" Trends in genetics : TIG **25**(5): 210-216.

Su, A. I., M. P. Cooke, et al. (2002). "Large-scale analysis of the human and mouse transcriptomes." Proc Natl Acad Sci U S A **99**(7): 4465-4470.

Thomas, P. D., V. Wood, et al. (2012). "On the Use of Gene Ontology Annotations to Assess Functional Similarity among Orthologs and Paralogs: A Short Report." PLoS computational biology **8**(2): e1002386.

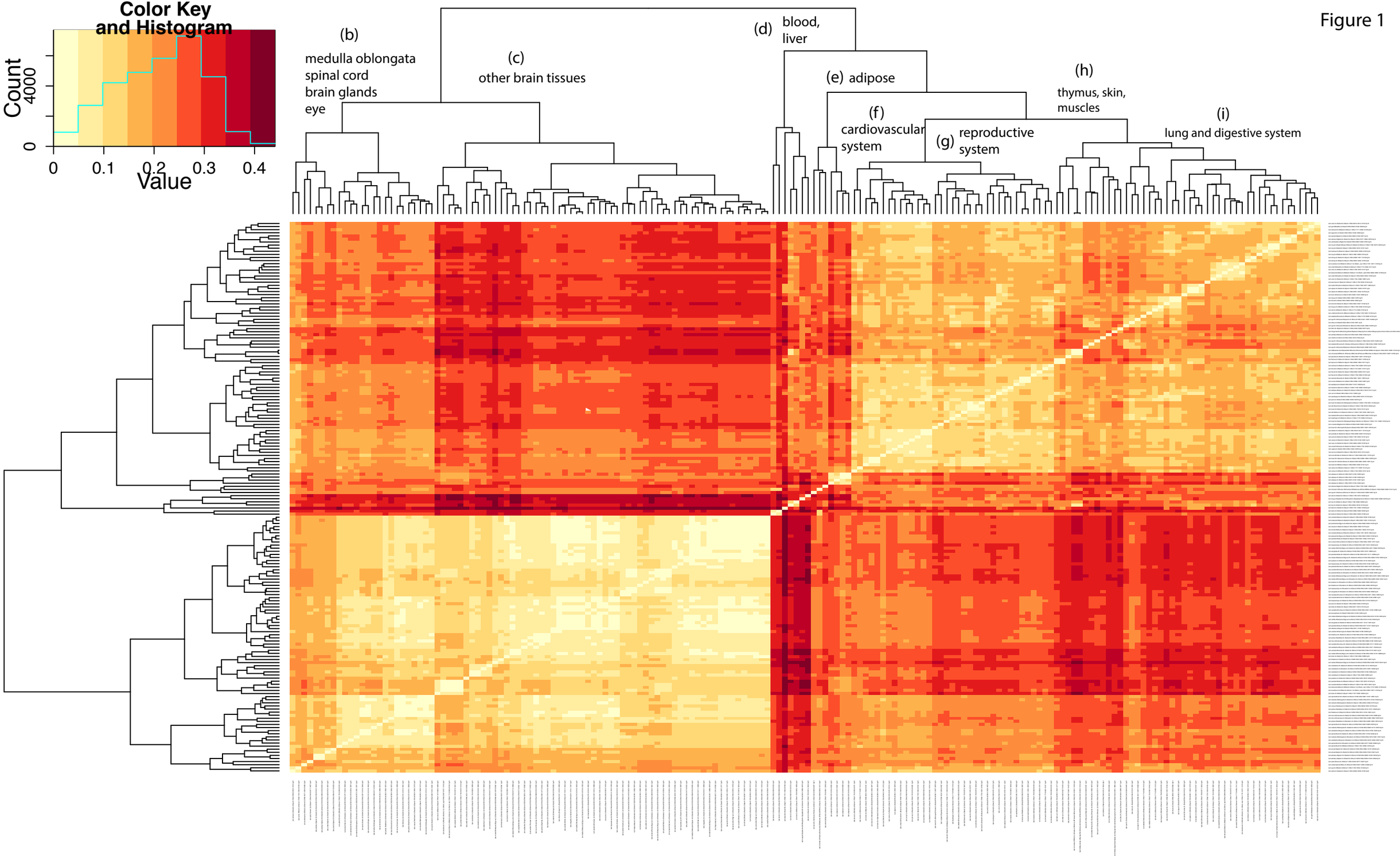
Color Key and Histogram
Count
4000
0
0
0.1
0.2
0.3
0.4
Value
(b)
medulla oblongata
spinal cord
brain glands
eye
(c)
other brain tissues
(d)
blood,
liver
(e) adipose
(f)
cardiovascular
system
(g)
reproductive
system
(h)
thymus, skin,
muscles
(i)
lung and digestive system

Figure 1

Figure 2

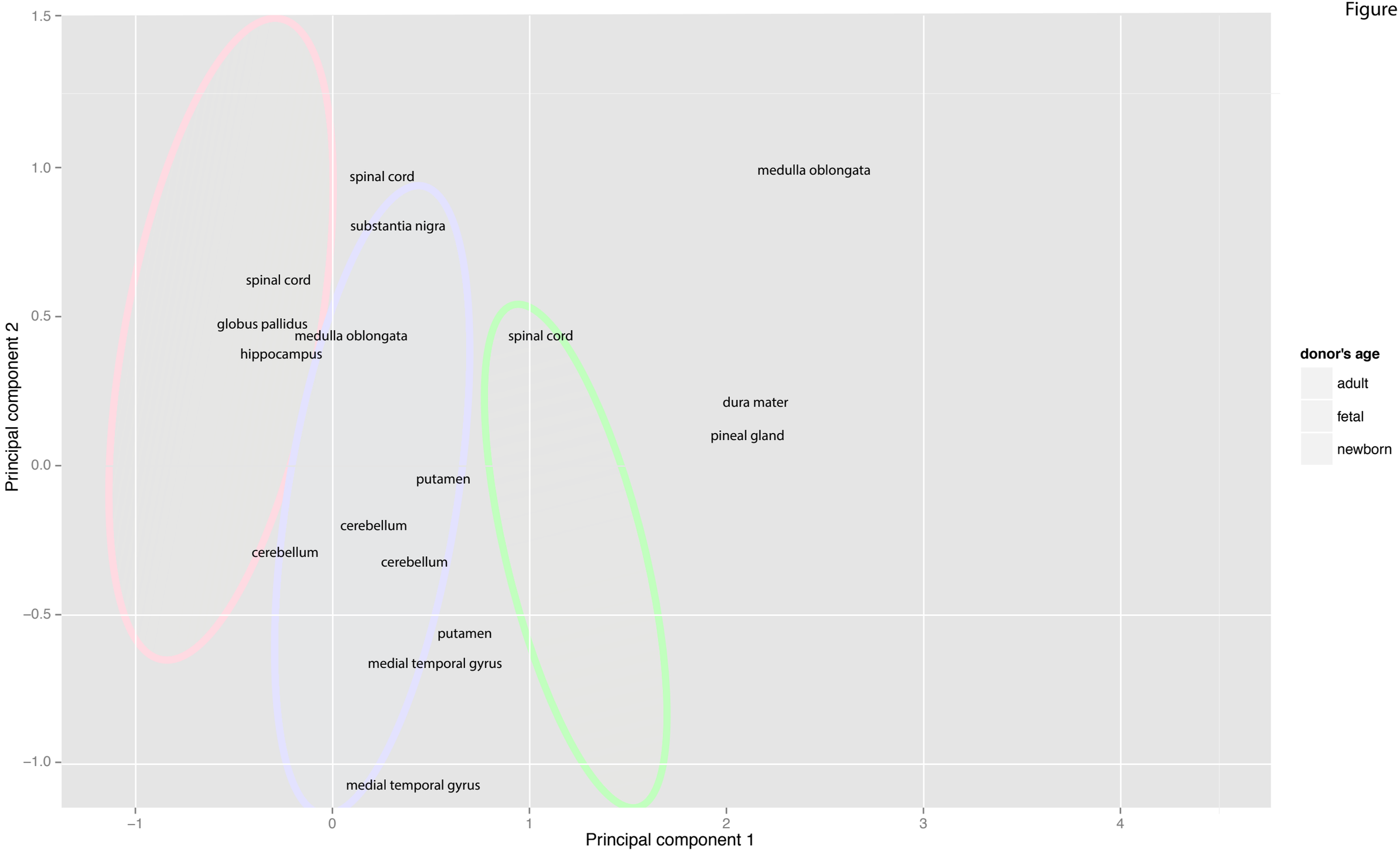
1.5
1.0
0.5
0.0
−0.5
−1.0
Principal component 2
−1
0
1
2
3
4
Principal component 1
spinal cord
substantia nigra
medulla oblongata
spinal cord
globus pallidus
medulla oblongata
hippocampus
spinal cord
dura mater
pineal gland
putamen
cerebellum
cerebellum
cerebellum
putamen
medial temporal gyrus
medial temporal gyrus
donor's age
adult
fetal
newborn

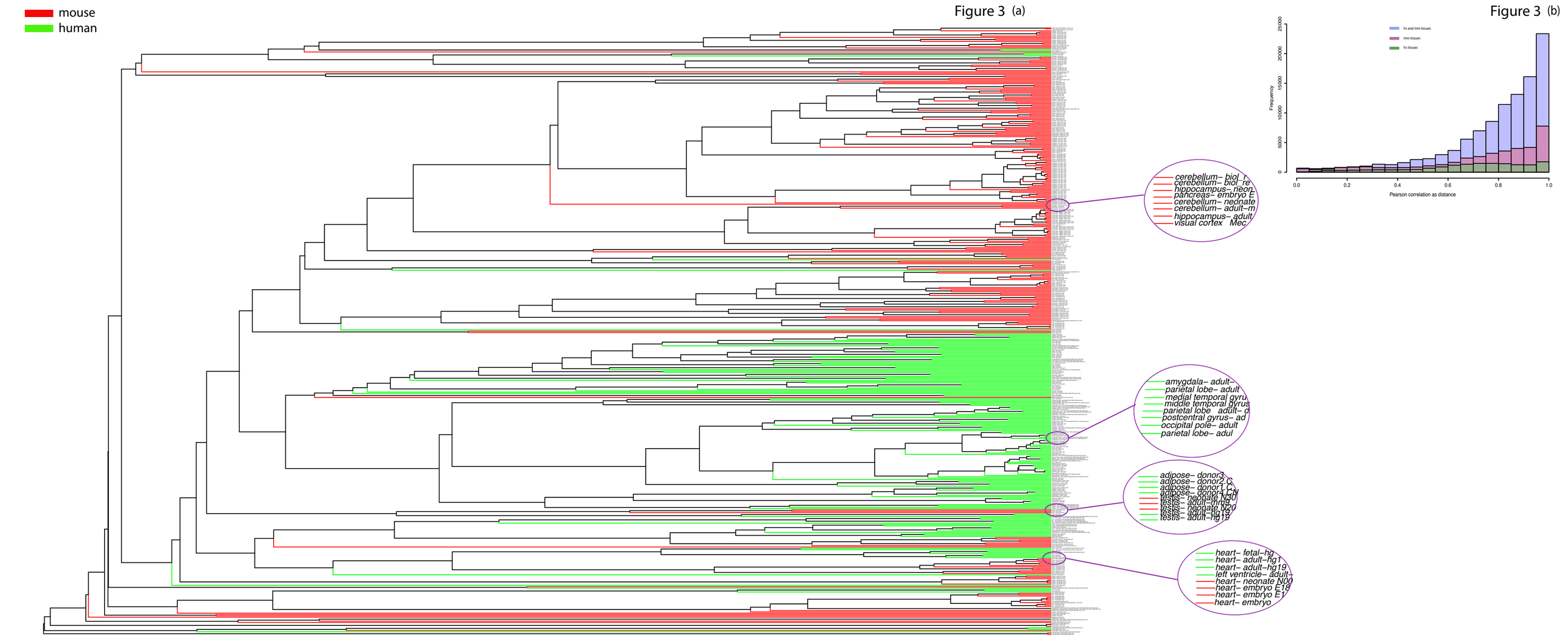
mouse
human
Figure 3 (a)
cerebellum– biol_1
cerebellum– biol_re
hippocampus– neon
pancreas– embryo E
cerebellum– neonate
cerebellum– adult–m
hippocampus– adult
visual cortex Mec
amygdala– adult–
parietal lobe– adult
medial temporal gyru
middle temporal gyrus
parietal lobe adult– d
postcentral gyrus– ad
occipital pole– adult
parietal lobe– adul
adipose– donor3 C
adipose– donor2 C
adipose– donor1 C
adipose– donor4 CN
testis– neonate N30
testis– adult–hrs2
testis– neonate N20
testis– adult–hg19
testis– adult–hg19
heart– fetal–hg
heart– adult–hg1
heart– adult–hg19
left ventricle– adult–
heart– neonate N00
heart– embryo E18
heart– embryo E1
heart– embryo
Figure 3 (b)
hs and mm tissues
mm tissues
hs tissues
Frequency
0
5000
10000
15000
20000
25000
0.0
0.2
0.4
0.6
0.8
1.0
Pearson correlation as distance

Figure 4

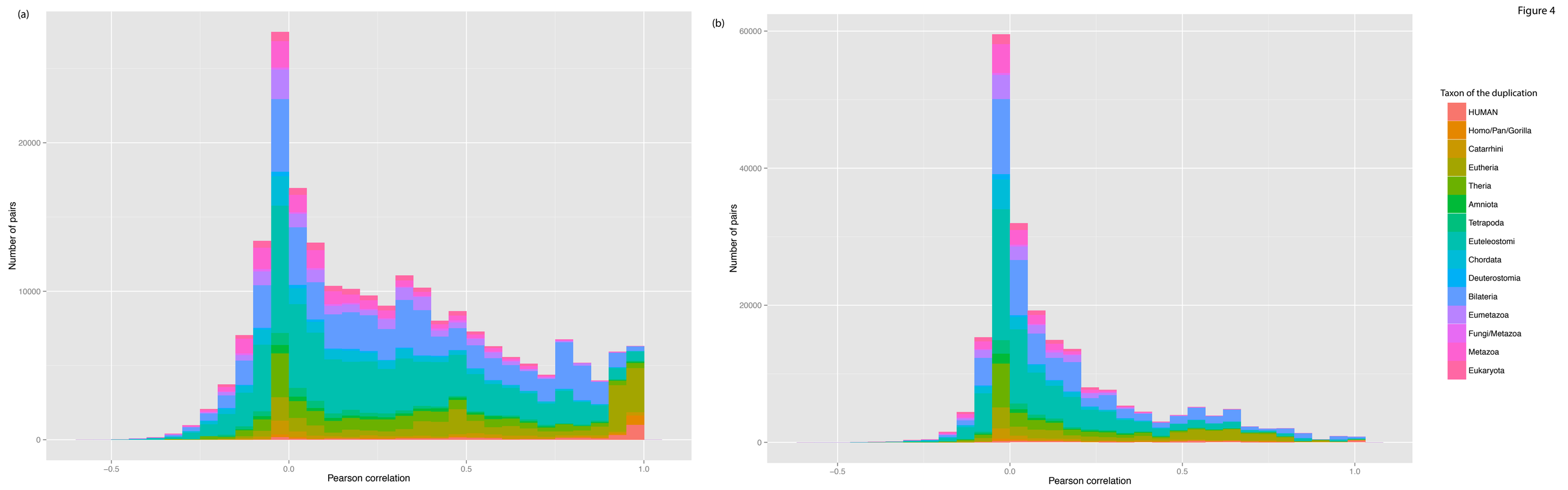
(a)
Number of pairs
20000
10000
0
−0.5
0.0
0.5
1.0
Pearson correlation
(b)
Number of pairs
60000
40000
20000
0
−0.5
0.0
0.5
1.0
Pearson correlation
Taxon of the duplication
HUMAN
Homo/Pan/Gorilla
Catarrhini
Eutheria
Theria
Amniota
Tetrapoda
Euteleostomi
Chordata
Deuterostomia
Bilateria
Eumetazoa
Fungi/Metazoa
Metazoa
Eukaryota

Figure 5

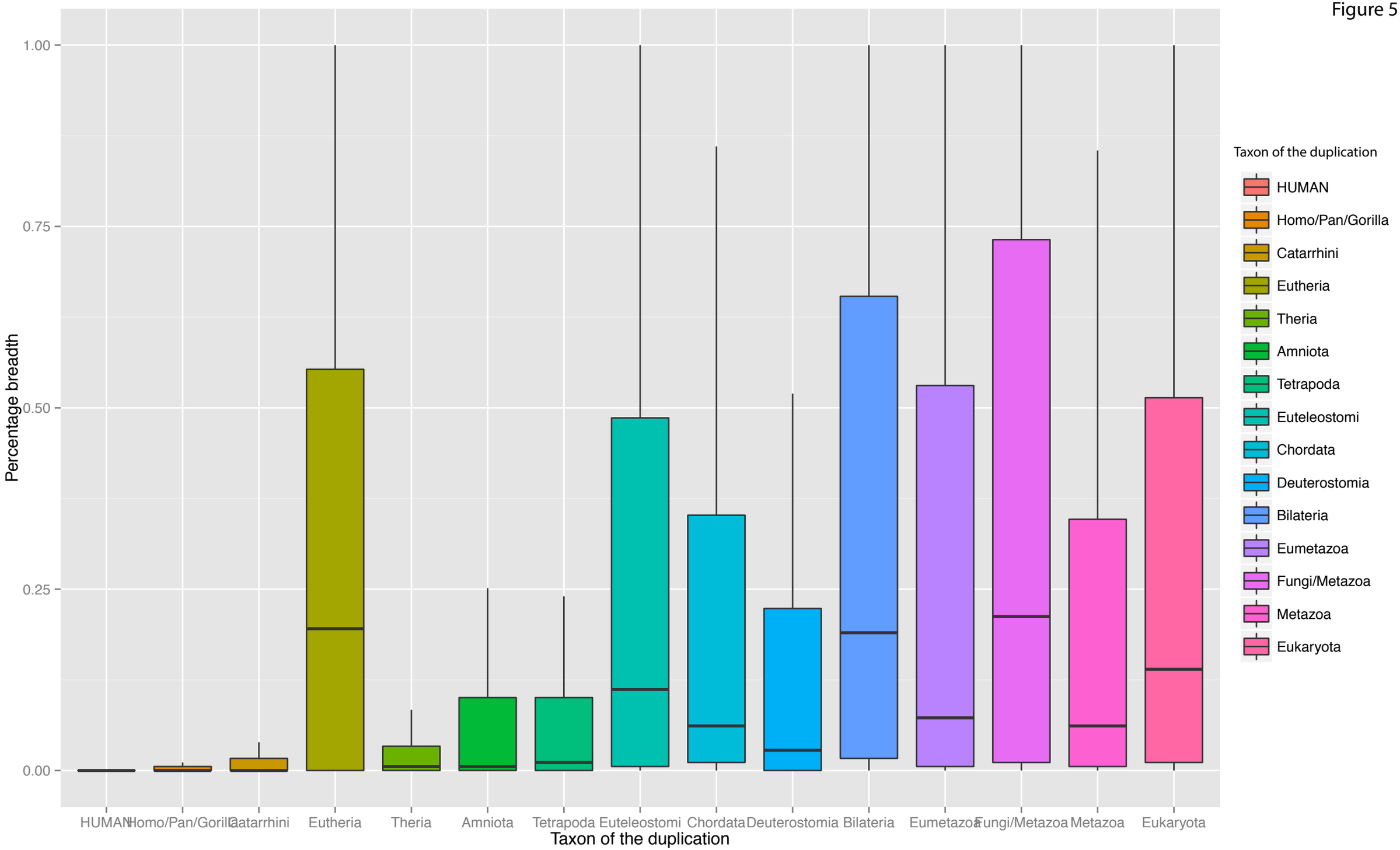
1.00
0.75
0.50
0.25
0.00
Percentage breadth
HUMAN
Homo/Pan/Gorilla
Catarrhini
Eutheria
Theria
Amniota
Tetrapoda
Euteleostomi
Chordata
Deuterostomia
Bilateria
Eumetazoa
Fungi/Metazoa
Metazoa
Eukaryota
Taxon of the duplication
Taxon of the duplication
HUMAN
Homo/Pan/Gorilla
Catarrhini
Eutheria
Theria
Amniota
Tetrapoda
Euteleostomi
Chordata
Deuterostomia
Bilateria
Eumetazoa
Fungi/Metazoa
Metazoa
Eukaryota

Figure 6

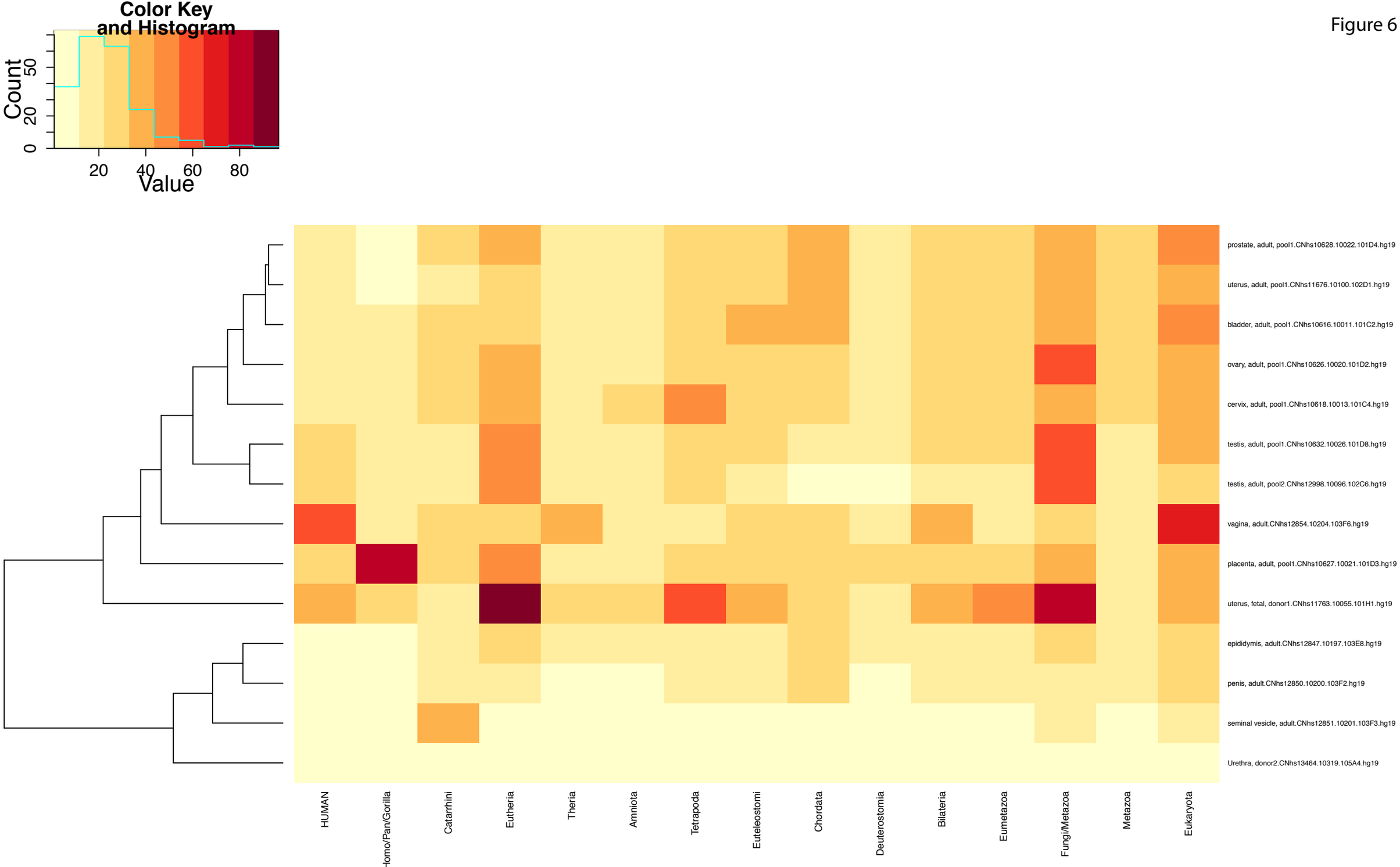
Color Key
and Histogram
Count
0
20
50
20
40
60
80
Value
prostate, adult, pool1.CNhs10628.10022.101D4.hg19
uterus, adult, pool1.CNhs11676.10100.102D1.hg19
bladder, adult, pool1.CNhs10616.10011.101C2.hg19
ovary, adult, pool1.CNhs10626.10020.101D2.hg19
cervix, adult, pool1.CNhs10618.10013.101C4.hg19
testis, adult, pool1.CNhs10632.10026.101D8.hg19
testis, adult, pool2.CNhs12998.10096.102C6.hg19
vagina, adult.CNhs12854.10204.103F6.hg19
placenta, adult, pool1.CNhs10627.10021.101D3.hg19
uterus, fetal, donor1.CNhs11763.10055.101H1.hg19
epididymis, adult.CNhs12847.10197.103E8.hg19
penis, adult.CNhs12850.10200.103F2.hg19
seminal vesicle, adult.CNhs12851.10201.103F3.hg19
Urethra, donor2.CNhs13464.10319.105A4.hg19
HUMAN
Homo/Pan/Gorilla
Catarrhini
Eutheria
Theria
Amniota
Tetrapoda
Euteleostomi
Chordata
Deuterostomia
Bilateria
Eumetazoa
Fungi/Metazoa
Metazoa
Eukaryota

Figure 7 (a)

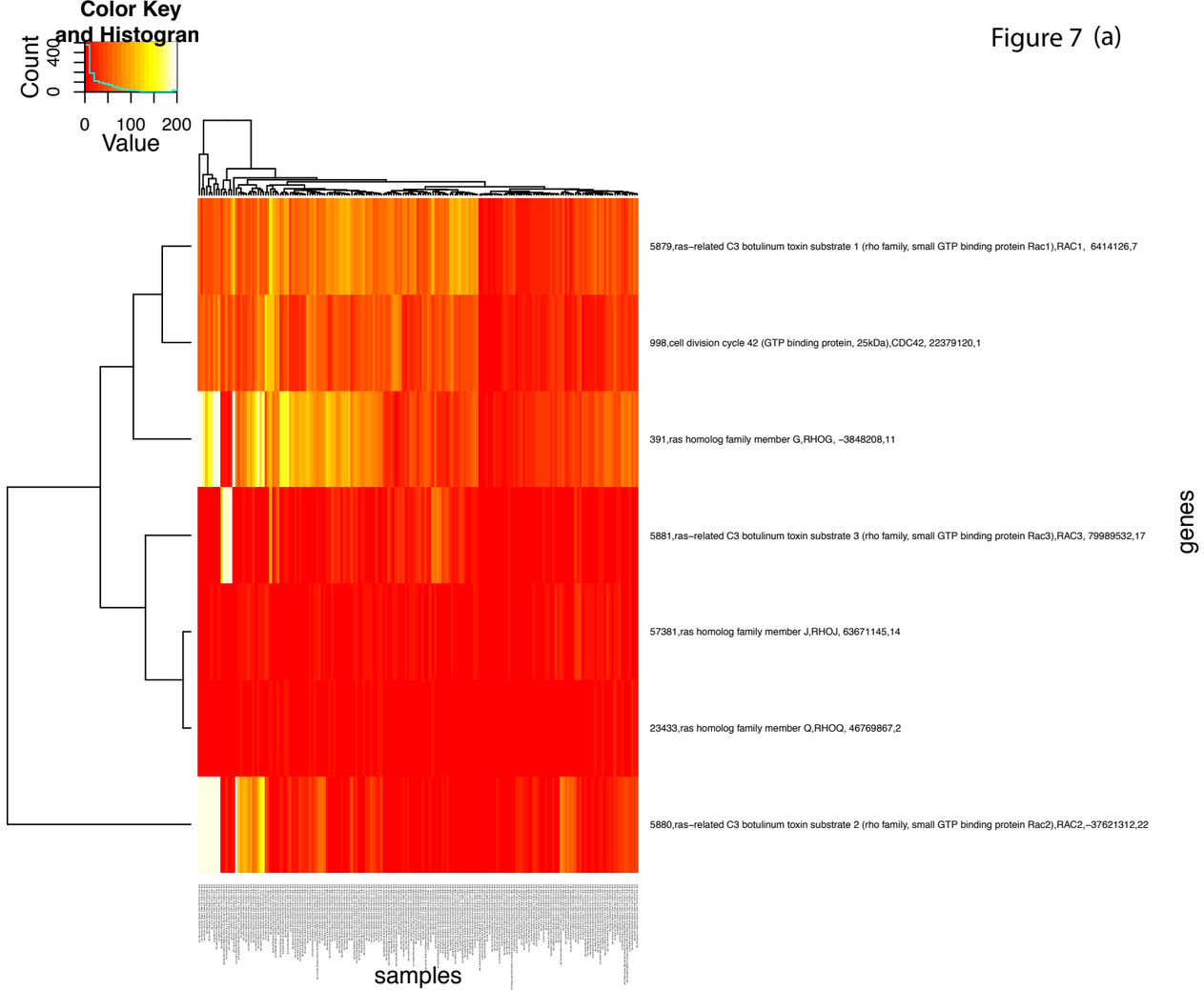

Figure 7 (b)

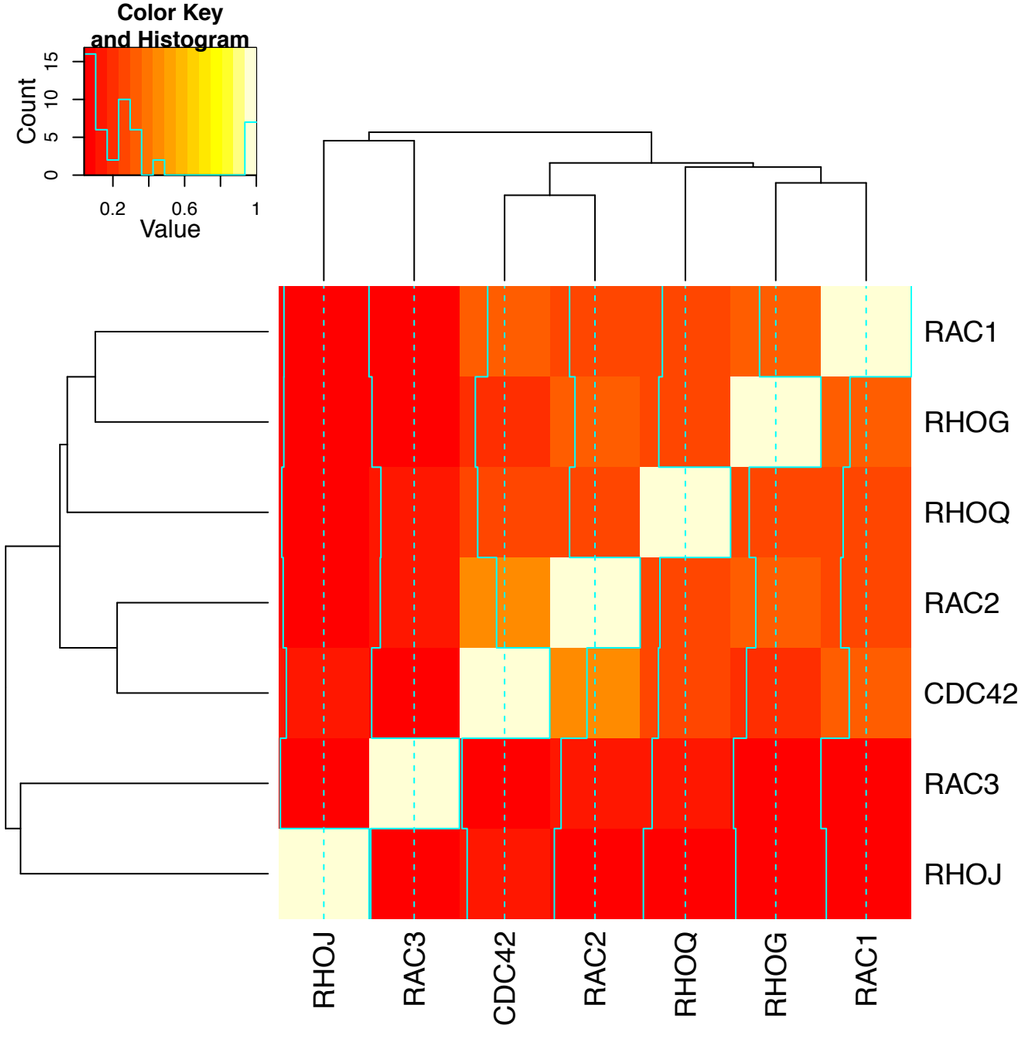

Figure 8


Scale
chr2:
50 kb
179490000
179500000
179510000
179520000
179530000
179540000
179550000
179560000
179570000
179580000
179590000
179600000
FFCP_FANTOM5_web_resource_link
RefSeq Genes
MIR548N
LOC100506866
TTN
H3K27Ac Mark (Often Found Near Active Regulatory Elements) on 7 cell lines from ENCODE
Transcription Factor ChIP-seq from ENCODE
Digital DNaseI Hypersensitivity Clusters from ENCODE
DNase Clusters
Simple Nucleotide Polymorphisms (dbSNP 135) Found in >= 1% of Samples
Common SNPs(135)
Simple Nucleotide Polymorphisms (dbSNP 132) Found in >= 1% of Samples
Common SNPs(132)
Human mRNAs from GenBank
Human mRNAs
Human ESTs That Have Been Spliced
Spliced ESTs
Placental Mammal Basewise Conservation by PhyloP
Mammal Cons
Multiz Alignments of 46 Vertebrates
Rhesus
Mouse
Dog
Elephant
Opossum
Chicken
X_tropicalis
Zebrafish
Repeating Elements by RepeatMasker
RepeatMasker
NHGRI Catalog of Published Genome-Wide Association Studies

Figure 9 (a)

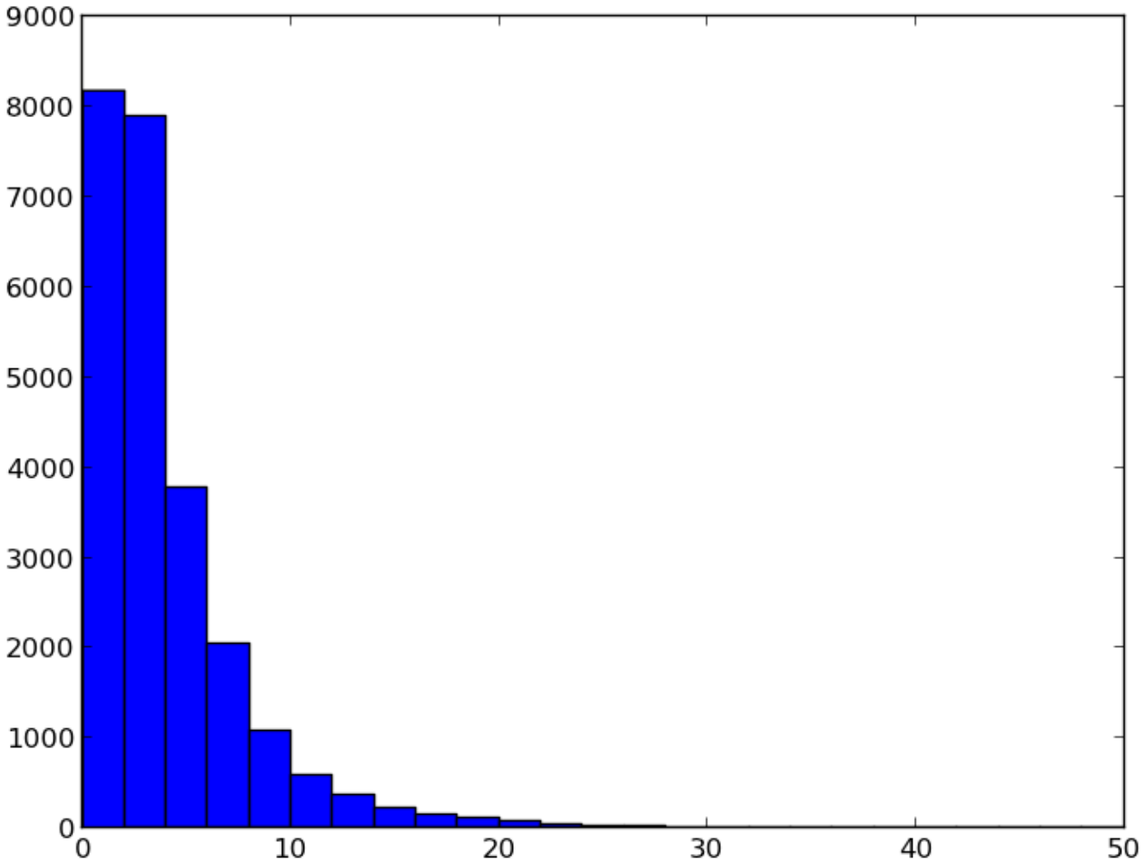

Figure 9 (b)

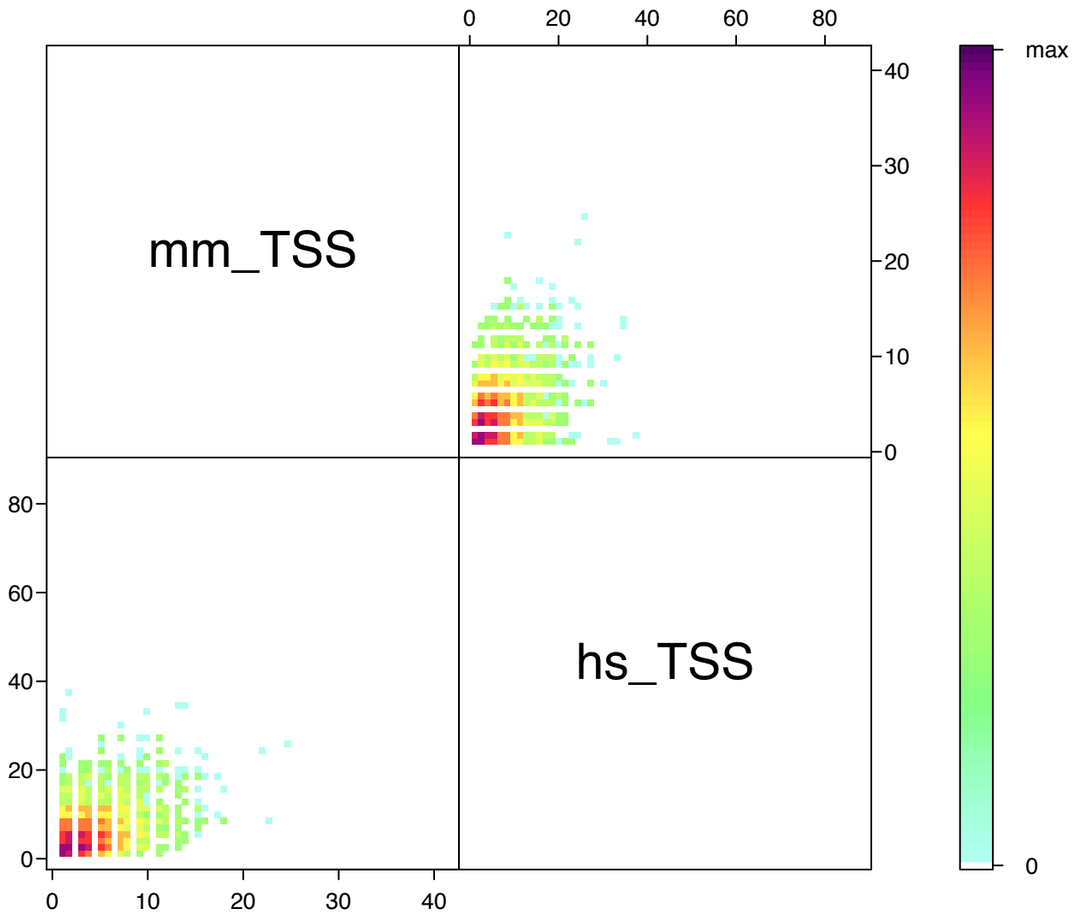

Figure 10

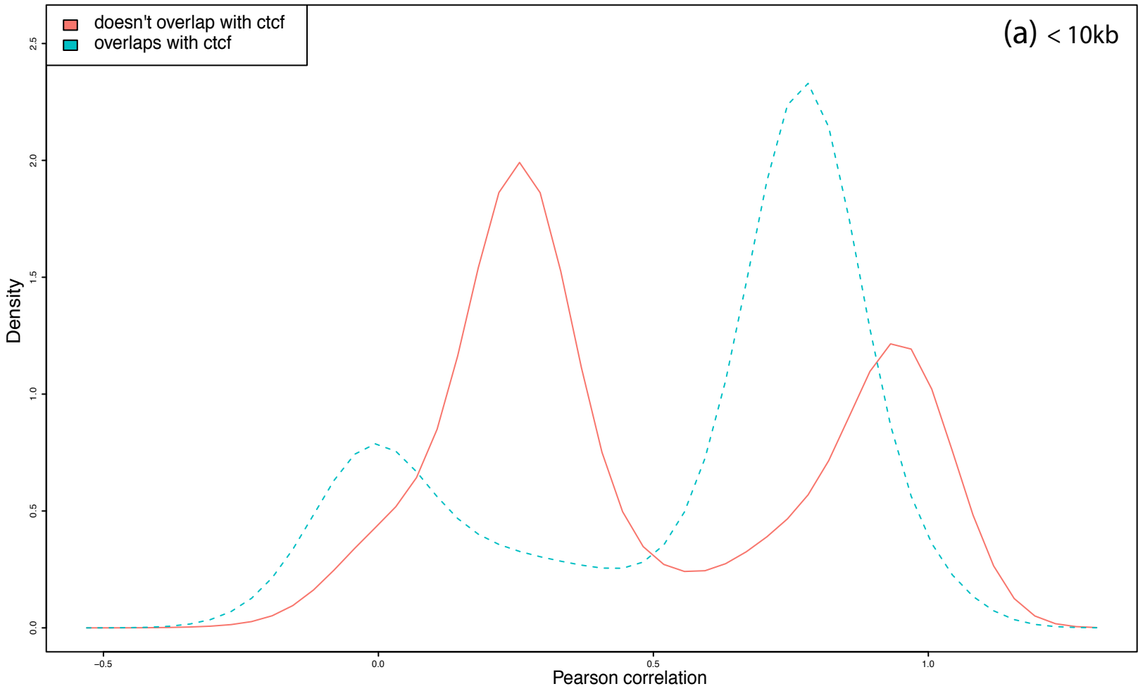
doesn't overlap with ctcf
overlaps with ctcf
(a) < 10kb
Density
Pearson correlation

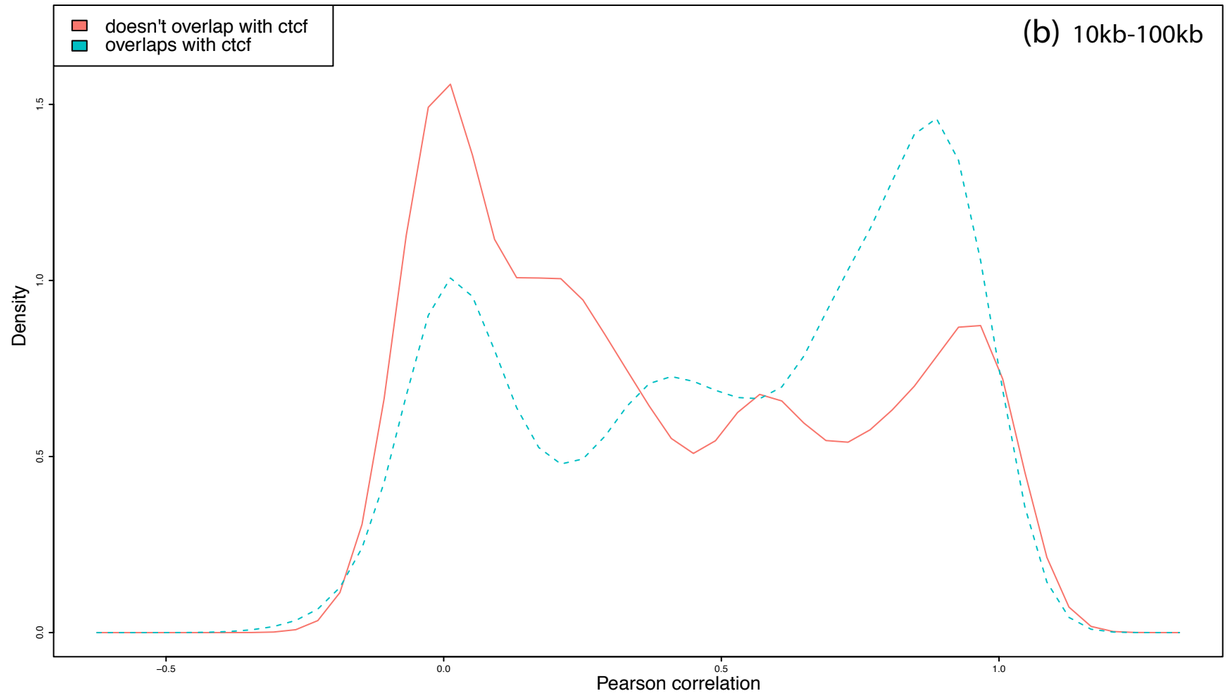
doesn't overlap with ctcf
overlaps with ctcf
(b) 10kb-100kb
Density
Pearson correlation

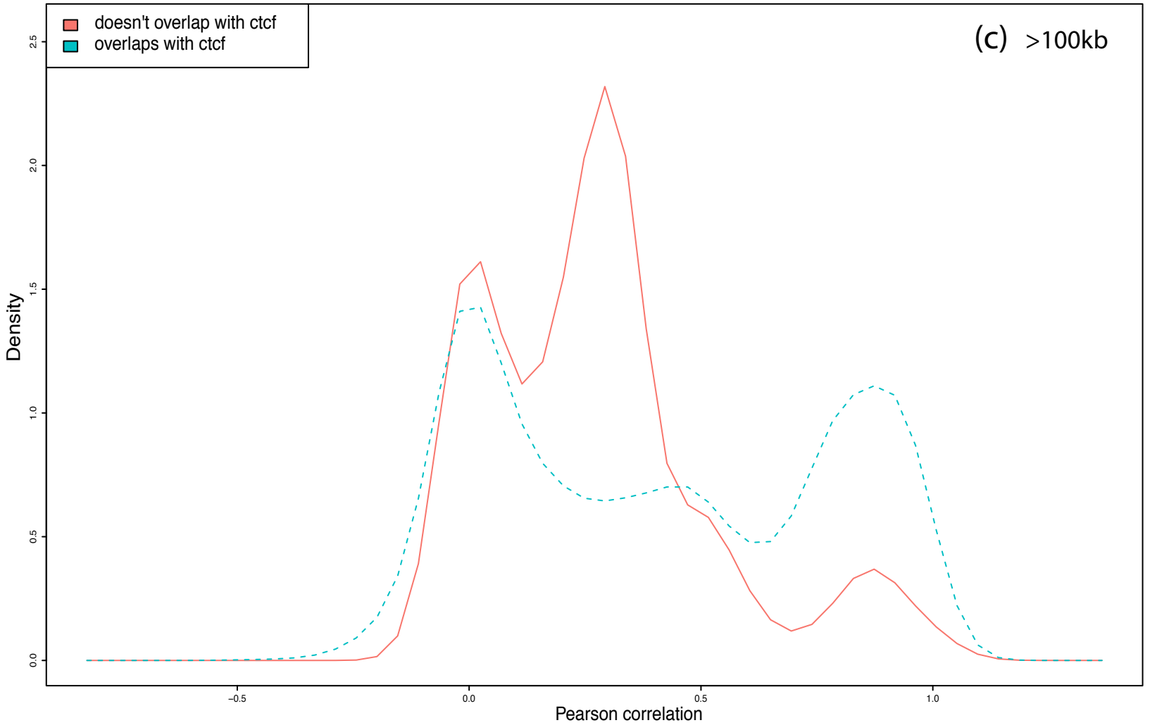
doesn't overlap with ctcf
overlaps with ctcf
(c) >100kb
Density
Pearson correlation

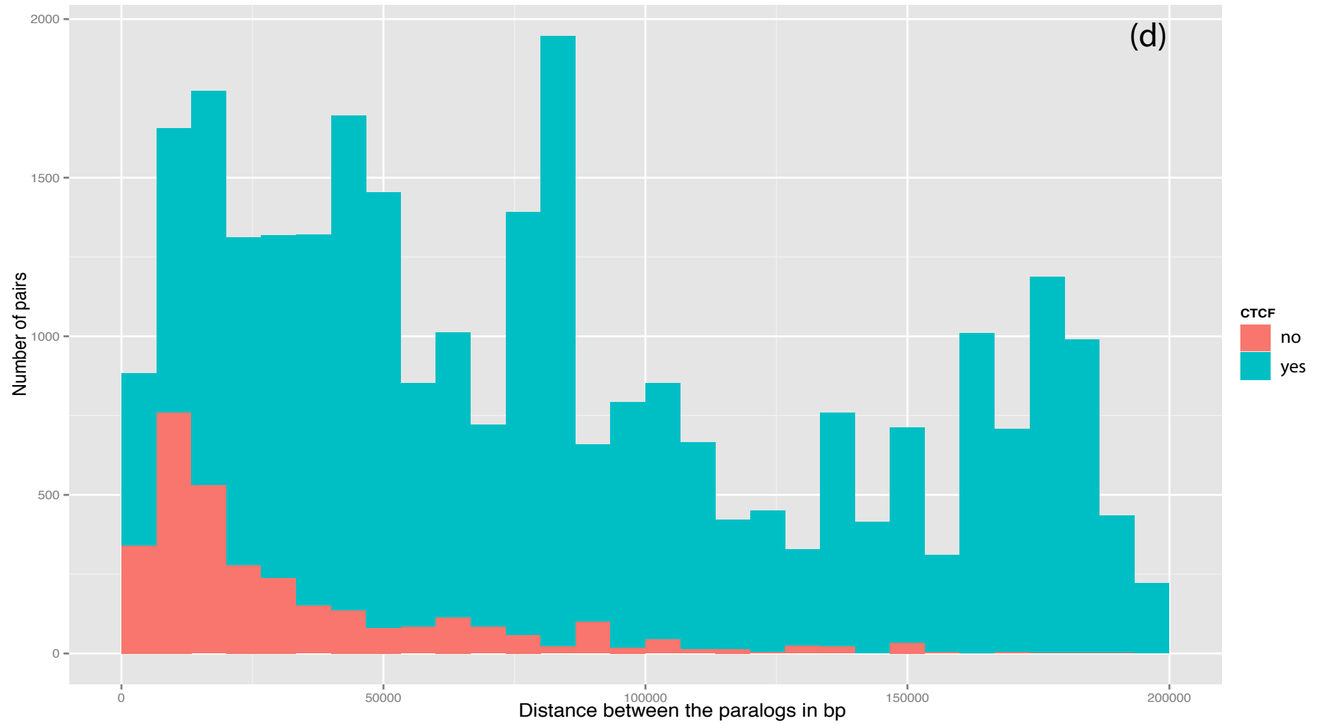
(d)
Number of pairs
Distance between the paralogs in bp
CTCF
no
yes

Figure 11

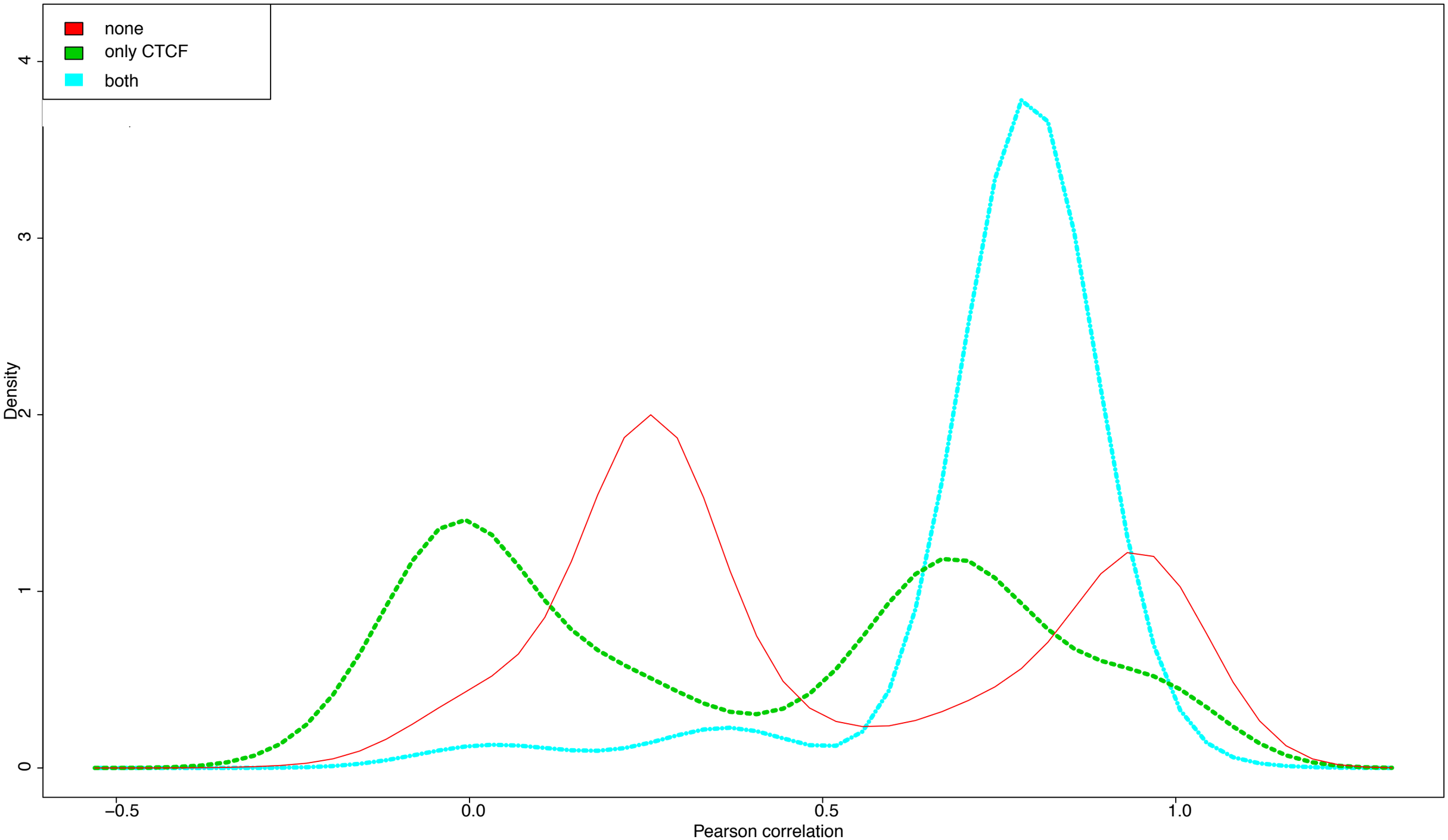
none
only CTCF
both
Density
0
1
2
3
4
−0.5
0.0
0.5
1.0
Pearson correlation

Figure S1 (a)

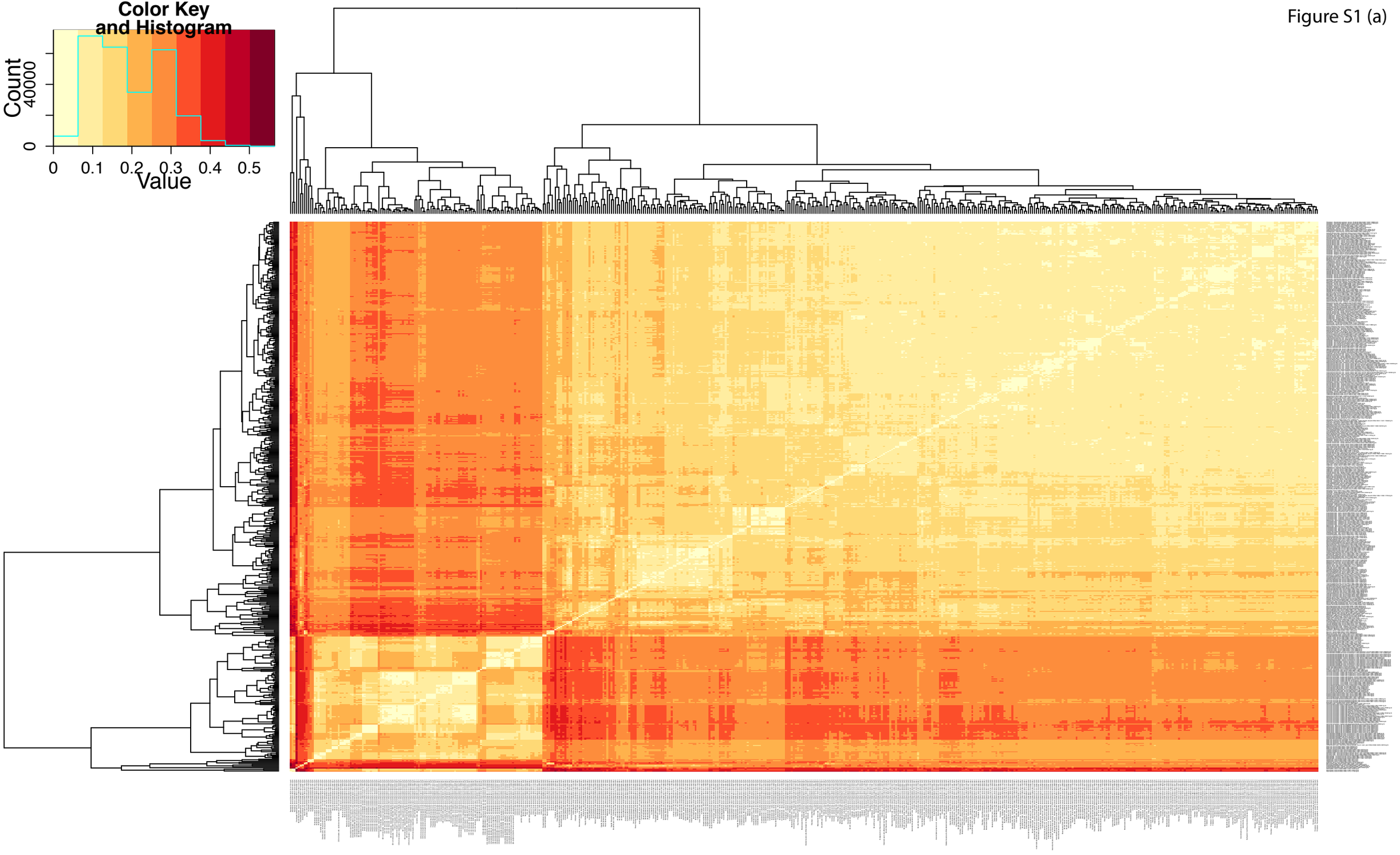

Figure S1 (b)

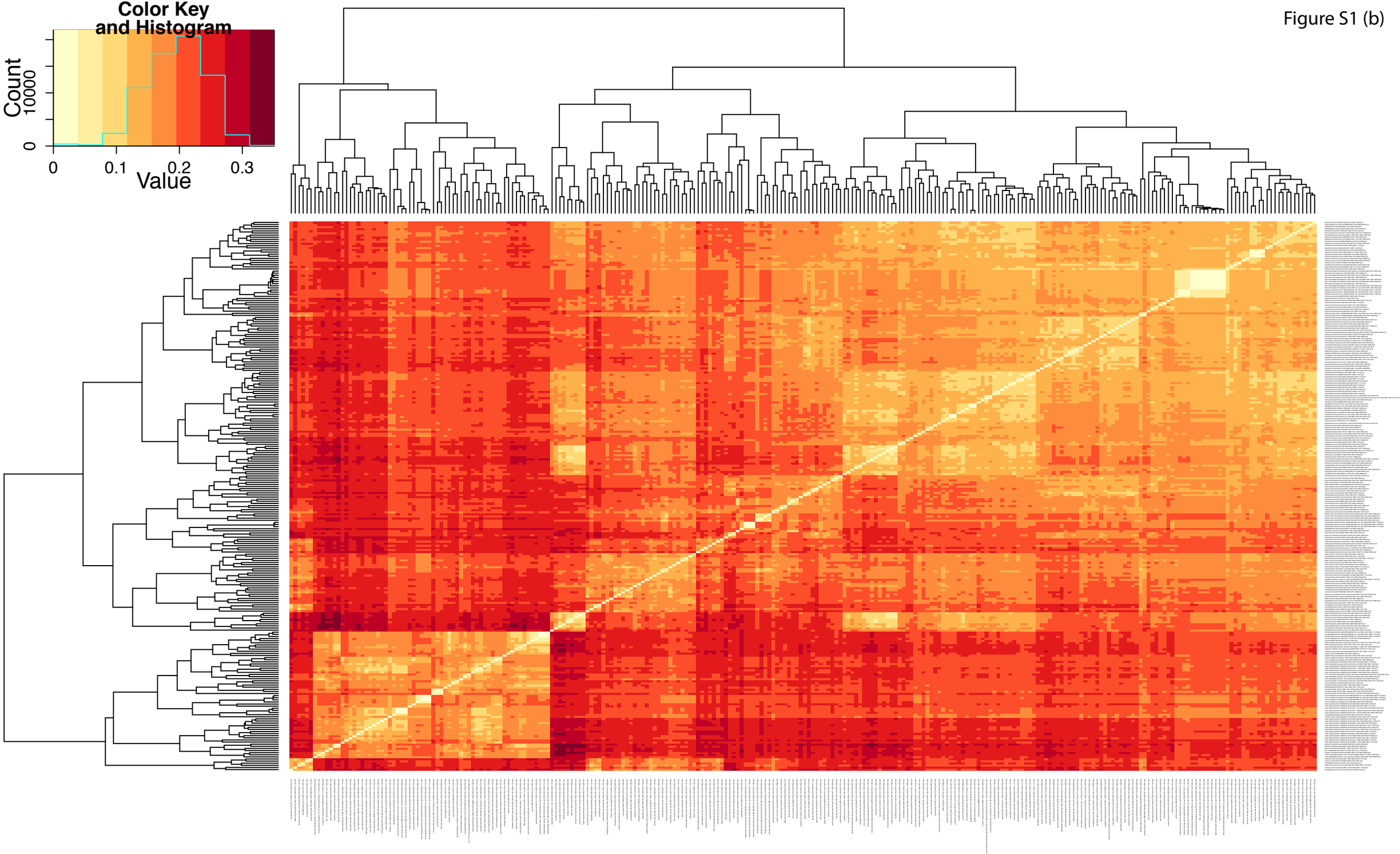

Figure S1 (c)

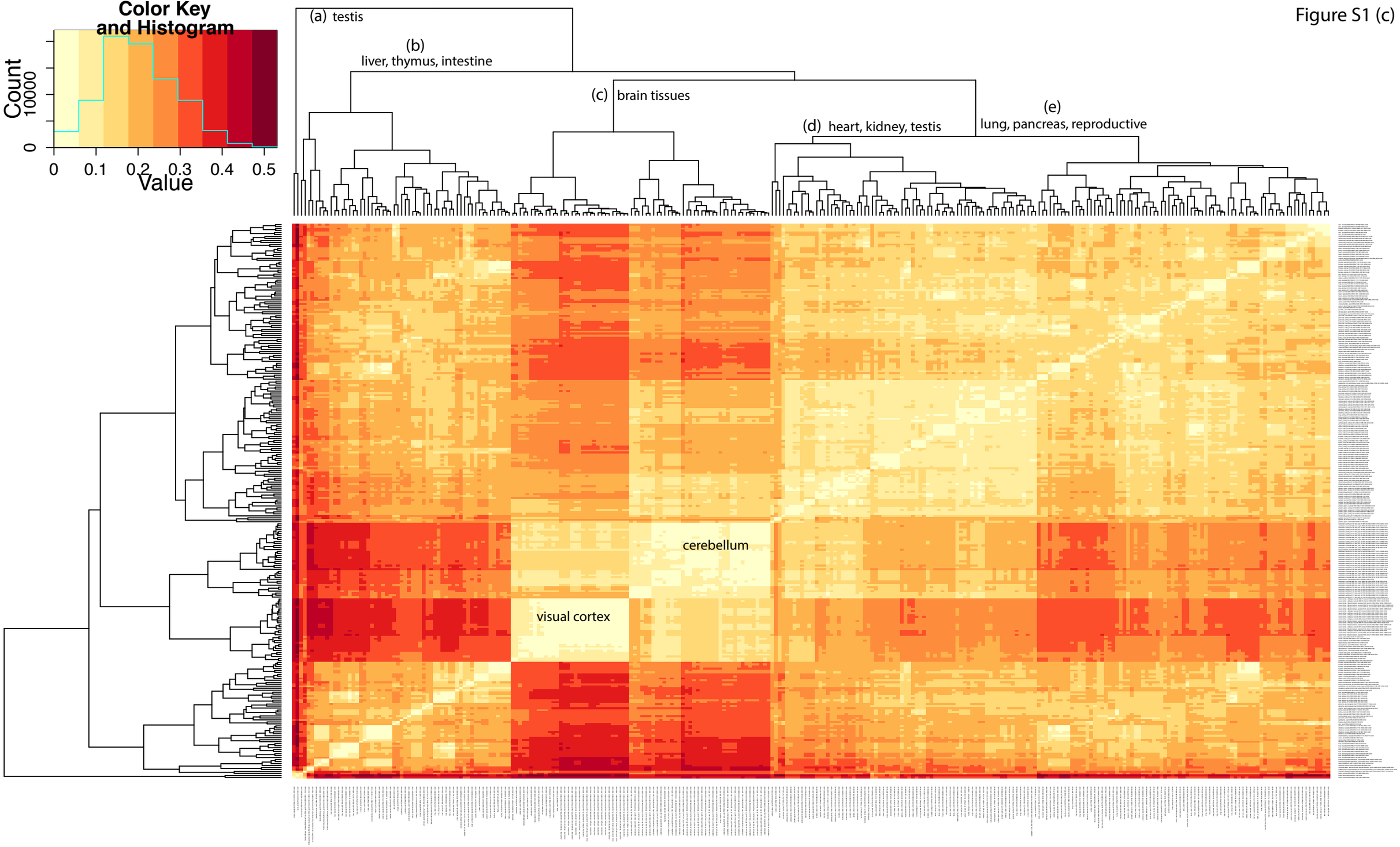
Color Key and Histogram
Count
10000
0
0
0.1
0.2
0.3
0.4
0.5
Value
(a) testis
(b)
liver, thymus, intestine
(c) brain tissues
(d) heart, kidney, testis
(e)
lung, pancreas, reproductive
cerebellum
visual cortex

Figure S1 (d)

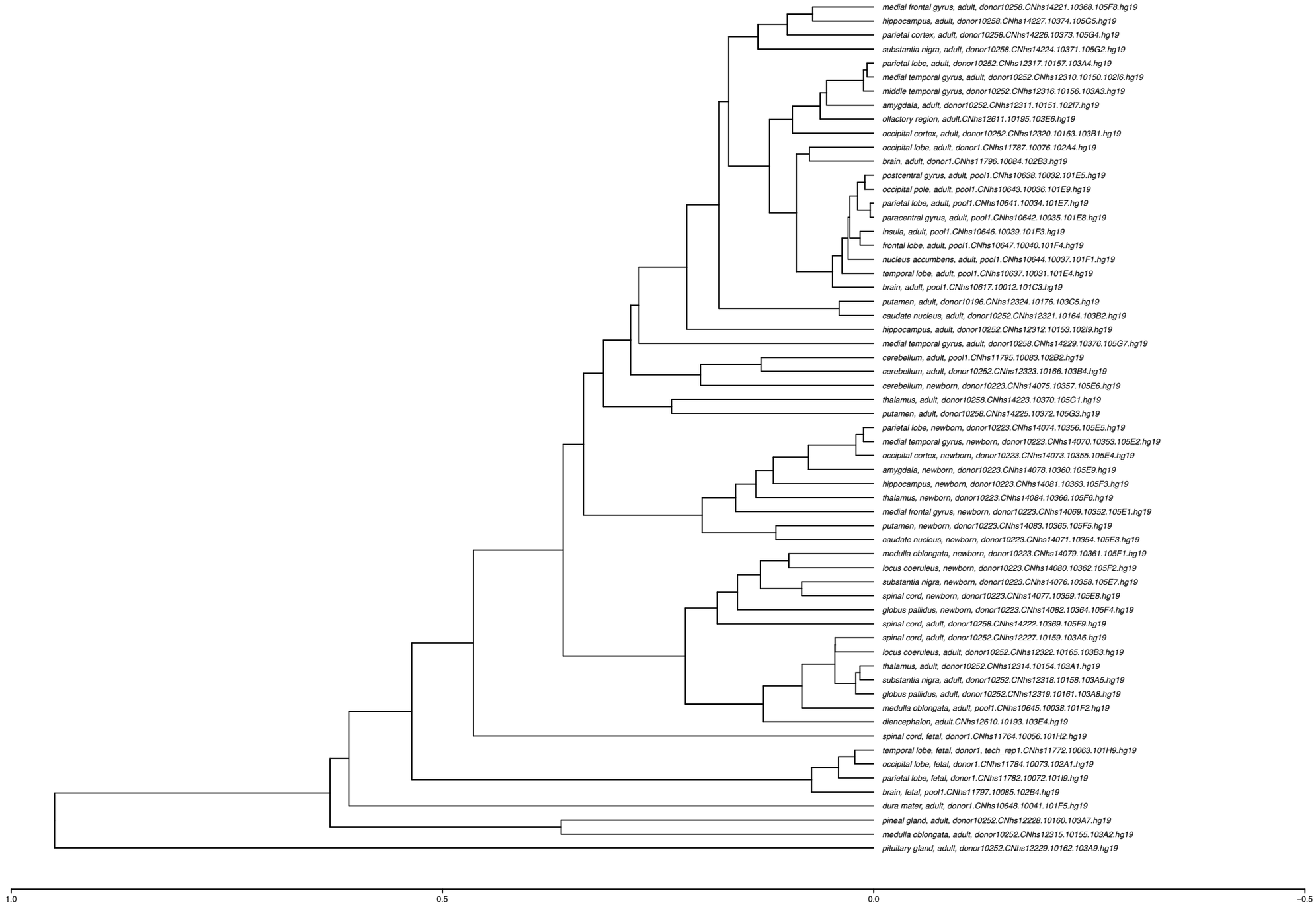
medial frontal gyrus, adult, donor10258.CNhs14221.10368.105F8.hg19
hippocampus, adult, donor10258.CNhs14227.10374.105G5.hg19
parietal cortex, adult, donor10258.CNhs14226.10373.105G4.hg19
substantia nigra, adult, donor10258.CNhs14224.10371.105G2.hg19
parietal lobe, adult, donor10252.CNhs12317.10157.103A4.hg19
medial temporal gyrus, adult, donor10252.CNhs12310.10150.102I6.hg19
middle temporal gyrus, donor10252.CNhs12316.10156.103A3.hg19
amygdala, adult, donor10252.CNhs12311.10151.102I7.hg19
olfactory region, adult.CNhs12611.10195.103E6.hg19
occipital cortex, adult, donor10252.CNhs12320.10163.103B1.hg19
occipital lobe, adult, donor1.CNhs11787.10076.102A4.hg19
brain, adult, donor1.CNhs11796.10084.102B3.hg19
postcentral gyrus, adult, pool1.CNhs10638.10032.101E5.hg19
occipital pole, adult, pool1.CNhs10643.10036.101E9.hg19
parietal lobe, adult, pool1.CNhs10641.10034.101E7.hg19
paracentral gyrus, adult, pool1.CNhs10642.10035.101E8.hg19
insula, adult, pool1.CNhs10646.10039.101F3.hg19
frontal lobe, adult, pool1.CNhs10647.10040.101F4.hg19
nucleus accumbens, adult, pool1.CNhs10644.10037.101F1.hg19
temporal lobe, adult, pool1.CNhs10637.10031.101E4.hg19
brain, adult, pool1.CNhs10617.10012.101C3.hg19
putamen, adult, donor10196.CNhs12324.10176.103C5.hg19
caudate nucleus, adult, donor10252.CNhs12321.10164.103B2.hg19
hippocampus, adult, donor10252.CNhs12312.10153.102I9.hg19
medial temporal gyrus, adult, donor10258.CNhs14229.10376.105G7.hg19
cerebellum, adult, pool1.CNhs11795.10083.102B2.hg19
cerebellum, adult, donor10252.CNhs12323.10166.103B4.hg19
cerebellum, newborn, donor10223.CNhs14075.10357.105E6.hg19
thalamus, adult, donor10258.CNhs14223.10370.105G1.hg19
putamen, adult, donor10258.CNhs14225.10372.105G3.hg19
parietal lobe, newborn, donor10223.CNhs14074.10356.105E5.hg19
medial temporal gyrus, newborn, donor10223.CNhs14070.10353.105E2.hg19
occipital cortex, newborn, donor10223.CNhs14073.10355.105E4.hg19
amygdala, newborn, donor10223.CNhs14078.10360.105E9.hg19
hippocampus, newborn, donor10223.CNhs14081.10363.105F3.hg19
thalamus, newborn, donor10223.CNhs14084.10366.105F6.hg19
medial frontal gyrus, newborn, donor10223.CNhs14069.10352.105E1.hg19
putamen, newborn, donor10223.CNhs14083.10365.105F5.hg19
caudate nucleus, newborn, donor10223.CNhs14071.10354.105E3.hg19
medulla oblongata, newborn, donor10223.CNhs14079.10361.105F1.hg19
locus coeruleus, newborn, donor10223.CNhs14080.10362.105F2.hg19
substantia nigra, newborn, donor10223.CNhs14076.10358.105E7.hg19
spinal cord, newborn, donor10223.CNhs14077.10359.105E8.hg19
globus pallidus, newborn, donor10223.CNhs14082.10364.105F4.hg19
spinal cord, adult, donor10258.CNhs14222.10369.105F9.hg19
spinal cord, adult, donor10252.CNhs12227.10159.103A6.hg19
locus coeruleus, adult, donor10252.CNhs12322.10165.103B3.hg19
thalamus, adult, donor10252.CNhs12314.10154.103A1.hg19
substantia nigra, adult, donor10252.CNhs12318.10158.103A5.hg19
globus pallidus, adult, donor10252.CNhs12319.10161.103A8.hg19
medulla oblongata, adult, pool1.CNhs10645.10038.101F2.hg19
diencephalon, adult.CNhs12610.10193.103E4.hg19
spinal cord, fetal, donor1.CNhs11764.10056.101H2.hg19
temporal lobe, fetal, donor1, tech_rep1.CNhs11772.10063.101H9.hg19
occipital lobe, fetal, donor1.CNhs11784.10073.102A1.hg19
parietal lobe, fetal, donor1.CNhs11782.10072.101I9.hg19
brain, fetal, pool1.CNhs11797.10085.102B4.hg19
dura mater, adult, donor1.CNhs10648.10041.101F5.hg19
pineal gland, adult, donor10252.CNhs12228.10160.103A7.hg19
medulla oblongata, adult, donor10252.CNhs12315.10155.103A2.hg19
pituitary gland, adult, donor10252.CNhs12229.10162.103A9.hg19
1.0
0.5
0.0
−0.5

Figure S1 (e)

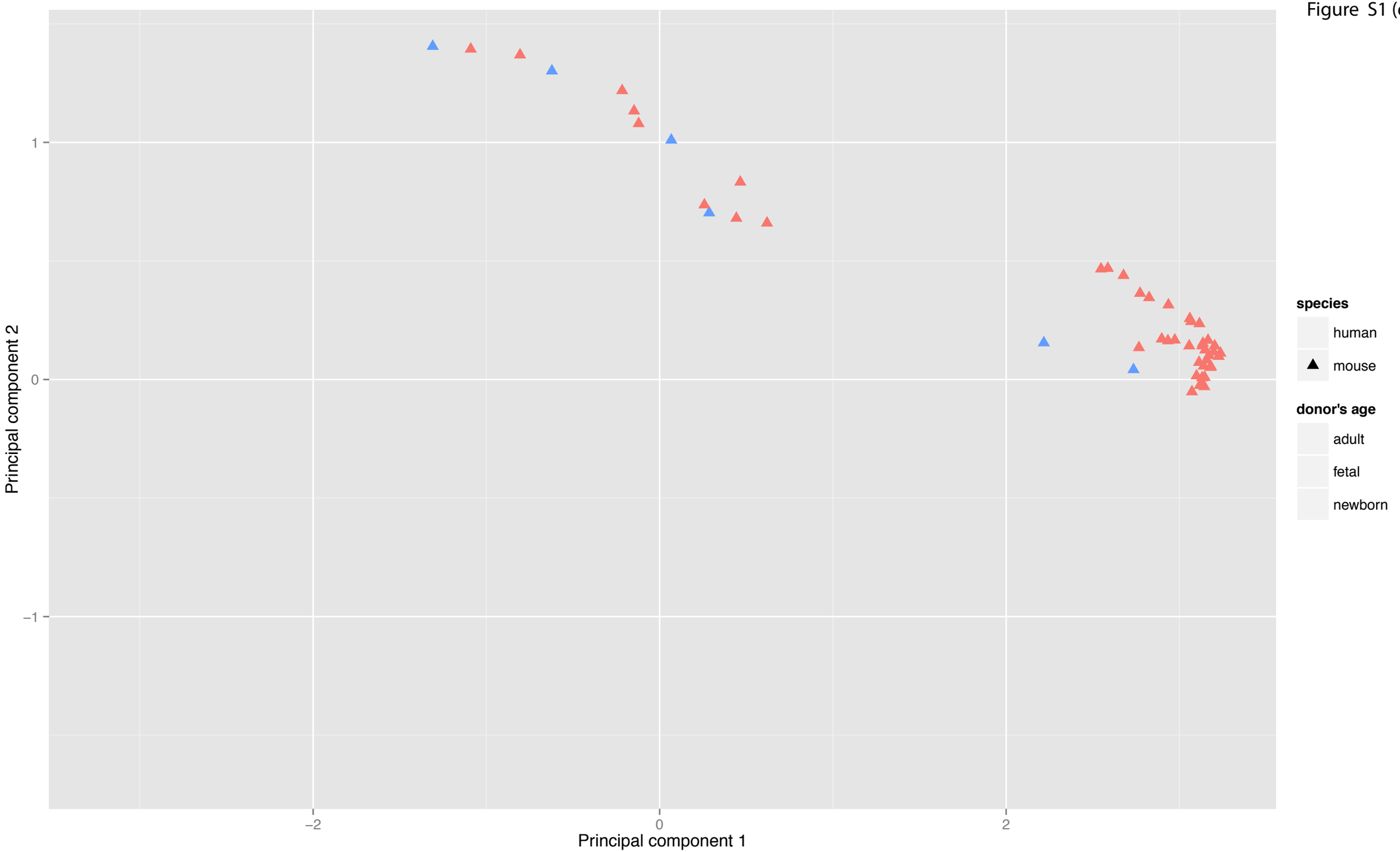
Principal component 2
1
0
−1
−2
0
2
Principal component 1
species
human
mouse
donor's age
adult
fetal
newborn

Figure S2

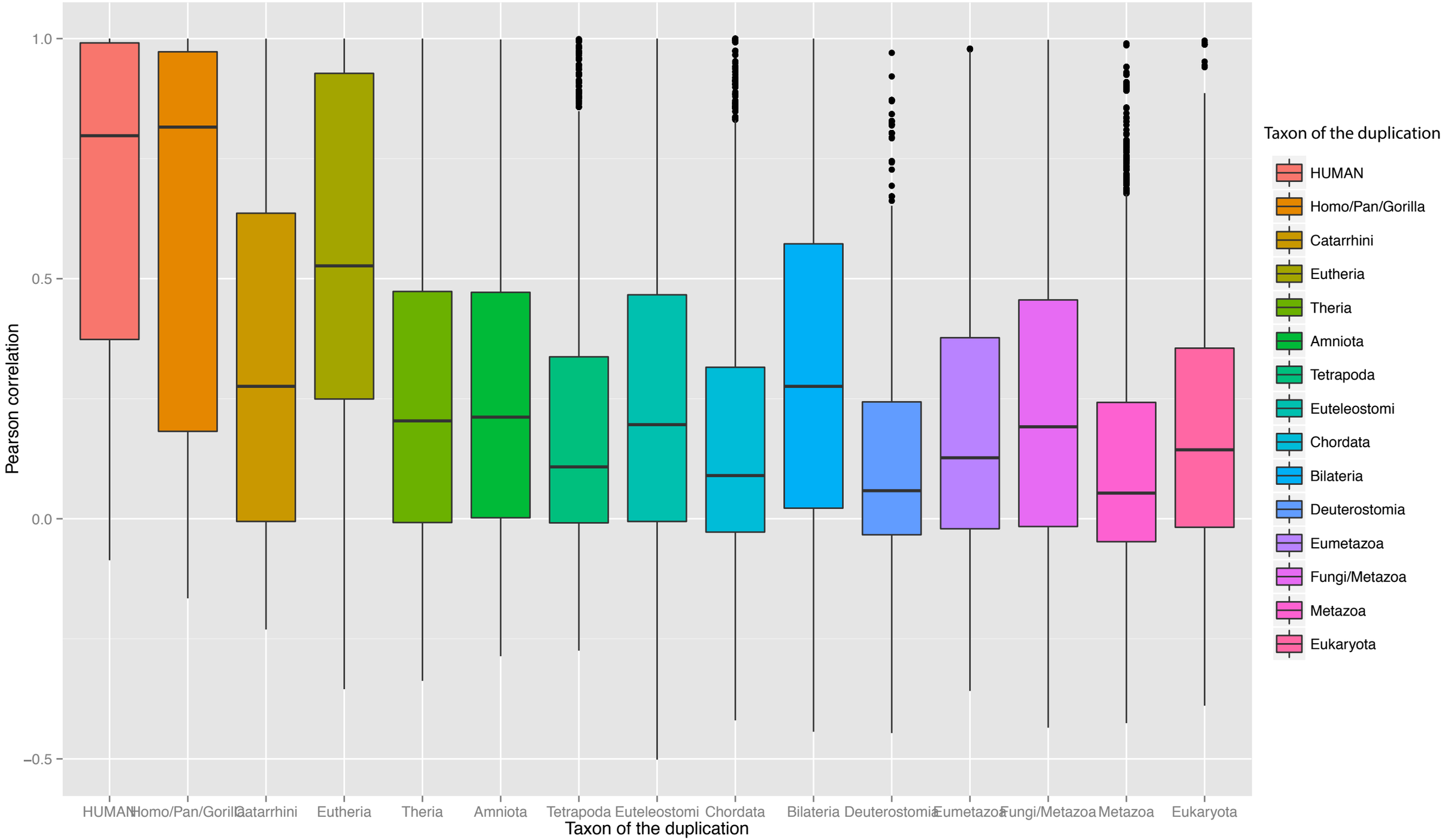
1.0
0.5
0.0
−0.5
Pearson correlation
HUMAN
Homo/Pan/Gorilla
Catarrhini
Eutheria
Theria
Amniota
Tetrapoda
Euteleostomi
Chordata
Bilateria
Deuterostomia
Eumetazoa
Fungi/Metazoa
Metazoa
Eukaryota
Taxon of the duplication
Taxon of the duplication
HUMAN
Homo/Pan/Gorilla
Catarrhini
Eutheria
Theria
Amniota
Tetrapoda
Euteleostomi
Chordata
Bilateria
Deuterostomia
Eumetazoa
Fungi/Metazoa
Metazoa
Eukaryota

Figure S3

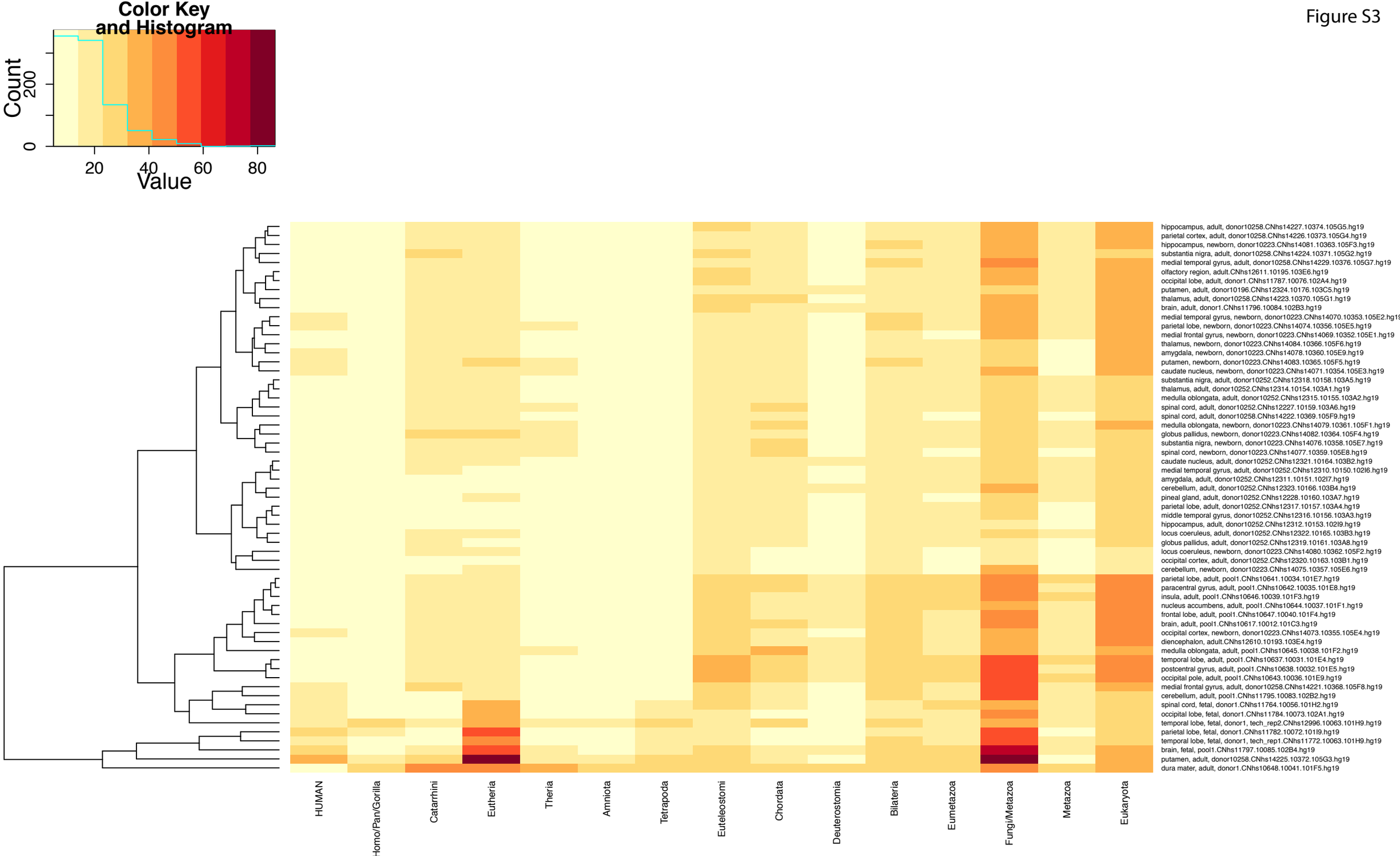
Color Key
and Histogram
Count
0
200
20
40
60
80
Value
hippocampus, adult, donor10258.CNhs14227.10374.105G5.hg19
parietal cortex, adult, donor10258.CNhs14226.10373.105G4.hg19
hippocampus, newborn, donor10223.CNhs14081.10363.105F3.hg19
substantia nigra, adult, donor10258.CNhs14224.10371.105G2.hg19
medial temporal gyrus, adult, donor10258.CNhs14229.10376.105G7.hg19
olfactory region, adult.CNhs12611.10195.103E6.hg19
occipital lobe, adult, donor1.CNhs11787.10076.102A4.hg19
putamen, adult, donor10196.CNhs12324.10176.103C5.hg19
thalamus, adult, donor10258.CNhs14223.10370.105G1.hg19
brain, adult, donor1.CNhs11796.10084.102B3.hg19
medial temporal gyrus, newborn, donor10223.CNhs14070.10353.105E2.hg19
parietal lobe, newborn, donor10223.CNhs14074.10356.105E5.hg19
medial frontal gyrus, newborn, donor10223.CNhs14069.10352.105E1.hg19
thalamus, newborn, donor10223.CNhs14084.10366.105F6.hg19
amygdala, newborn, donor10223.CNhs14078.10360.105E9.hg19
putamen, newborn, donor10223.CNhs14083.10365.105F5.hg19
caudate nucleus, newborn, donor10223.CNhs14071.10354.105E3.hg19
substantia nigra, adult, donor10252.CNhs12318.10158.103A5.hg19
thalamus, adult, donor10252.CNhs12314.10154.103A1.hg19
medulla oblongata, adult, donor10252.CNhs12315.10155.103A2.hg19
spinal cord, adult, donor10252.CNhs12227.10159.103A6.hg19
spinal cord, adult, donor10258.CNhs14222.10369.105F9.hg19
medulla oblongata, newborn, donor10223.CNhs14079.10361.105F1.hg19
globus pallidus, newborn, donor10223.CNhs14082.10364.105F4.hg19
substantia nigra, newborn, donor10223.CNhs14076.10358.105E7.hg19
spinal cord, newborn, donor10223.CNhs14077.10359.105E8.hg19
caudate nucleus, adult, donor10252.CNhs12321.10164.103B2.hg19
medial temporal gyrus, adult, donor10252.CNhs12310.10150.102I6.hg19
amygdala, adult, donor10252.CNhs12311.10151.102I7.hg19
cerebellum, adult, donor10252.CNhs12323.10166.103B4.hg19
pineal gland, adult, donor10252.CNhs12228.10160.103A7.hg19
parietal lobe, adult, donor10252.CNhs12317.10157.103A4.hg19
middle temporal gyrus, donor10252.CNhs12316.10156.103A3.hg19
hippocampus, adult, donor10252.CNhs12312.10153.102I9.hg19
locus coeruleus, adult, donor10252.CNhs12322.10165.103B3.hg19
globus pallidus, adult, donor10252.CNhs12319.10161.103A8.hg19
locus coeruleus, newborn, donor10223.CNhs14080.10362.105F2.hg19
occipital cortex, adult, donor10252.CNhs12320.10163.103B1.hg19
cerebellum, newborn, donor10223.CNhs14075.10357.105E6.hg19
parietal lobe, adult, pool1.CNhs10641.10034.101E7.hg19
paracentral gyrus, adult, pool1.CNhs10642.10035.101E8.hg19
insula, adult, pool1.CNhs10646.10039.101F3.hg19
nucleus accumbens, adult, pool1.CNhs10644.10037.101F1.hg19
frontal lobe, adult, pool1.CNhs10647.10040.101F4.hg19
brain, adult, pool1.CNhs10617.10012.101C3.hg19
occipital cortex, newborn, donor10223.CNhs14073.10355.105E4.hg19
diencephalon, adult.CNhs12610.10193.103E4.hg19
medulla oblongata, adult, pool1.CNhs10645.10038.101F2.hg19
temporal lobe, adult, pool1.CNhs10637.10031.101E4.hg19
postcentral gyrus, adult, pool1.CNhs10638.10032.101E5.hg19
occipital pole, adult, pool1.CNhs10643.10036.101E9.hg19
medial frontal gyrus, adult, donor10258.CNhs14221.10368.105F8.hg19
cerebellum, adult, pool1.CNhs11795.10083.102B2.hg19
spinal cord, fetal, donor1.CNhs11764.10056.101H2.hg19
occipital lobe, fetal, donor1.CNhs11784.10073.102A1.hg19
temporal lobe, fetal, donor1, tech_rep2.CNhs12996.10063.101H9.hg19
parietal lobe, fetal, donor1.CNhs11782.10072.101I9.hg19
temporal lobe, fetal, donor1, tech_rep1.CNhs11772.10063.101H9.hg19
brain, fetal, pool1.CNhs11797.10085.102B4.hg19
putamen, adult, donor10258.CNhs14225.10372.105G3.hg19
dura mater, adult, donor1.CNhs10648.10041.101F5.hg19
HUMAN
Homo/Pan/Gorilla
Catarrhini
Eutheria
Theria
Amniota
Tetrapoda
Euteleostomi
Chordata
Deuterostomia
Bilateria
Eumetazoa
Fungi/Metazoa
Metazoa
Eukaryota

Figure S4

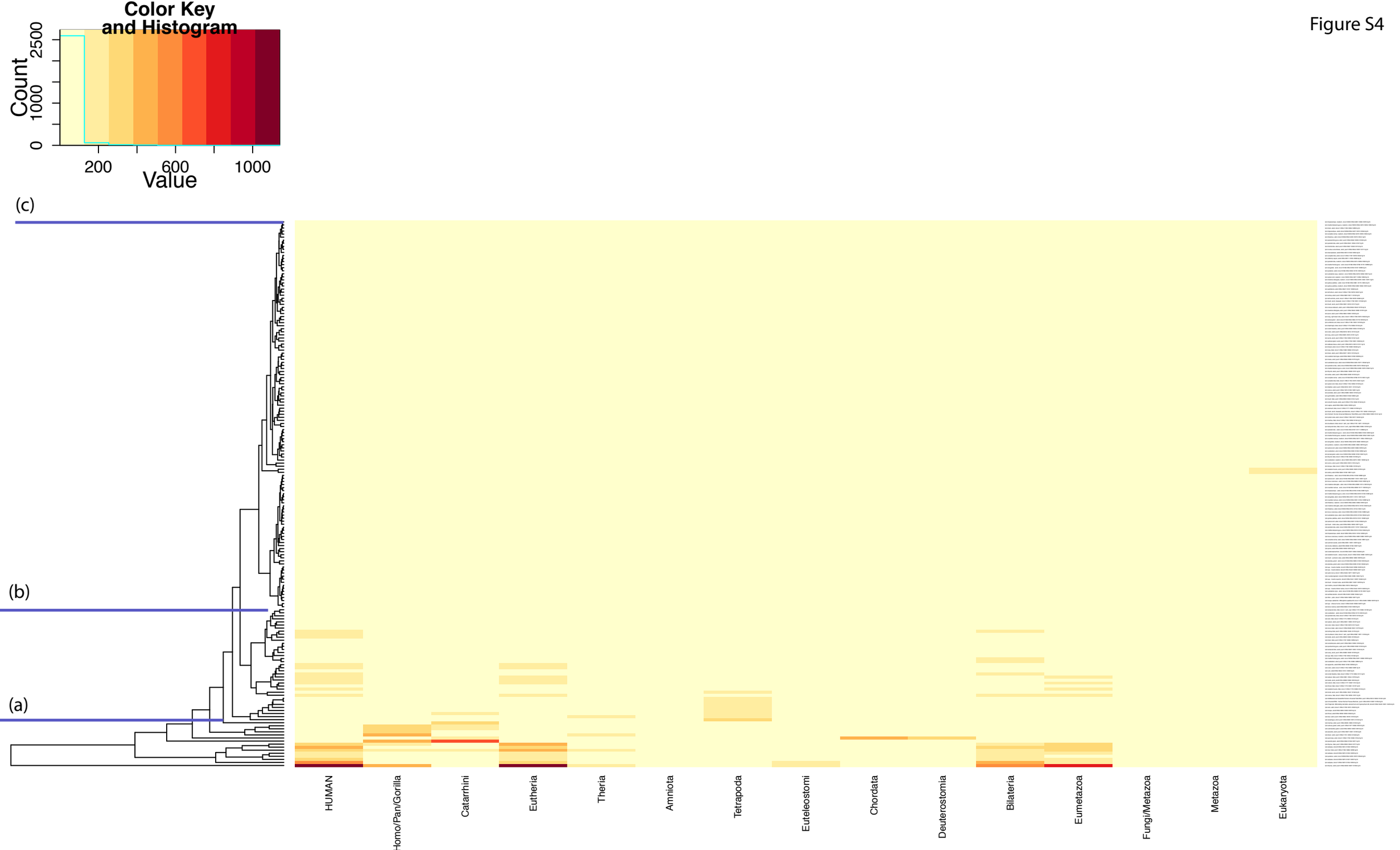
Color Key
and Histogram
Count
0
1000
2500
200
600
1000
Value
(c)
(b)
(a)
HUMAN
Homo/Pan/Gorilla
Catarrhini
Eutheria
Theria
Amniota
Tetrapoda
Euteleostomi
Chordata
Deuterostomia
Bilateria
Eumetazoa
Fungi/Metazoa
Metazoa
Eukaryota

Figure S5

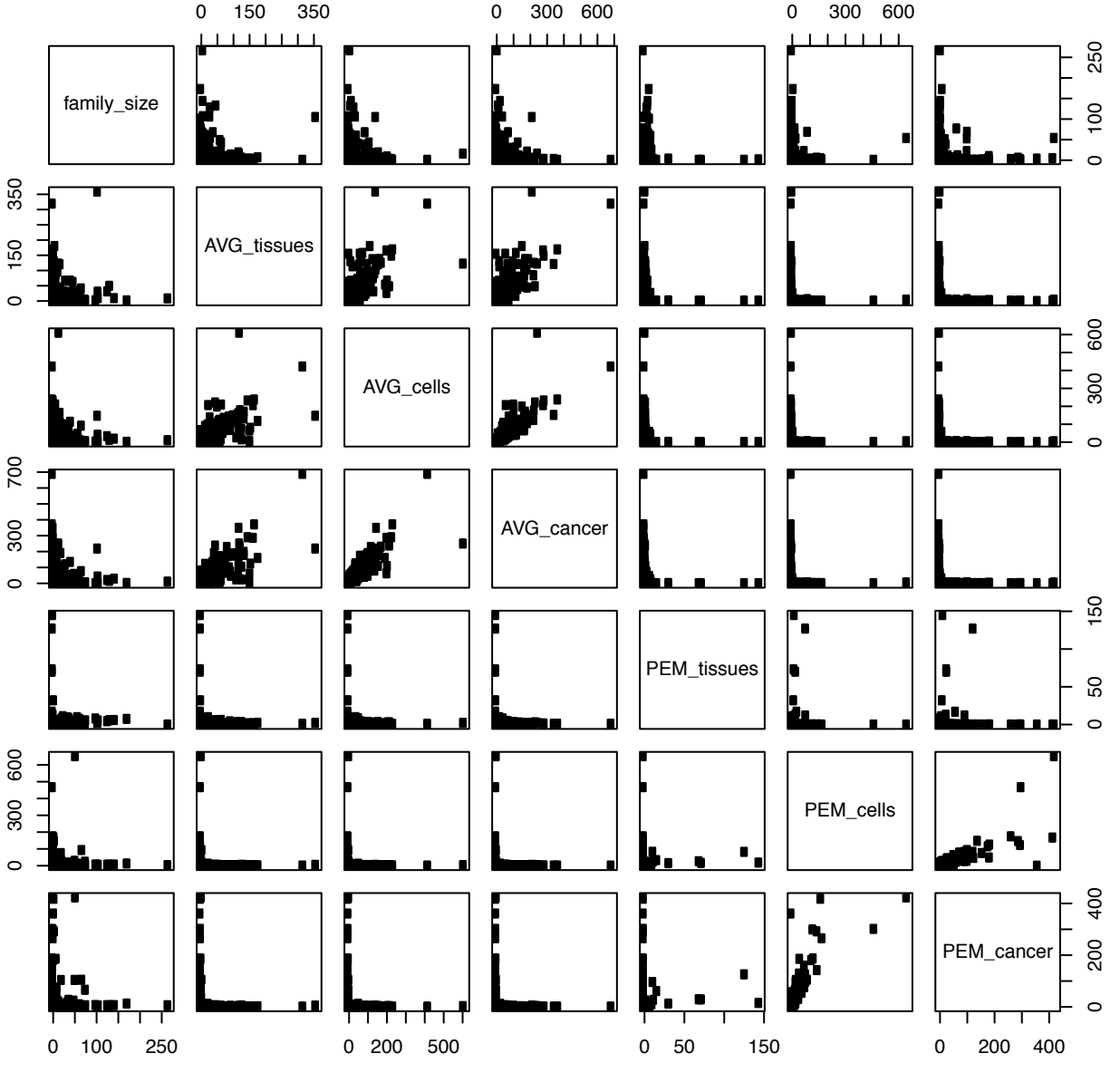
family_size
AVG_tissues
AVG_cells
AVG_cancer
PEM_tissues
PEM_cells
PEM_cancer
0 150 350
0 300 600
0 300 600
0 100 250
0 150 350
0 300 600
0 300 700
0 50 150
0 300 600
0 200 400
0 100 250
0 200 500
0 50 150
0 200 400

Figure 6 (a)

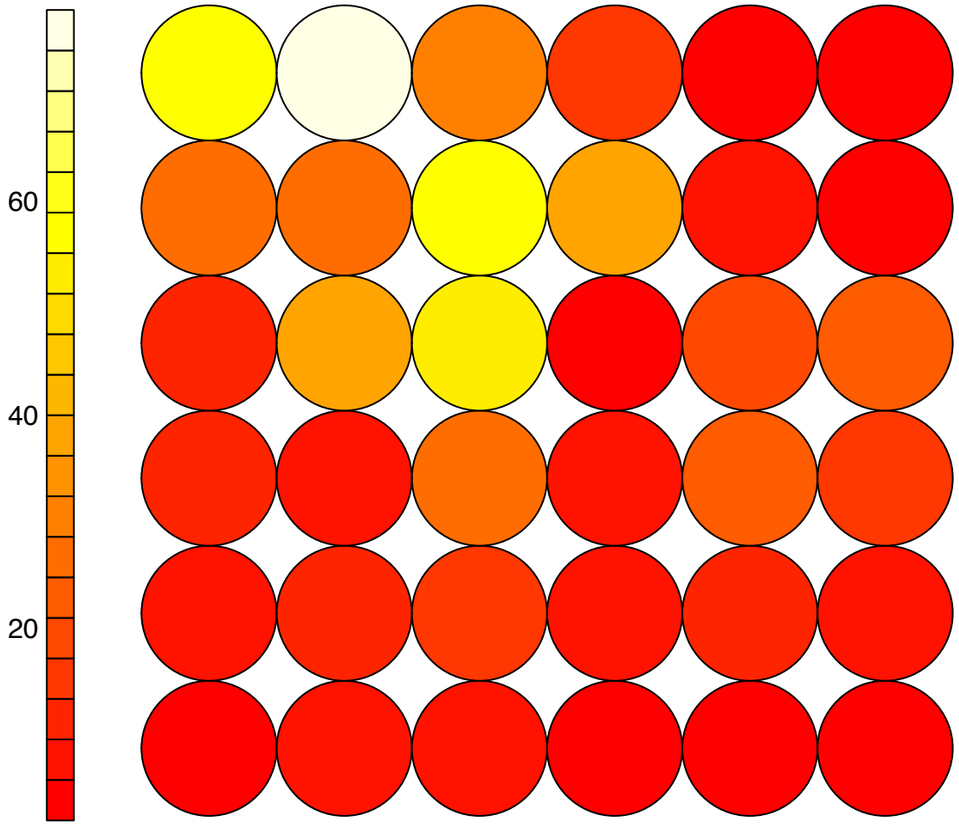

Figure 6 (b)

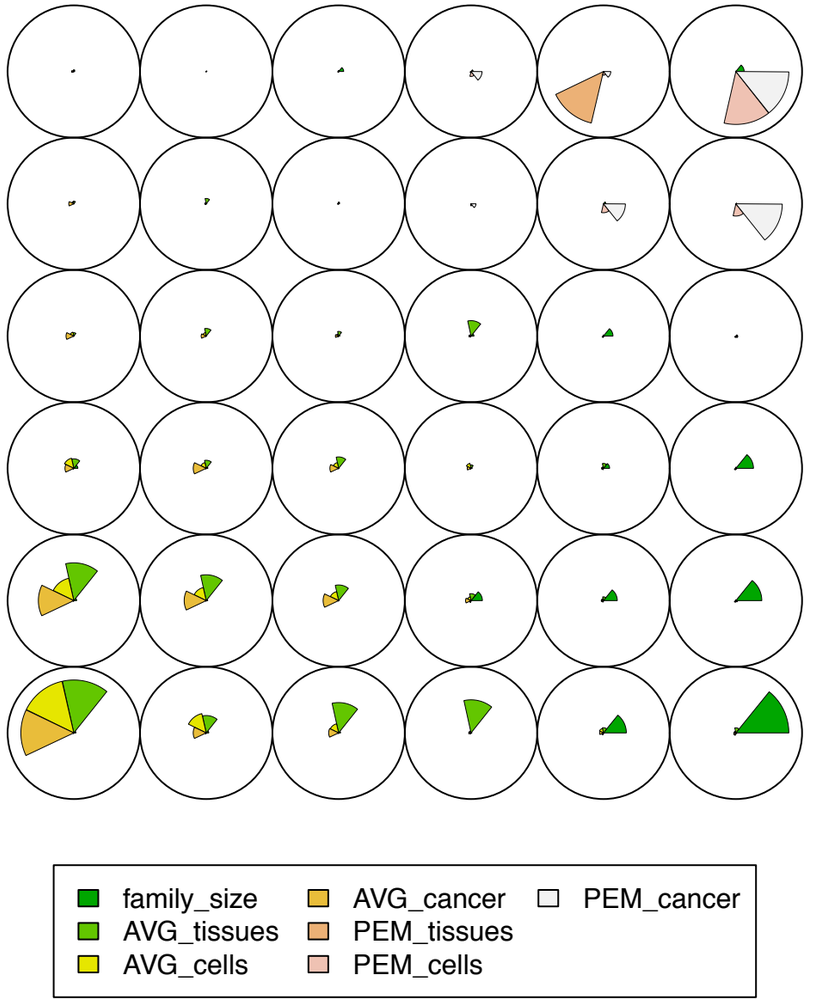

Gene Set Name [# Genes (K)]	Description	# Genes in Overlap (k)	k/K	p value
MODULE_11 [540]	Genes in the cancer module 11	10		$2.27\ e^{-10}$
MODULE_66 [552]	Genes in the cancer module 66	10		$2.81\ e^{-10}$
SMID_BREAST_CANCER_NORMAL_LIKE_UP [476]	Genes up-regulated in the normal-like subtype of breast cancer.	9		$1.73\ e^{-9}$
PICCALUGA_ANGIOIMMUNOBLASTIC_LYMPHOMA_MA_UP [205]	Up-regulated genes in angioimmunoblastic lymphoma (AILT) compared to normal T lymphocytes.	7		$2.38\ e^{-9}$
WONG_ADULT_TISSUE_STEM_MODULE [721]	The 'adult tissue stem' module: genes coordinately up-regulated in a compendium of adult tissue stem cells.	10		$3.66\ e^{-9}$
MODULE_12 [360]	Genes in the cancer module 12	8		$4.45\ e^{-9}$
MODULE_47 [225]	Genes in the cancer module 47	7		$4.55\ e^{-9}$
V$ATF1_Q6 [231]	Genes with promoter regions [-2kb,2kb] around transcription start site containing the motif CYYTGACGTCA which matches annotation for ATF1: activating transcription factor 1	7		$5.46\ e^{-9}$
MODULE_100 [544]	Genes in the cancer module 100	9		$5.51\ e^{-9}$
MODULE_137 [546]	Genes in the cancer module 137	9		$5.69\ e^{-9}$

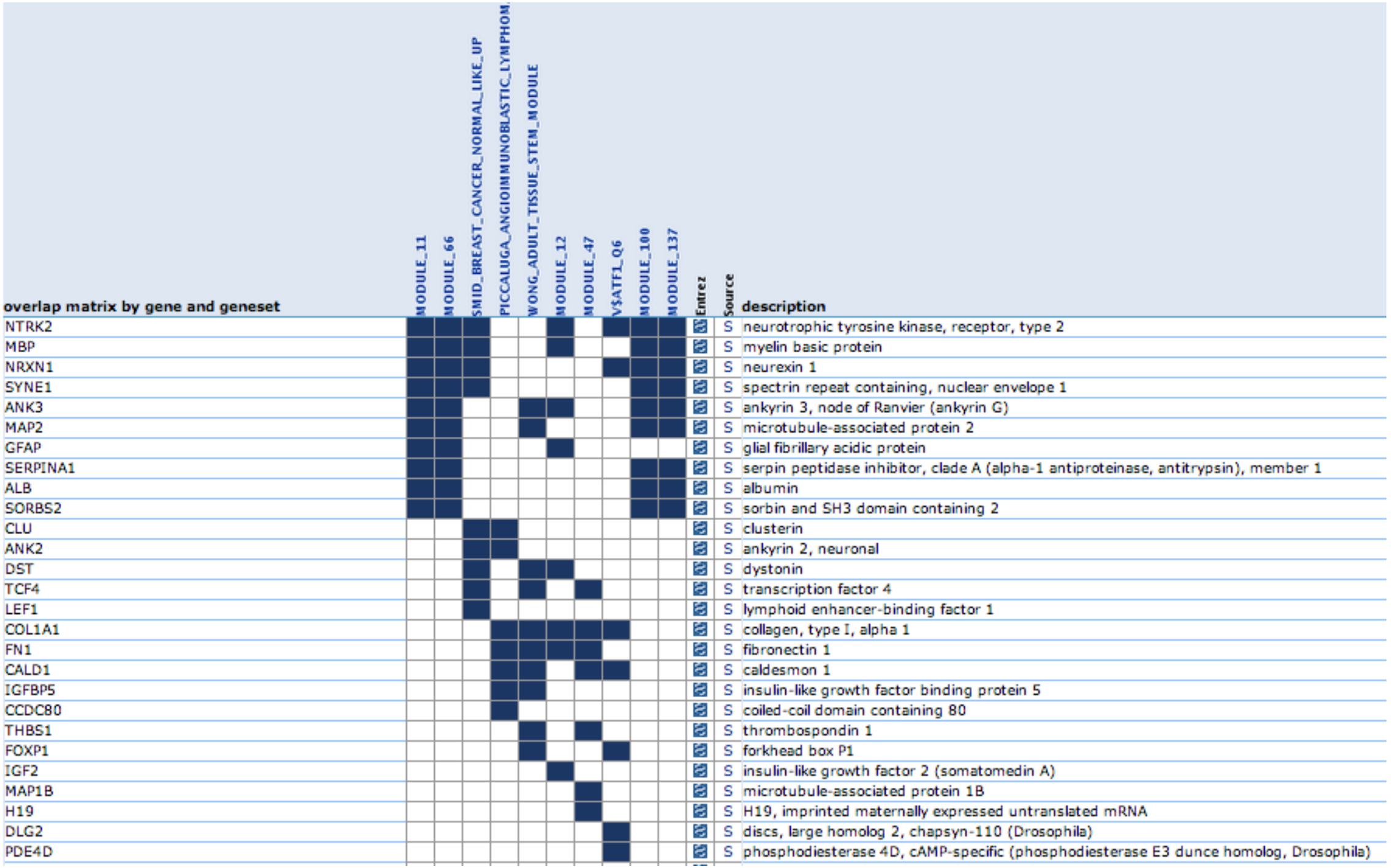

overlap matrix by gene and geneset	MODULE_11	MODULE_66	SMID_BREAST_CANCER_NORMAL_LIKE_UP	PICCALUGA_ANGIOIMMUNOBLASTIC_LYMPHOM	WONG_ADULT_TISSUE_STEM_MODULE	MODULE_12	MODULE_47	V$ATF1_Q6	MODULE_100	MODULE_137	Entrez	Source	description
NTRK2	■	■	■			■		■	■	■		S	neurotrophic tyrosine kinase, receptor, type 2
MBP	■	■	■			■			■	■		S	myelin basic protein
NRXN1	■	■	■					■	■	■		S	neurexin 1
SYNE1	■	■	■						■	■		S	spectrin repeat containing, nuclear envelope 1
ANK3	■	■			■	■			■	■		S	ankyrin 3, node of Ranvier (ankyrin G)
MAP2	■	■			■				■	■		S	microtubule-associated protein 2
GFAP	■	■				■						S	glial fibrillary acidic protein
SERPINA1	■	■							■	■		S	serpin peptidase inhibitor, clade A (alpha-1 antiproteinase, antitrypsin), member 1
ALB	■	■							■	■		S	albumin
SORBS2	■	■							■	■		S	sorbin and SH3 domain containing 2
CLU			■	■								S	clusterin
ANK2			■	■								S	ankyrin 2, neuronal
DST			■		■	■						S	dystonin
TCF4			■		■		■					S	transcription factor 4
LEF1			■									S	lymphoid enhancer-binding factor 1
COL1A1				■	■	■	■	■				S	collagen, type I, alpha 1
FN1				■	■	■	■					S	fibronectin 1
CALD1				■	■		■	■				S	caldesmon 1
IGFBP5				■	■							S	insulin-like growth factor binding protein 5
CCDC80				■								S	coiled-coil domain containing 80
THBS1					■		■					S	thrombospondin 1
FOXP1					■			■				S	forkhead box P1
IGF2						■						S	insulin-like growth factor 2 (somatomedin A)
MAP1B							■					S	microtubule-associated protein 1B
H19							■					S	H19, imprinted maternally expressed untranslated mRNA
DLG2								■				S	discs, large homolog 2, chapsyn-110 (Drosophila)
PDE4D								■				S	phosphodiesterase 4D, cAMP-specific (phosphodiesterase E3 dunce homolog, Drosophila)

Gene Set Name [# Genes (K)]	Description	# Genes in Overlap (k)	k/K	p value
WANG_SMARCE1_TARGETS_UP [280]	Genes up-regulated in BT549 cells (breast cancer) by expression of SMARCE1 [GeneID=6605] off a retroviral vector.	6		$5\ e^{-9}$
TTGTTT_V$FOXO4_01 [2061]	Genes with promoter regions [-2kb,2kb] around transcription start site containing the motif TTGTTT which matches annotation for MLLT7: myeloid/lymphoid or mixed-lineage leukemia (trithorax homolog, Drosophila); translocated to, 7	10		$1.61\ e^{-8}$
MODULE_12 [360]	Genes in the cancer module 12	6		$2.23\ e^{-8}$
WILCOX_PRESPONSE_TO_ROGESTERONE_DN [66]	Genes down-regulated in primary cultures of ovarian surface epithlium cells exposed to progesterone [PubChem=5994] for 5 days.	4		$3.92\ e^{-8}$
TGCCAAR_V$NF1_Q6 [722]	Genes with promoter regions [-2kb,2kb] around transcription start site containing the motif TGCCAAR which matches annotation for NF1: neurofibromin 1 (neurofibromatosis, von Recklinghausen disease, Watson disease)	7		$4.77\ e^{-8}$
GU_PDEF_TARGETS_UP [71]	Integrin, VEGF, Wnt and TGFbeta signaling pathway genes up-regulated in PC-3 cells (prostate cancer) after knockdown of PDEF [GeneID=25803] by RNAi.	4		$5.28\ e^{-8}$
MODULE_47 [225]	Genes in the cancer module 47	5		$9.72\ e^{-8}$
PILON_KLF1_TARGETS_UP [504]	Genes up-regulated in erythroid progenitor cells from fetal livers of E13.5 embryos with KLF1 [GeneID=10661] knockout compared to those from the wild type embryos.	6		$1.63\ e^{-7}$
MODULE_23 [565]	Genes in the cancer module 23	6		$3.18\ e^{-7}$
HOOI_ST7_TARGETS_DN [123]	Genes down-regulated in PC-3 cells (prostate cancer) stably expressing ST7 [GeneID=7982] off a plasmid vector.	4		$4.85\ e^{-7}$

overlap matrix by gene and geneset	WANG_SMARCE1_TARGETS_UP	TTGTTT_V$FOX04_01	MODULE_12	WILCOX_PRESPONSE_TO_ROGESTERONE_DN	TGCCAAR_V$NF1_Q6	GU_PDEF_TARGETS_UP	MODULE_47	PILON_KLF1_TARGETS_UP	MODULE_23	HOOI_ST7_TARGETS_DN	Entrez	Source	description
COL1A1	■	■	■	■		■	■	■	■	■		S	collagen, type I, alpha 1
FN1	■	■	■	■		■	■	■	■	■		S	fibronectin 1
NTRK2	■	■	■									S	neurotrophic tyrosine kinase, receptor, type 2
MAP1B	■	■					■					S	microtubule-associated protein 1B
IGFBP5	■			■						■		S	insulin-like growth factor binding protein 5
CALD1	■				■		■	■				S	caldesmon 1
DST		■	■	■	■							S	dystonin
TCF4		■			■	■	■					S	transcription factor 4
ALB		■			■			■	■			S	albumin
SORBS2		■			■				■			S	sorbin and SH3 domain containing 2
TTN		■								■		S	titin
PDE4D		■										S	phosphodiesterase 4D, cAMP-specific (phosphodiesterase E3 dunce homolog, Drosophila)
GFAP			■		■							S	glial fibrillary acidic protein
IGF2			■					■	■			S	insulin-like growth factor 2 (somatomedin A)
LEF1					■	■						S	lymphoid enhancer-binding factor 1
APOB								■	■			S	apolipoprotein B (including Ag(x) antigen)
AKAP13												S	A kinase (PRKA) anchor protein 13

Figure S11

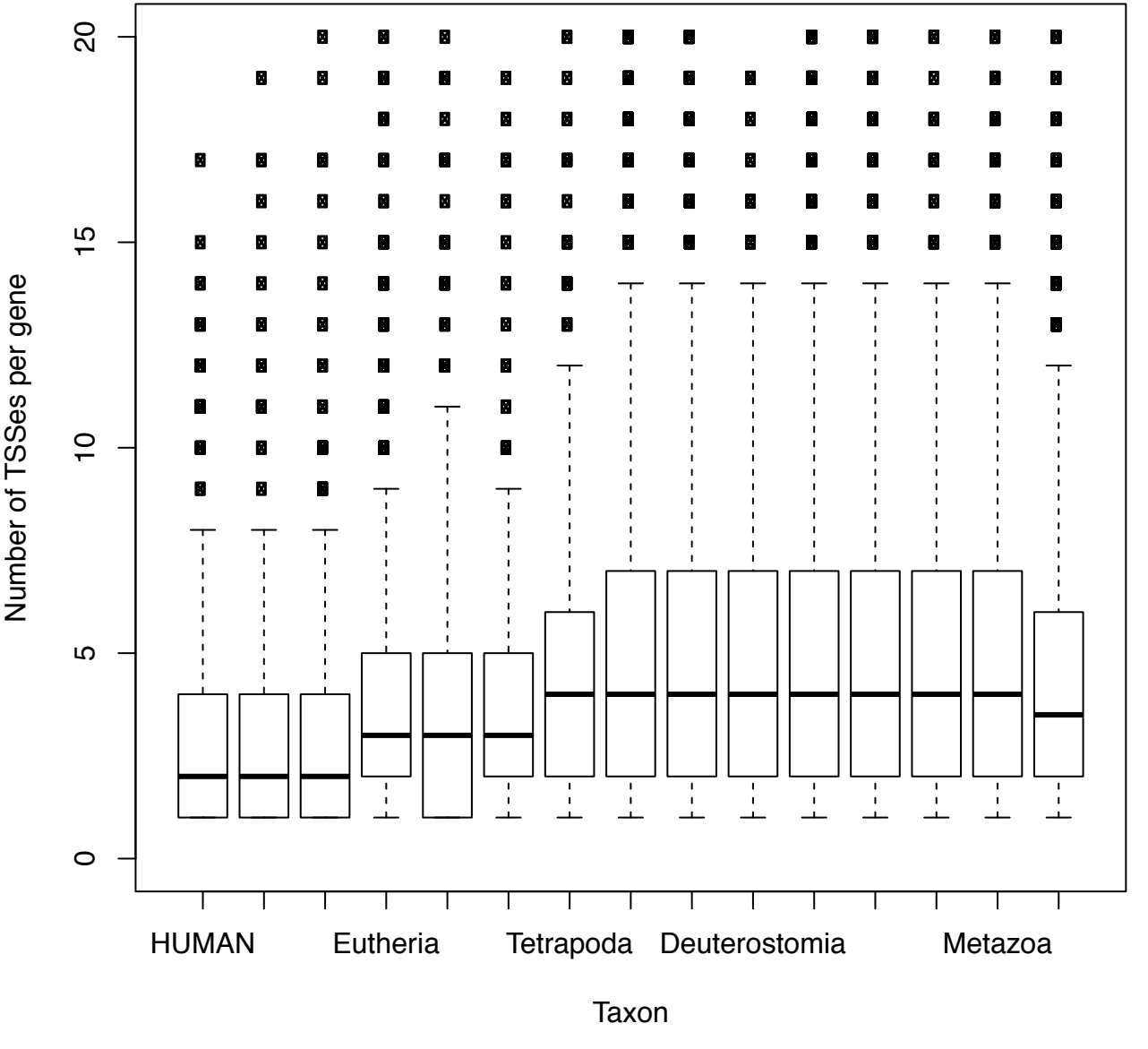
Number of TSSes per gene
0
5
10
15
20
HUMAN
Eutheria
Tetrapoda
Deuterostomia
Metazoa
Taxon

Figure S12

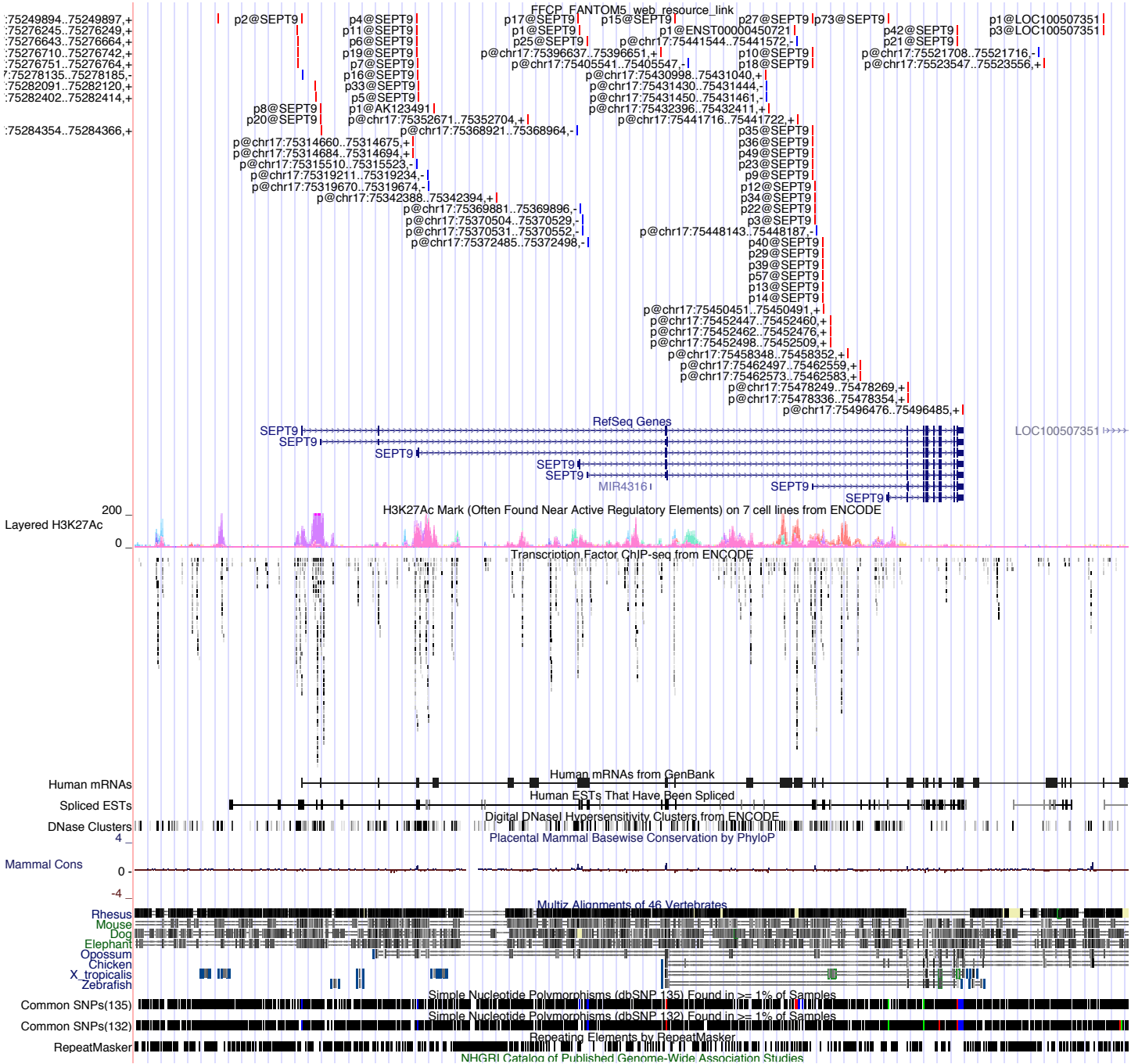
FFCP_FANTOM5_web_resource_link
RefSeq Genes
SEPT9
LOC100507351
MIR4316
H3K27Ac Mark (Often Found Near Active Regulatory Elements) on 7 cell lines from ENCODE
Layered H3K27Ac
Transcription Factor ChIP-seq from ENCODE
Human mRNAs
Human mRNAs from GenBank
Spliced ESTs
Human ESTs That Have Been Spliced
DNase Clusters
Digital DNaseI Hypersensitivity Clusters from ENCODE
Placental Mammal Basewise Conservation by PhyloP
Mammal Cons
Multiz Alignments of 46 Vertebrates
Rhesus
Mouse
Dog
Elephant
Opossum
Chicken
X_tropicalis
Zebrafish
Common SNPs(135)
Simple Nucleotide Polymorphisms (dbSNP 135) Found in >= 1% of Samples
Common SNPs(132)
Simple Nucleotide Polymorphisms (dbSNP 132) Found in >= 1% of Samples
RepeatMasker
Repeating Elements by RepeatMasker
NHGRI Catalog of Published Genome-Wide Association Studies

Figure S13

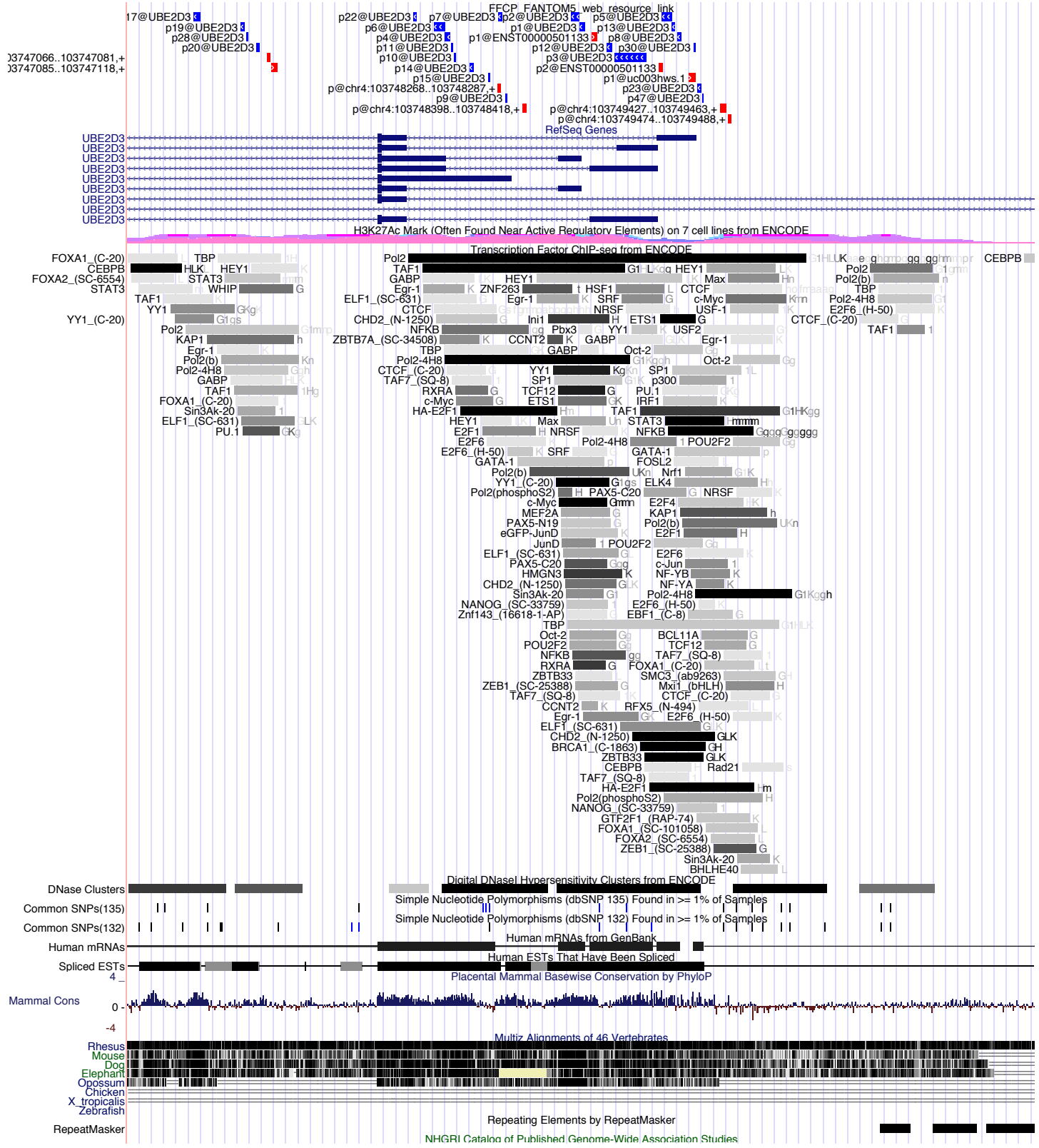
FFCP_FANTOM5_web_resource_link
RefSeq Genes
H3K27Ac Mark (Often Found Near Active Regulatory Elements) on 7 cell lines from ENCODE
Transcription Factor ChIP-seq from ENCODE
Digital DNaseI Hypersensitivity Clusters from ENCODE
DNase Clusters
Simple Nucleotide Polymorphisms (dbSNP 135) Found in >= 1% of Samples
Common SNPs(135)
Simple Nucleotide Polymorphisms (dbSNP 132) Found in >= 1% of Samples
Common SNPs(132)
Human mRNAs from GenBank
Human mRNAs
Human ESTs That Have Been Spliced
Spliced ESTs
Placental Mammal Basewise Conservation by PhyloP
Mammal Cons
Multiz Alignments of 46 Vertebrates
Rhesus
Mouse
Dog
Elephant
Opossum
Chicken
X_tropicalis
Zebrafish
Repeating Elements by RepeatMasker
RepeatMasker
NHGRI Catalog of Published Genome-Wide Association Studies

Figure S14

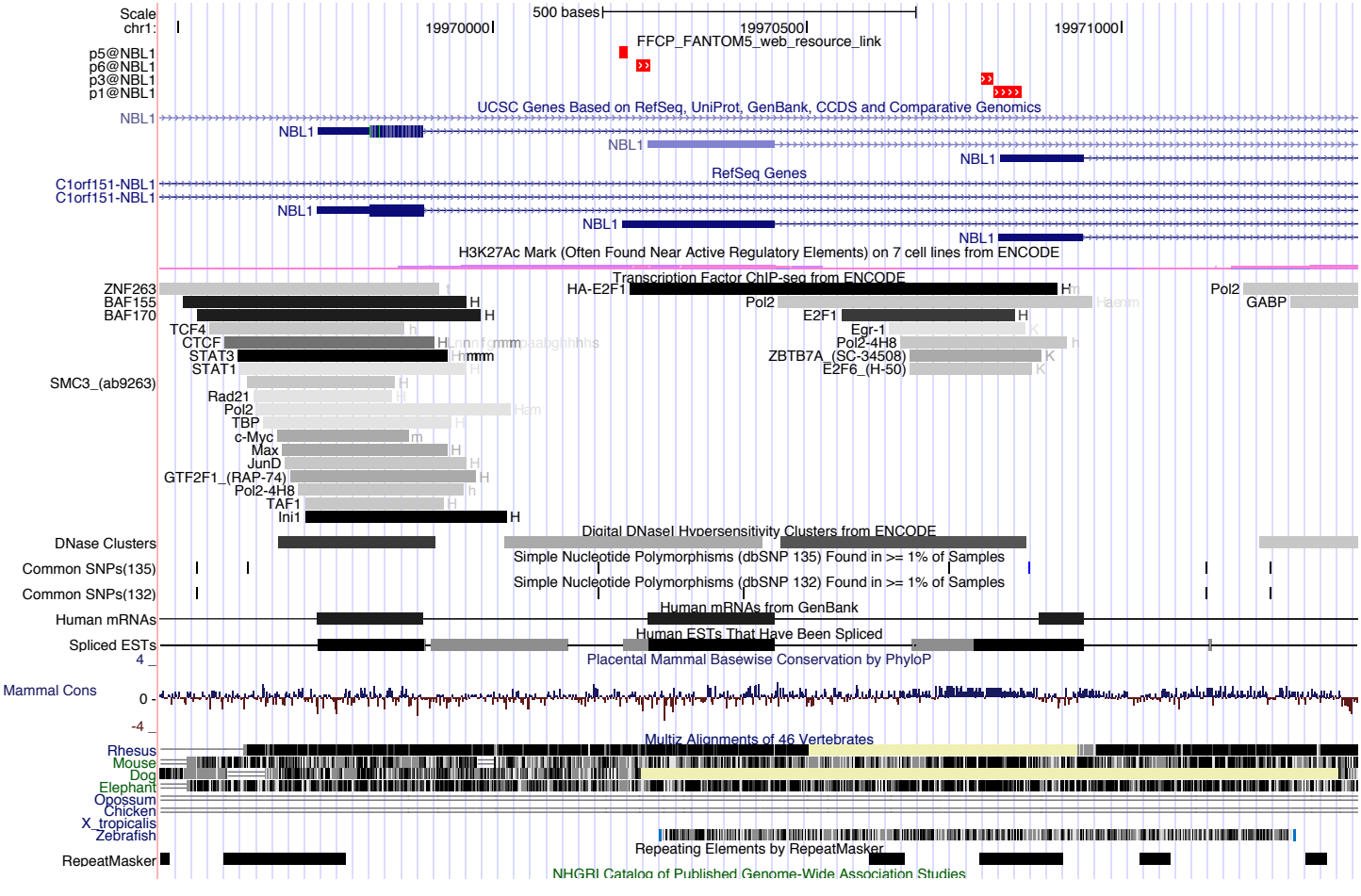
Scale
chr1:
500 bases
19970000
19970500
19971000
FFCP_FANTOM5_web_resource_link
p5@NBL1
p6@NBL1
p3@NBL1
p1@NBL1
UCSC Genes Based on RefSeq, UniProt, GenBank, CCDS and Comparative Genomics
NBL1
RefSeq Genes
C1orf151-NBL1
H3K27Ac Mark (Often Found Near Active Regulatory Elements) on 7 cell lines from ENCODE
Transcription Factor ChIP-seq from ENCODE
ZNF263
BAF155
BAF170
TCF4
CTCF
STAT3
STAT1
SMC3_(ab9263)
Rad21
Pol2
TBP
c-Myc
Max
JunD
GTF2F1_(RAP-74)
Pol2-4H8
TAF1
Ini1
HA-E2F1
E2F1
Egr-1
ZBTB7A_(SC-34508)
E2F6_(H-50)
GABP
DNase Clusters
Digital DNaseI Hypersensitivity Clusters from ENCODE
Common SNPs(135)
Simple Nucleotide Polymorphisms (dbSNP 135) Found in >= 1% of Samples
Common SNPs(132)
Simple Nucleotide Polymorphisms (dbSNP 132) Found in >= 1% of Samples
Human mRNAs
Human mRNAs from GenBank
Spliced ESTs
Human ESTs That Have Been Spliced
Placental Mammal Basewise Conservation by PhyloP
Mammal Cons
Multiz Alignments of 46 Vertebrates
Rhesus
Mouse
Dog
Elephant
Opossum
Chicken
X_tropicalis
Zebrafish
Repeating Elements by RepeatMasker
RepeatMasker
NHGRI Catalog of Published Genome-Wide Association Studies

Figure S15

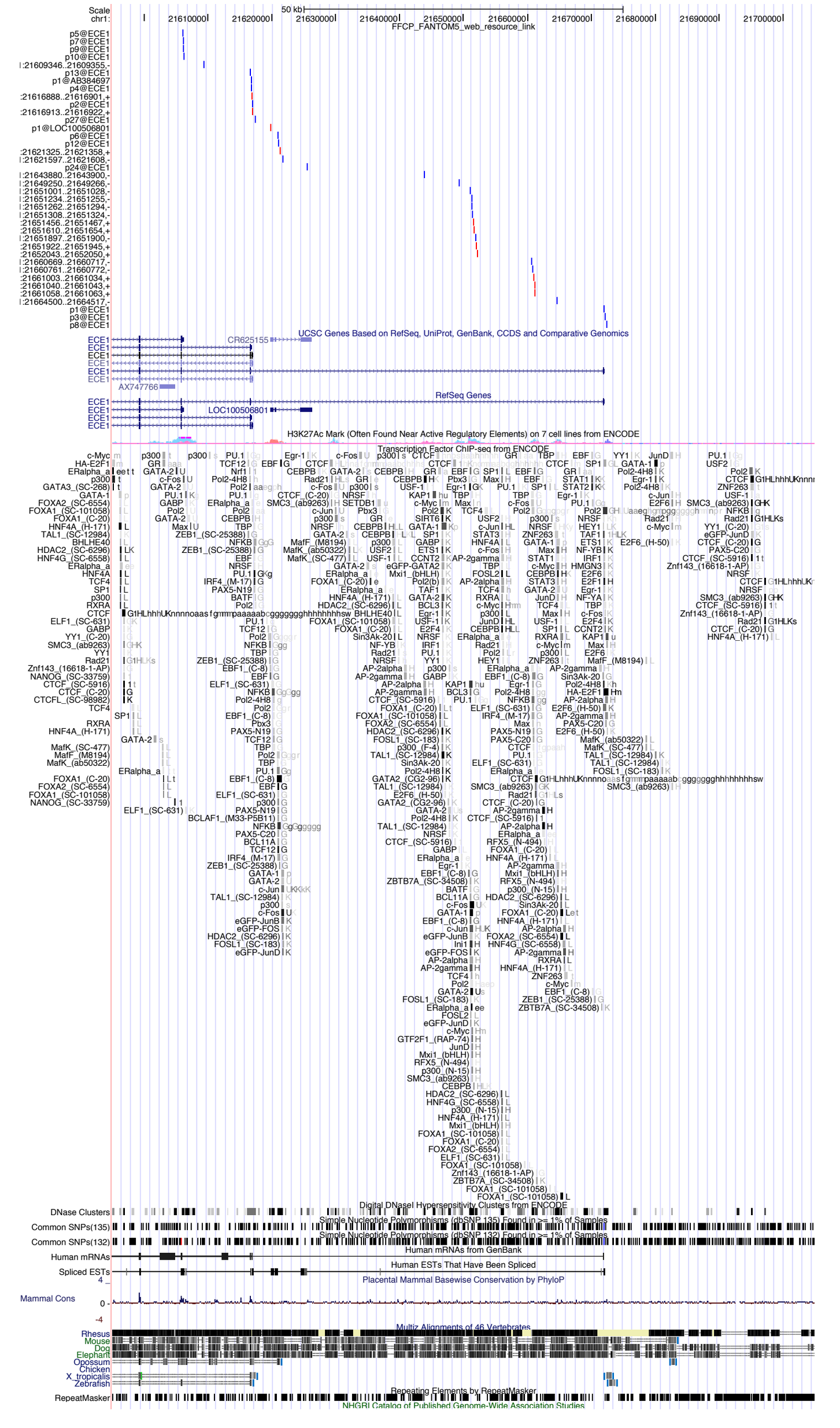
Scale
chr1:
50 kb
21610000
21620000
21630000
21640000
21650000
21660000
21670000
21680000
21690000
21700000
FFCP_FANTOM5_web_resource_link
p5@ECE1
p7@ECE1
p9@ECE1
p10@ECE1
l:21609346..21609355,-
p13@ECE1
p1@AB384697
p4@ECE1
:21616888..21616901,+
p2@ECE1
:21616913..21616922,+
p27@ECE1
p1@LOC100506801
p6@ECE1
p12@ECE1
:21621325..21621358,+
l:21621597..21621608,-
p24@ECE1
l:21643880..21643900,-
l:21649250..21649266,-
l:21651001..21651028,-
l:21651234..21651255,-
l:21651262..21651294,-
l:21651308..21651324,-
:21651456..21651467,+
:21651610..21651654,+
l:21651897..21651900,-
:21651922..21651945,+
:21652043..21652050,+
l:21660669..21660717,-
l:21660761..21660772,-
:21661003..21661034,+
:21661040..21661043,+
:21661058..21661063,+
l:21664500..21664517,-
p1@ECE1
p3@ECE1
p8@ECE1
UCSC Genes Based on RefSeq, UniProt, GenBank, CCDS and Comparative Genomics
ECE1
CR625155
AX747766
RefSeq Genes
LOC100506801
H3K27Ac Mark (Often Found Near Active Regulatory Elements) on 7 cell lines from ENCODE
Transcription Factor ChIP-seq from ENCODE
c-Myc
HA-E2F1
ERalpha_a
p300
GATA3_(SC-268)
GATA-1
FOXA2_(SC-6554)
FOXA1_(SC-101058)
FOXA1_(C-20)
HNF4A_(H-171)
TAL1_(SC-12984)
BHLHE40
HDAC2_(SC-6296)
HNF4G_(SC-6558)
ERalpha_a
HNF4A
TCF4
SP1
p300
RXRA
CTCF
ELF1_(SC-631)
GABP
YY1_(C-20)
SMC3_(ab9263)
YY1
Rad21
Znf143_(16618-1-AP)
NANOG_(SC-33759)
CTCF_(SC-5916)
CTCF_(C-20)
CTCFL_(SC-98982)
TCF4
RXRA
HNF4A_(H-171)
MafK_(SC-477)
MafF_(M8194)
MafK_(ab50322)
FOXA1_(C-20)
FOXA2_(SC-6554)
FOXA1_(SC-101058)
NANOG_(SC-33759)
DNase Clusters
Digital DNaseI Hypersensitivity Clusters from ENCODE
Common SNPs(135)
Simple Nucleotide Polymorphisms (dbSNP 135) Found in >= 1% of Samples
Common SNPs(132)
Simple Nucleotide Polymorphisms (dbSNP 132) Found in >= 1% of Samples
Human mRNAs
Human mRNAs from GenBank
Spliced ESTs
Human ESTs That Have Been Spliced
Placental Mammal Basewise Conservation by PhyloP
Mammal Cons
4
0
-4
Multiz Alignments of 46 Vertebrates
Rhesus
Mouse
Dog
Elephant
Opossum
Chicken
X_tropicalis
Zebrafish
Repeating Elements by RepeatMasker
RepeatMasker
NHGRI Catalog of Published Genome-Wide Association Studies

Figure S16

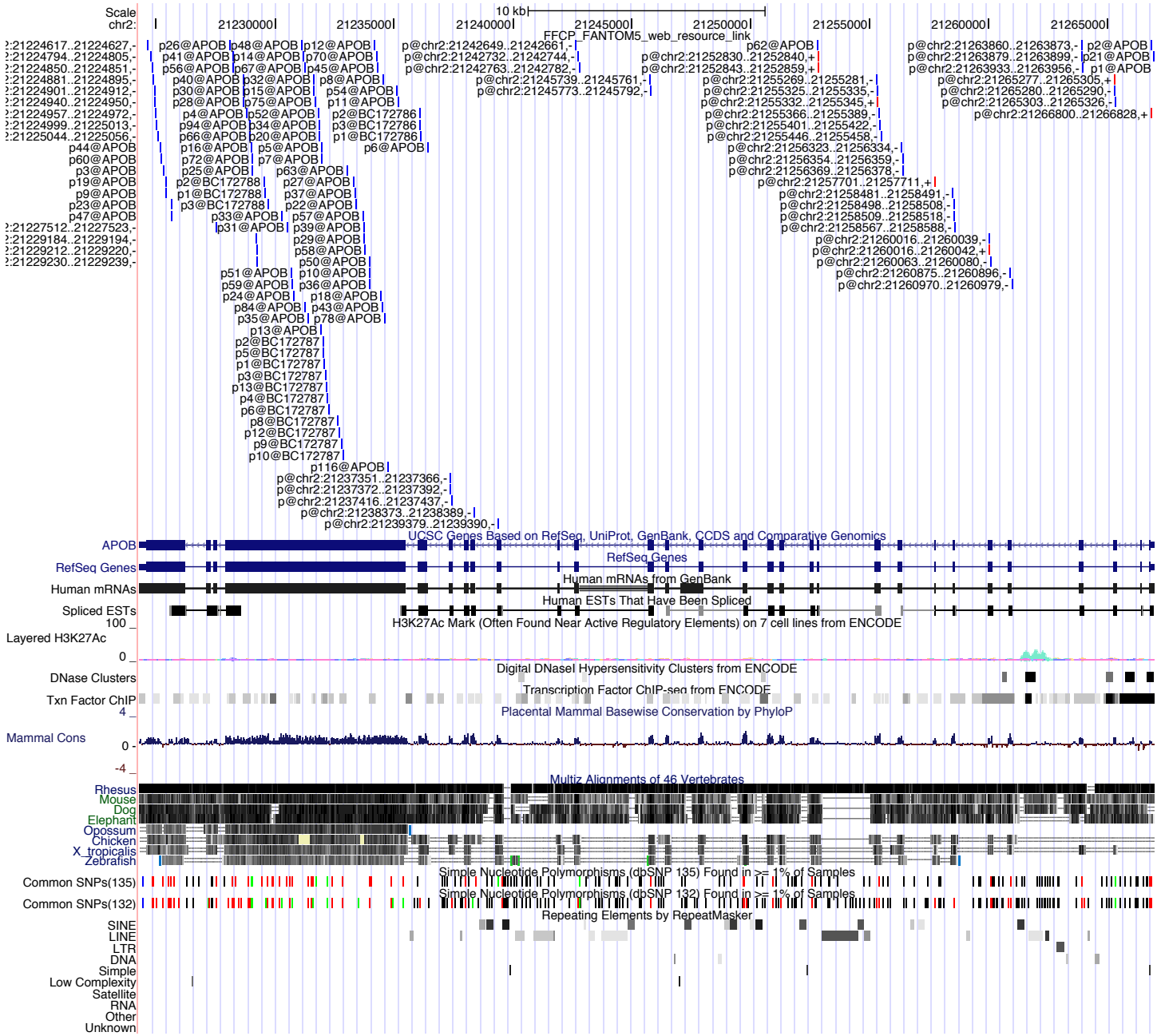
Scale
chr2:
10 kb
21230000
21235000
21240000
21245000
21250000
21255000
21260000
21265000
FFCP_FANTOM5_web_resource_link
UCSC Genes Based on RefSeq, UniProt, GenBank, CCDS and Comparative Genomics
APOB
RefSeq Genes
Human mRNAs
Spliced ESTs
Human mRNAs from GenBank
Human ESTs That Have Been Spliced
H3K27Ac Mark (Often Found Near Active Regulatory Elements) on 7 cell lines from ENCODE
Layered H3K27Ac
DNase Clusters
Digital DNaseI Hypersensitivity Clusters from ENCODE
Txn Factor ChIP
Transcription Factor ChIP-seq from ENCODE
Placental Mammal Basewise Conservation by PhyloP
Mammal Cons
Multiz Alignments of 46 Vertebrates
Rhesus
Mouse
Dog
Elephant
Opossum
Chicken
X_tropicalis
Zebrafish
Common SNPs(135)
Simple Nucleotide Polymorphisms (dbSNP 135) Found in >= 1% of Samples
Common SNPs(132)
Simple Nucleotide Polymorphisms (dbSNP 132) Found in >= 1% of Samples
Repeating Elements by RepeatMasker
SINE
LINE
LTR
DNA
Simple
Low Complexity
Satellite
RNA
Other
Unknown

Figure S17

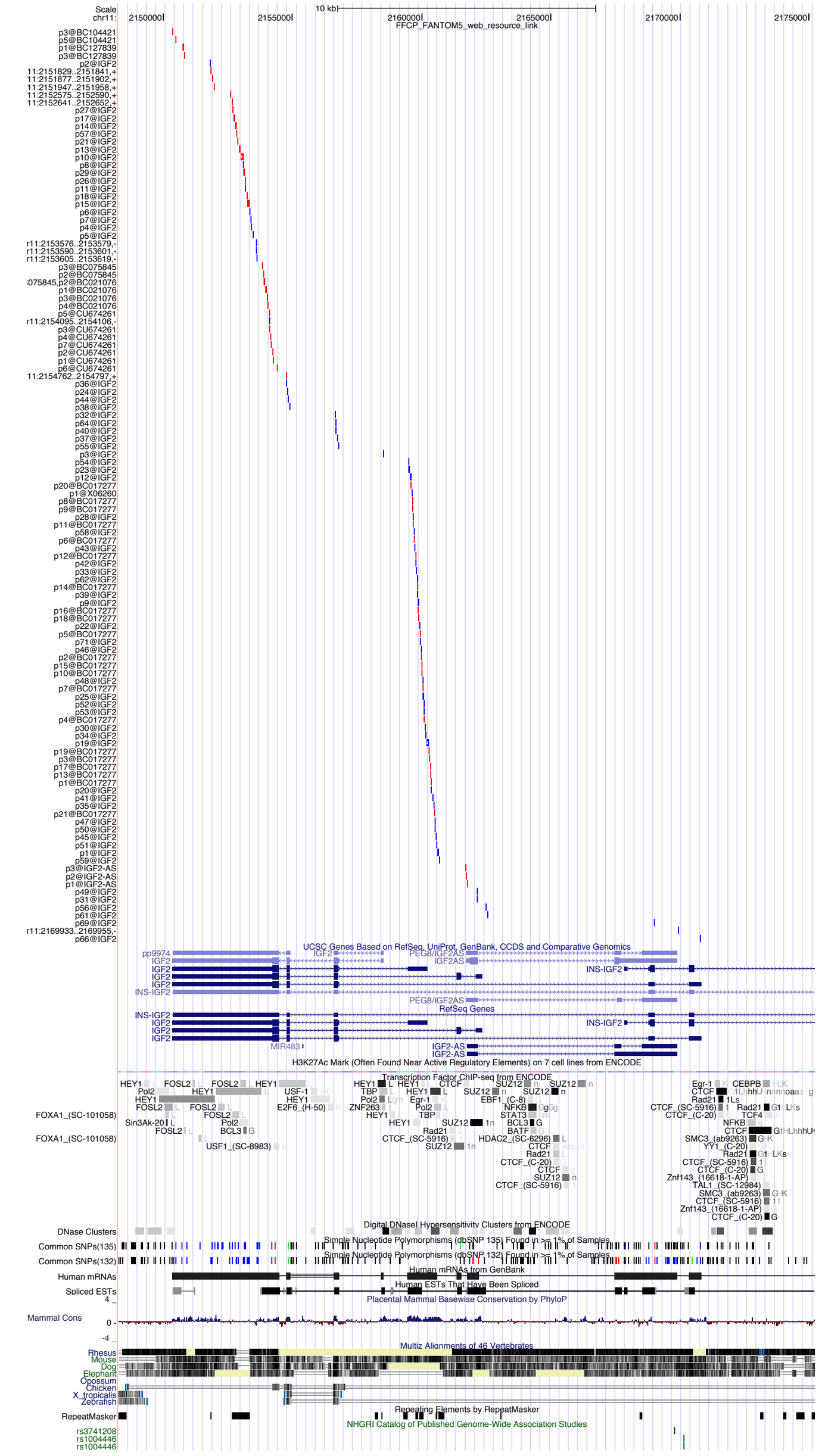
Scale
chr11:
10 kb
2150000
2155000
2160000
2165000
2170000
2175000
FFCP_FANTOM5_web_resource_link
UCSC Genes Based on RefSeq, UniProt, GenBank, CCDS and Comparative Genomics
RefSeq Genes
H3K27Ac Mark (Often Found Near Active Regulatory Elements) on 7 cell lines from ENCODE
Transcription Factor ChIP-seq from ENCODE
FOXA1_(SC-101058)
FOXA1_(SC-101058)
Digital DNaseI Hypersensitivity Clusters from ENCODE
DNase Clusters
Simple Nucleotide Polymorphisms (dbSNP 135) Found in >= 1% of Samples
Common SNPs(135)
Simple Nucleotide Polymorphisms (dbSNP 132) Found in >= 1% of Samples
Common SNPs(132)
Human mRNAs from GenBank
Human mRNAs
Human ESTs That Have Been Spliced
Spliced ESTs
Placental Mammal Basewise Conservation by PhyloP
Mammal Cons
Multiz Alignments of 46 Vertebrates
Rhesus
Mouse
Dog
Elephant
Opossum
Chicken
X_tropicalis
Zebrafish
Repeating Elements by RepeatMasker
RepeatMasker
NHGRI Catalog of Published Genome-Wide Association Studies
rs3741208
rs1004446
rs1004446

Figure S18

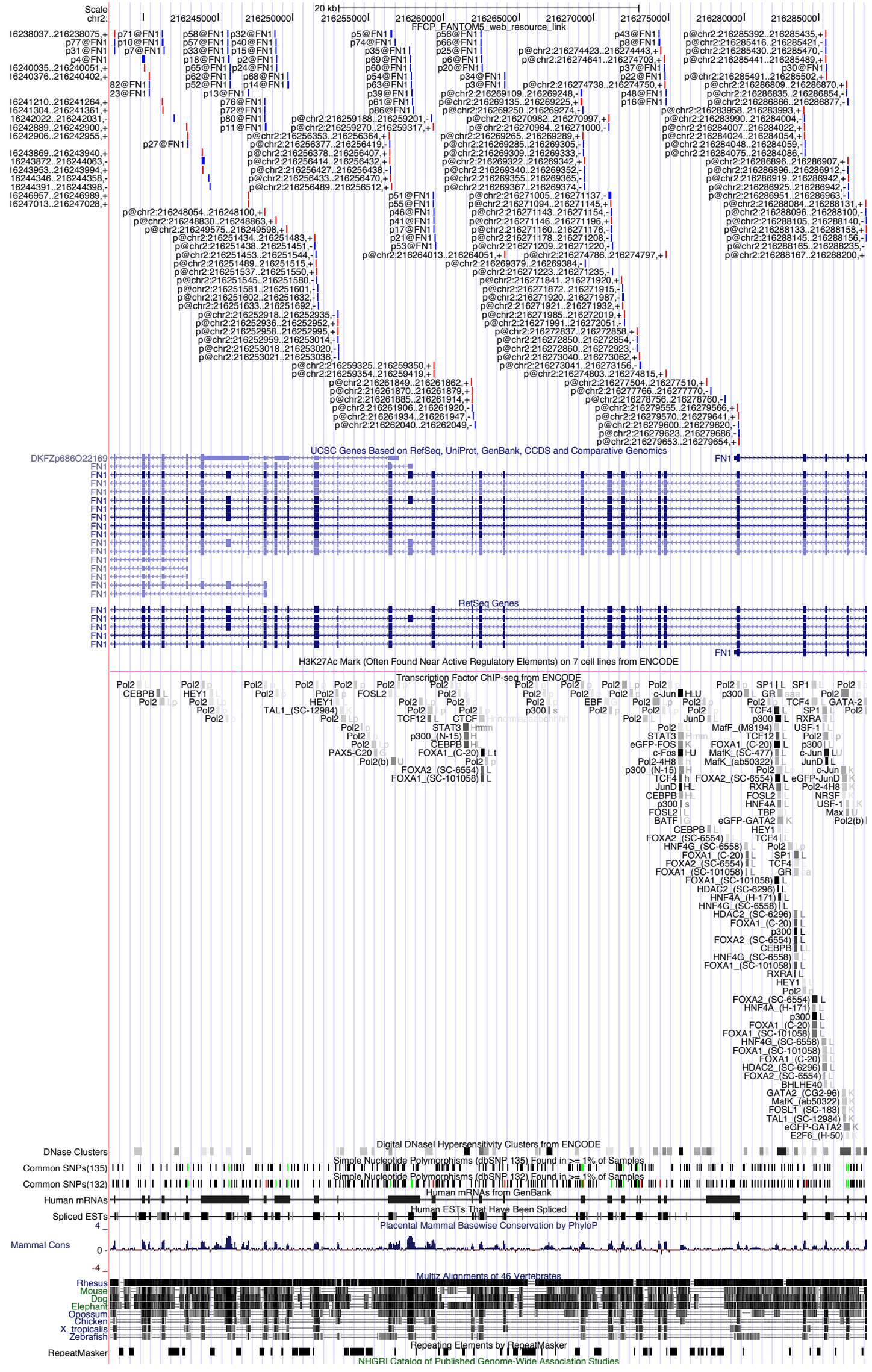
Scale
chr2:
20 kb
216245000
216250000
216255000
216260000
216265000
216270000
216275000
216280000
216285000
FFCP_FANTOM5_web_resource_link
UCSC Genes Based on RefSeq, UniProt, GenBank, CCDS and Comparative Genomics
DKFZp686O22169
FN1
RefSeq Genes
H3K27Ac Mark (Often Found Near Active Regulatory Elements) on 7 cell lines from ENCODE
Transcription Factor ChIP-seq from ENCODE
Digital DNaseI Hypersensitivity Clusters from ENCODE
DNase Clusters
Common SNPs(135)
Simple Nucleotide Polymorphisms (dbSNP 135) Found in >= 1% of Samples
Common SNPs(132)
Simple Nucleotide Polymorphisms (dbSNP 132) Found in >= 1% of Samples
Human mRNAs
Human mRNAs from GenBank
Spliced ESTs
Human ESTs That Have Been Spliced
Placental Mammal Basewise Conservation by PhyloP
Mammal Cons
Multiz Alignments of 46 Vertebrates
Rhesus
Mouse
Dog
Elephant
Opossum
Chicken
X_tropicalis
Zebrafish
RepeatMasker
Repeating Elements by RepeatMasker
NHGRI Catalog of Published Genome-Wide Association Studies

Figure 19 (a)

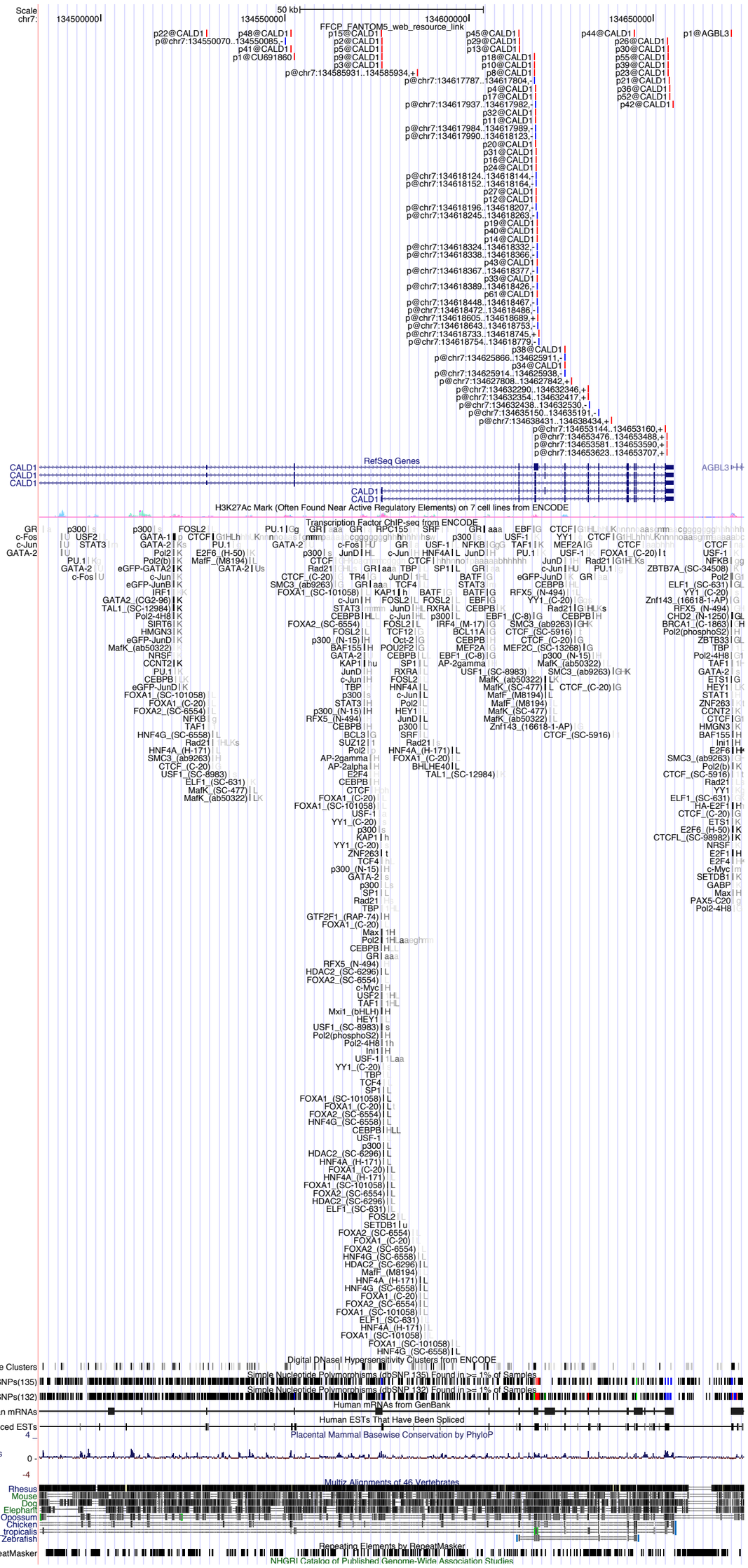

Figure 19 (b)

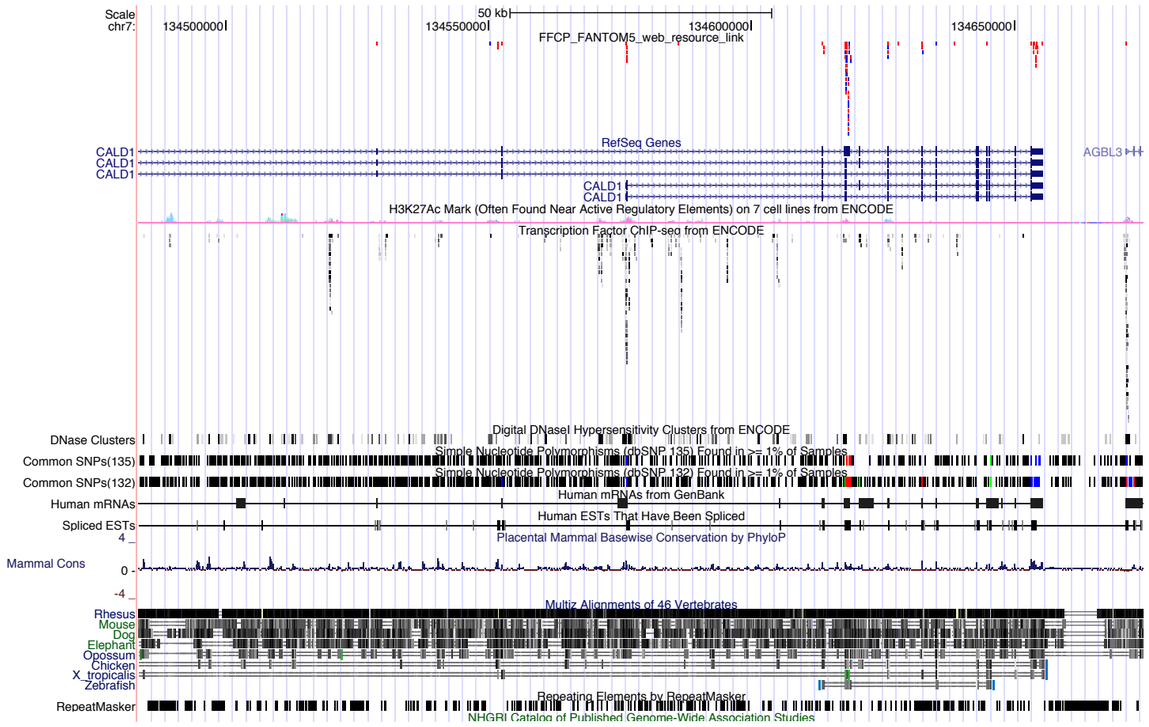

Figure S20

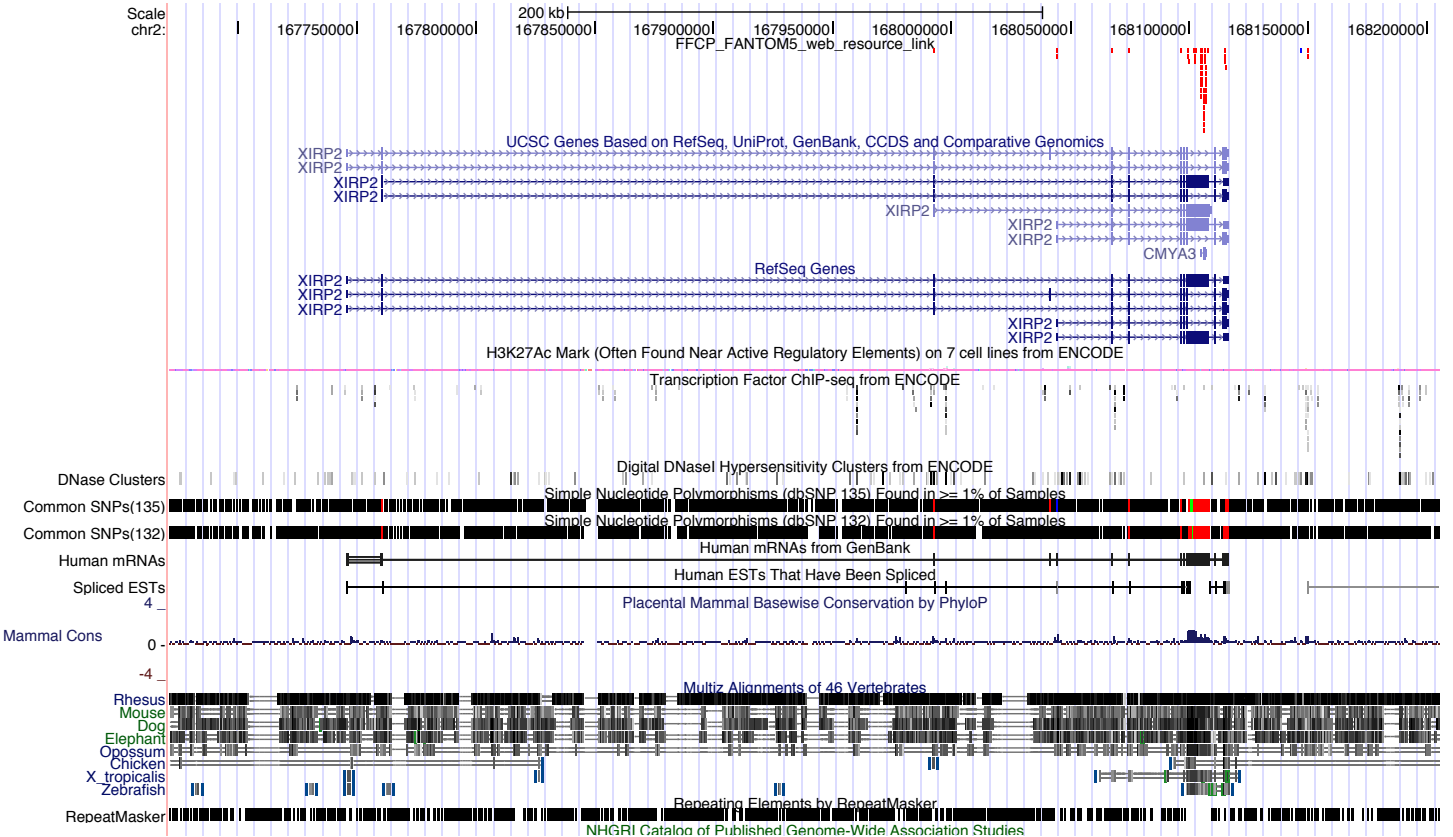
Scale
chr2:
200 kb
167750000
167800000
167850000
167900000
167950000
168000000
168050000
168100000
168150000
168200000
FFCP_FANTOM5_web_resource_link
UCSC Genes Based on RefSeq, UniProt, GenBank, CCDS and Comparative Genomics
XIRP2
CMYA3
RefSeq Genes
H3K27Ac Mark (Often Found Near Active Regulatory Elements) on 7 cell lines from ENCODE
Transcription Factor ChIP-seq from ENCODE
Digital DNaseI Hypersensitivity Clusters from ENCODE
DNase Clusters
Common SNPs(135)
Simple Nucleotide Polymorphisms (dbSNP 135) Found in >= 1% of Samples
Common SNPs(132)
Simple Nucleotide Polymorphisms (dbSNP 132) Found in >= 1% of Samples
Human mRNAs
Human mRNAs from GenBank
Spliced ESTs
Human ESTs That Have Been Spliced
Placental Mammal Basewise Conservation by PhyloP
Mammal Cons
4
0
-4
Multiz Alignments of 46 Vertebrates
Rhesus
Mouse
Dog
Elephant
Opossum
Chicken
X_tropicalis
Zebrafish
RepeatMasker
Repeating Elements by RepeatMasker
NHGRI Catalog of Published Genome-Wide Association Studies

Figure S21

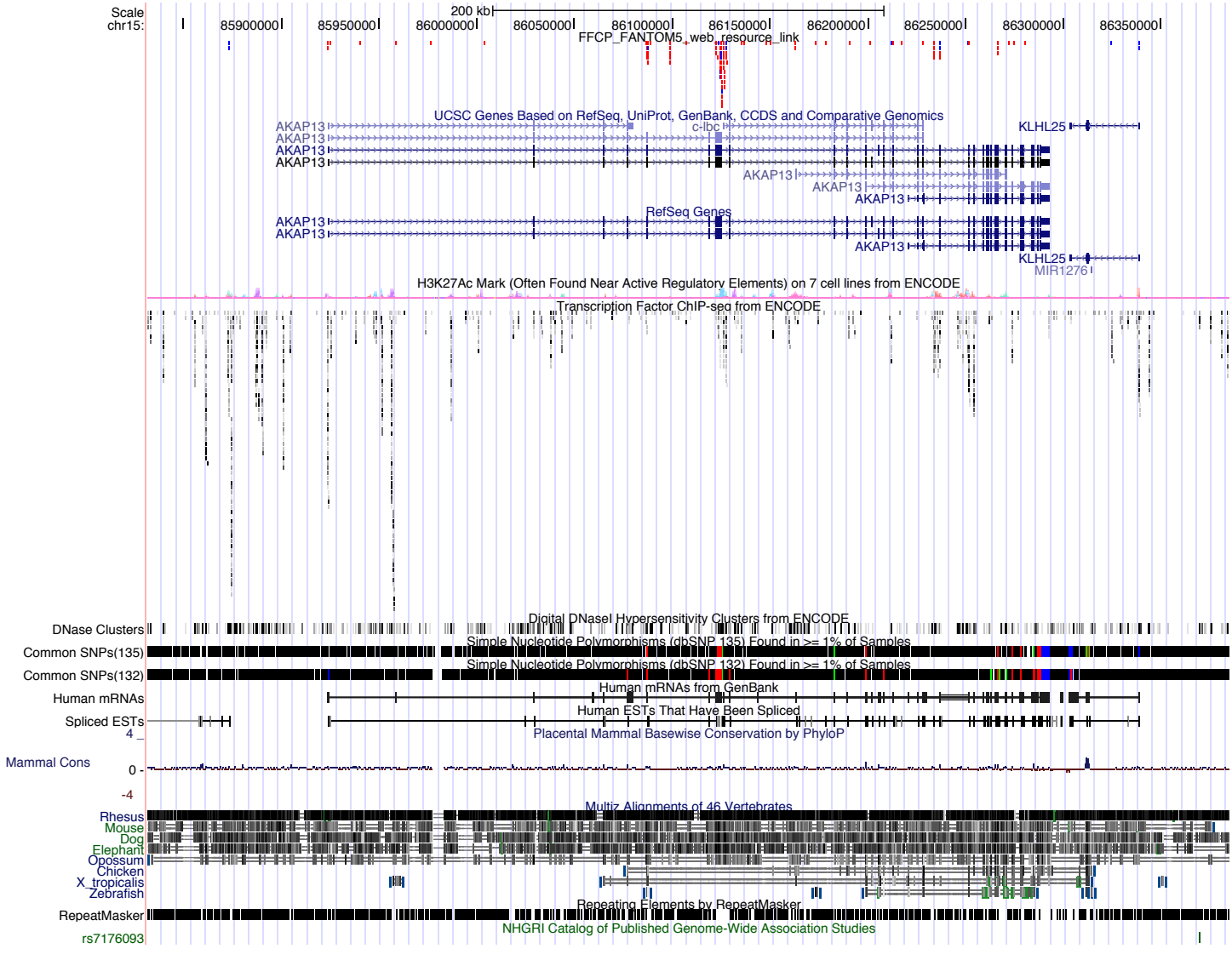
Scale
chr15:
200 kb
85900000
85950000
86000000
86050000
86100000
86150000
86200000
86250000
86300000
86350000
FFCP_FANTOM5_web_resource_link
UCSC Genes Based on RefSeq, UniProt, GenBank, CCDS and Comparative Genomics
AKAP13
c-lbc
KLHL25
RefSeq Genes
MIR1276
H3K27Ac Mark (Often Found Near Active Regulatory Elements) on 7 cell lines from ENCODE
Transcription Factor ChIP-seq from ENCODE
DNase Clusters
Digital DNaseI Hypersensitivity Clusters from ENCODE
Common SNPs(135)
Simple Nucleotide Polymorphisms (dbSNP 135) Found in >= 1% of Samples
Common SNPs(132)
Simple Nucleotide Polymorphisms (dbSNP 132) Found in >= 1% of Samples
Human mRNAs
Human mRNAs from GenBank
Spliced ESTs
Human ESTs That Have Been Spliced
4
Placental Mammal Basewise Conservation by PhyloP
Mammal Cons
0
-4
Multiz Alignments of 46 Vertebrates
Rhesus
Mouse
Dog
Elephant
Opossum
Chicken
X_tropicalis
Zebrafish
RepeatMasker
Repeating Elements by RepeatMasker
rs7176093
NHGRI Catalog of Published Genome-Wide Association Studies

Table S2 (a)

Cluster name	Human	Mouse
lung	tpm.lung, adult, pool1.CNhs10625.10019-101D1.hg19 tpm.lung, fetal, donor1.CNhs11680.10068-101I5.hg19 tpm.lung, right lower lobe, adult, donor1.CNhs11786.10075-102A3.hg19	tpm.lung, embryo E14.CNhs10604.404-26F8.mm9 tpm.lung, embryo E15.CNhs11020.432-17C5.mm9 tpm.lung, embryo E16.CNhs10998.458-17B6.mm9 tpm.lung, embryo E17.CNhs10605.480-44A6.mm9 tpm.lung, embryo E18.CNhs10583.1287-20I6.mm9 tpm.lung, neonate N00.CNhs11224.640-42C6.mm9 tpm.lung, neonate N06.CNhs11212.683-20E5.mm9 tpm.lung, neonate N07.CNhs11111.715-19A3.mm9 tpm.lung, neonate N10.CNhs11219.750-23E6.mm9 tpm.lung, neonate N20.CNhs11109.822-18A4.mm9 tpm.lung, neonate N25.CNhs11119.1359-25C7.mm9 tpm.lung, neonate N30.CNhs11133.1394-42H2.mm9 tpm.lung, adult.CNhs10474.28-22B1.mm9 tpm.lung, embryo E12.CNhs10522.354-16G2.mm9
colon	tpm.colon, adult, donor1.CNhs11794.10082-102B1.hg19 tpm.colon, adult, pool1.CNhs10619.10014-101C5.hg19 tpm.colon, fetal, donor1.CNhs11780.10070-101I7.hg19	tpm.colon, adult.CNhs10468.36-18H7.mm9
diencephalon	tpm.diencephalon, adult.CNhs12610.10193-103E4.hg19	tpm.diencephalon, adult.CNhs10482.20-12F2.mm9 tpm.diencephalon, neonate N30.CNhs11201.1388-42B2.mm9
skin	tpm.skin, fetal, donor1.CNhs11774.10065-101I2.hg19 tpm.skin, adult, donor1.CNhs11785.10074-102A2.hg19 tpm.Skin - palm, donor1.CNhs13458.10286-104F7.hg19	tpm.skin, adult.CNhs10492.30-1C3.mm9 tpm.skin, neonate N00.CNhs11124.650-25G4.mm9 tpm.skin, neonate N03.CNhs11215.662-22H3.mm9 tpm.skin, neonate N06.CNhs11097.693-20I5.mm9 tpm.skin, neonate N10.CNhs11108.762-6C4.mm9
kidney	tpm.kidney, adult, pool1.CNhs10622.10017-101C8.hg19 tpm.kidney, fetal, pool1.CNhs10652.10045-101F9.hg19	tpm.kidney, neonate N25.CNhs11122.1353-25F3.mm9 tpm.kidney, neonate N30.CNhs11203.1385-42H1.mm9 tpm.kidney, embryo E14.CNhs10606.411-4I9.mm9 tpm.kidney, embryo E15.CNhs10997.434-16F8.mm9 tpm.kidney, embryo E16.CNhs10584.464-22A5.mm9 tpm.kidney, embryo E17.CNhs11028.483-18I2.mm9 tpm.kidney, embryo E18.CNhs11001.1288-20C7.mm9 tpm.kidney, neonate N00.CNhs11214.646-21G7.mm9 tpm.kidney, neonate N10.CNhs11206.758-6D5.mm9 tpm.kidney, neonate N20.CNhs11113.832-19I1.mm9
liver	tpm.liver, adult, pool1.CNhs10624.10018-101C9.hg19 tpm.liver, fetal, pool1.CNhs11798.10086-102B5.hg19	tpm.liver, embryo E15.CNhs10520.433-16D7.mm9 tpm.liver, embryo E16.CNhs10523.462-17F5.mm9 tpm.liver, embryo E17.CNhs10510.481-18A3.mm9 tpm.liver, embryo E18.CNhs10579.499-43G4.mm9 tpm.liver, neonate N00.CNhs11117.641-24F4.mm9 tpm.liver, neonate N03.CNhs11123.1345-25G2.mm9 tpm.liver, neonate N06.CNhs11101.684-20A8.mm9 tpm.liver, neonate N07.CNhs11103.716-20H2.mm9 tpm.liver, neonate N10.CNhs11115.751-24B9.mm9 tpm.liver, neonate N20.CNhs11220.823-25A3.mm9 tpm.liver, neonate N25.CNhs11198.1368-26H1.mm9 tpm.liver, neonate N30.CNhs11106.1382-42D1.mm9 tpm.liver, adult pregnant day01.CNhs10466.508-5B2.mm9 tpm.liver, embryo E12.CNhs10601.355-15F8.mm9 tpm.liver, embryo E13.CNhs10524.378-3H6.mm9 tpm.liver, embryo E14.CNhs10594.409-16E1.mm9
uterus	tpm.uterus, adult, pool1.CNhs11676.10100-102D1.hg19 tpm.uterus, fetal, donor1.CNhs11763.10055-101H1.hg19	tpm.uterus, adult pregnant day19.CNhs10497.590-15F5.mm9 tpm.uterus, adult.CNhs10509.92-27E5.mm9
tongue	tpm.tongue, fetal, donor1.CNhs11768.10059-101H5.hg19	tpm.tongue, adult.CNhs10499.32-1B4.mm9

	tpm.tongue, adult.CNhs12853.10203-103F5.hg19 tpm.tongue epidermis (fungiform papillae), donor1.CNhs13460.10288-104F9.hg19	
stomach	tpm.stomach, fetal, donor1.CNhs11771.10062-101H8.hg19	tpm.stomach, neonate N03.CNhs11193.1340-24B8.mm9 tpm.stomach, neonate N07.CNhs11210.718-18A9.mm9 tpm.stomach, neonate N25.CNhs11104.1355-25E4.mm9 tpm.stomach, neonate N30.CNhs11134.1386-42I1.mm9 tpm.stomach, adult.CNhs10503.33-1H6.mm9 tpm.stomach, embryo E12.CNhs10588.356-43E3.mm9 tpm.stomach, embryo E15.CNhs10603.1252-16G8.mm9 tpm.stomach, embryo E16.CNhs11022.459-17D4.mm9 tpm.stomach, embryo E17.CNhs11006.1035-18D5.mm9 tpm.stomach, embryo E18.CNhs10999.1286-20C6.mm9
ovary	tpm.ovary, adult, pool1.CNhs10626.10020-101D2.hg19	tpm.ovary, adult.CNhs10507.91-2I7.mm9 tpm.ovary, embryo E18.CNhs11040.505-44H7.mm9 tpm.ovary, neonate N00.CNhs11217.1299-22I4.mm9
aorta	tpm.aorta, adult, pool1.CNhs11760.10052-101G7.hg19	tpm.aorta, adult.CNhs10498.46-23H1.mm9
heart	tpm.heart, adult, diseased post-infarction, donor1.CNhs11757.10050-101G5.hg19 tpm.heart, adult, diseased, donor1.CNhs11758.10051-101G6.hg19 tpm.heart, adult, pool1.CNhs10621.10016-101C7.hg19 tpm.heart, fetal, pool1.CNhs10653.10046-101G1.hg19	tpm.heart, embryo E17.CNhs11025.479-18E5.mm9 tpm.heart, embryo E18.CNhs11030.1283-20G3.mm9 tpm.heart, neonate N00.CNhs11213.639-21E3.mm9 tpm.heart, neonate N03.CNhs11221.1349-25I2.mm9 tpm.heart, neonate N10.CNhs11118.749-24G1.mm9 tpm.heart, neonate N16.CNhs11209.782-15G1.mm9 tpm.heart, neonate N20.CNhs11127.821-26I6.mm9 tpm.heart, neonate N25.CNhs11196.1351-25D3.mm9 tpm.heart, neonate N30.CNhs11202.1390-42D2.mm9 tpm.heart, embryo E11.CNhs10586.331-24E9.mm9 tpm.heart, embryo E12.CNhs11015.353-12F5.mm9 tpm.heart, embryo E13.CNhs11013.376-3I9.mm9 tpm.heart, embryo E14.CNhs10597.403-26D4.mm9 tpm.heart, embryo E15.CNhs11017.431-16C8.mm9 tpm.heart, embryo E16.CNhs11021.457-17C6.mm9
prostate	tpm.prostate, adult, pool1.CNhs10628.10022-101D4.hg19	tpm.prostate, adult.CNhs10470.859-1F8.mm9
vagina	tpm.vagina, adult.CNhs12854.10204-103F6.hg19	tpm.vagina, adult.CNhs10502.89-27D5.mm9
spleen	tpm.spleen, adult, pool1.CNhs10631.10025-101D7.hg19 tpm.spleen, fetal, pool1.CNhs10651.10044-101F8.hg19	tpm.spleen, adult.CNhs10465.25-2G2.mm9 tpm.spleen, embryo E16.CNhs11035.461-43C1.mm9 tpm.spleen, embryo E18.CNhs11011.1271-21F2.mm9 tpm.spleen, neonate N10.CNhs11116.752-24D1.mm9 tpm.spleen, neonate N20.CNhs11112.824-19H1.mm9 tpm.spleen, neonate N25.CNhs11099.1354-25G3.mm9
placenta	tpm.placenta, adult, pool1.CNhs10627.10021-101D3.hg19	tpm.placenta, adult pregnant day10.CNhs10472.539-13I7.mm9 tpm.placenta, adult pregnant day17.CNhs10464.577-18G3.mm9
pancreas	tpm.pancreas, adult, donor1.CNhs11756.10049-101G4.hg19	tpm.pancreas, neonate N25.CNhs11094.1555-45E2.mm9 tpm.pancreas, neonate N30.CNhs11182.1548-44H5.mm9 tpm.pancreas, adult.CNhs10486.34-16E4.mm9

		tpm.pancreas, embryo E14.CNhs11012.405-44F4.mm9 tpm.pancreas, embryo E15.CNhs11042.1556-45F2.mm9 tpm.pancreas, embryo E16.CNhs11003.460-26E5.mm9 tpm.pancreas, embryo E17.CNhs10599.1558-45G3.mm9 tpm.pancreas, embryo E18.CNhs10580.1535-43I7.mm9 tpm.pancreas, neonate N00.CNhs11105.645-26G9.mm9 tpm.pancreas, neonate N01.CNhs11138.1531-43D7.mm9 tpm.pancreas, neonate N02.CNhs11139.1539-43D8.mm9 tpm.pancreas, neonate N16.CNhs11136.787-43B6.mm9
testis	tpm.testis, adult, pool1.CNhs10632.10026-101D8.hg19 tpm.testis, adult, pool2.CNhs12998.10096-102C6.hg19	tpm.testis, neonate N30.CNhs11130.1391-42E2.mm9 tpm.testis, adult.CNhs10504.57-7G5.mm9 tpm.testis, embryo E13.CNhs11031.389-23F5.mm9 tpm.testis, embryo E15.CNhs11034.443-27C5.mm9 tpm.testis, embryo E16.CNhs11033.470-26G5.mm9 tpm.testis, embryo E17.CNhs11029.486-18I5.mm9 tpm.testis, embryo E18.CNhs11027.503-18G5.mm9 tpm.testis, neonate N00.CNhs11189.1300-22B7.mm9 tpm.testis, neonate N07.CNhs11222.726-26I4.mm9 tpm.testis, neonate N10.CNhs11204.763-44D9.mm9 tpm.testis, neonate N20.CNhs11110.839-18H3.mm9
small intestine	tpm.small intestine, fetal, donor1.CNhs11773.10064-101I1.hg19 tpm.small intestine, adult, pool1.CNhs10630.10024-101D6.hg19	tpm.small intestine, neonate N16.CNhs11114.790-21I1.mm9
medulla oblongata	tpm.medulla oblongata, adult, donor10252.CNhs12315.10155-103A2.hg19 tpm.medulla oblongata, adult, pool1.CNhs10645.10038-101F2.hg19 tpm.medulla oblongata, newborn, donor10223.CNhs14079.10361-105F1.hg19	tpm.medulla oblongata, adult.CNhs10477.17-12C2.mm9 tpm.medulla oblongata, neonate N30.CNhs11200.1396-42A3.mm9
adrenal gland	tpm.adrenal gland, adult, pool1.CNhs11793.10081-102A9.hg19	tpm.adrenal gland, adult.CNhs10508.49-24D7.mm9 tpm.adrenal gland, embryo E14.CNhs11038.406-44C5.mm9 tpm.adrenal gland, embryo E16.CNhs11004.1254-43D6.mm9 tpm.adrenal gland, embryo E17.CNhs11043.1263-45I1.mm9 tpm.adrenal gland, embryo E18.CNhs11026.1262-18F5.mm9 tpm.adrenal gland, neonate N00.CNhs11191.1311-23C1.mm9 tpm.adrenal gland, neonate N25.CNhs11223.1377-27I3.mm9
spinal cord	tpm.spinal cord, adult, donor10258.CNhs14222.10369-105F9.hg19 tpm.spinal cord, fetal, donor1.CNhs11764.10056-101H2.hg19 tpm.spinal cord, newborn, donor10223.CNhs14077.10359-105E8.hg19 tpm.spinal cord, adult, donor10252.CNhs12227.10159-103A6.hg19	tpm.spinal cord, adult.CNhs10505.24-13C9.mm9
pituitary gland	tpm.pituitary gland, adult, donor10252.CNhs12229.10162-103A9.hg19	tpm.pituitary gland, embryo E13.CNhs11009.370-44C7.mm9 tpm.pituitary gland, embryo E14.CNhs11037.398-44A5.mm9 tpm.pituitary gland, embryo E15.CNhs10592.427-16B9.mm9 tpm.pituitary gland, embryo E16.CNhs11036.449-43F6.mm9 tpm.pituitary gland, embryo E17.CNhs11039.1265-

		44F5.mm9 tpm.pituitary gland, neonate N00.CNhs11190.1308-22E9.mm9 tpm.pituitary gland, adult.CNhs10493.21-1G8.mm9 tpm.pituitary gland, embryo E12.CNhs11018.346-16E6.mm9
thymus	tpm.thymus, adult, pool1.CNhs10633.10027-101D9.hg19 tpm.thymus, fetal, pool1.CNhs10650.10043-101F7.hg19	tpm.thymus, adult.CNhs10471.38-12B5.mm9 tpm.thymus, embryo E14.CNhs11041.402-44I4.mm9 tpm.thymus, embryo E15.CNhs11005.430-45I2.mm9 tpm.thymus, embryo E16.CNhs11002.456-26C5.mm9 tpm.thymus, embryo E17.CNhs10581.478-18C1.mm9 tpm.thymus, embryo E18.CNhs10595.1273-19G4.mm9 tpm.thymus, neonate N02.CNhs11181.1541-43F8.mm9 tpm.thymus, neonate N03.CNhs11137.2104-43C7.mm9 tpm.thymus, neonate N06.CNhs11197.681-26C4.mm9 tpm.thymus, neonate N07.CNhs11211.713-19D3.mm9 tpm.thymus, neonate N10.CNhs11194.748-24E4.mm9 tpm.thymus, neonate N20.CNhs11186.820-7A2.mm9 tpm.thymus, neonate N25.CNhs11125.1362-25G7.mm9 tpm.thymus, neonate N30.CNhs11132.1393-42G2.mm9
hippocampus	tpm.hippocampus, adult, donor10252.CNhs12312.10153-102I9.hg19 tpm.hippocampus, adult, donor10258.CNhs14227.10374-105G5.hg19 tpm.hippocampus, newborn, donor10223.CNhs14081.10363-105F3.hg19	tpm.hippocampus, adult.CNhs10478.13-16E8.mm9 tpm.hippocampus, neonate N00.CNhs11228.627-43G1.mm9
cerebellum	tpm.cerebellum, adult, donor10252.CNhs12323.10166-103B4.hg19 tpm.cerebellum, adult, pool1.CNhs11795.10083-102B2.hg19 tpm.cerebellum, newborn, donor10223.CNhs14075.10357-105E6.hg19	tpm.cerebellum, embryo E16, biol_rep3 (E16R3).CNhs13019.10143-102H8.mm9 tpm.cerebellum, embryo E17, biol_rep1 (E17R1).CNhs12818.10120-102F3.mm9 tpm.cerebellum, embryo E17, biol_rep2 (E17R2).CNhs13008.10132-102G6.mm9 tpm.cerebellum, embryo E17, biol_rep3 (E17R3).CNhs13020.10144-102H9.mm9 tpm.cerebellum, embryo E18, biol_rep1 (E18R1).CNhs12962.10121-102F4.mm9 tpm.cerebellum, embryo E18, biol_rep2 (E18R2).CNhs13009.10133-102G7.mm9 tpm.cerebellum, embryo E18, biol_rep3 (E18R3).CNhs13021.10145-102I1.mm9 tpm.cerebellum, neonate N00, biol_rep1 (P0R1).CNhs12963.10122-102F5.mm9 tpm.cerebellum, neonate N00, biol_rep2 (P0R2).CNhs13010.10134-102G8.mm9 tpm.cerebellum, neonate N00, biol_rep3 (P0R3).CNhs13022.10146-102I2.mm9 tpm.cerebellum, neonate N03, biol_rep1 (P3R1).CNhs13001.10123-102F6.mm9 tpm.cerebellum, neonate N03, biol_rep2 (P3R2).CNhs13011.10135-102G9.mm9 tpm.cerebellum, neonate N03, biol_rep3 (P3R3).CNhs13024.10147-102I3.mm9 tpm.cerebellum, neonate N06, biol_rep1 (P6R1).CNhs12819.10124-102F7.mm9 tpm.cerebellum, neonate N06, biol_rep2 (P6R2).CNhs13012.10136-102H1.mm9 tpm.cerebellum, neonate N06, biol_rep3 (P6R3).CNhs13025.10148-102I4.mm9 tpm.cerebellum, neonate N09, biol_rep1 (P9R1).CNhs12820.10125-102F8.mm9

		tpm.cerebellum, neonate N09, biol_rep2 (P9R2).CNhs13013.10137-102H2.mm9 tpm.cerebellum, neonate N09, biol_rep3 (P9R3).CNhs13026.10149-102I5.mm9 tpm.cerebellum, neonate N30.CNhs11135.1395-42I2.mm9 tpm.cerebellum, adult.CNhs10494.15-8B2.mm9 tpm.cerebellum, embryo E11, biol_rep1 (E11R1).CNhs12956.10114-102E6.mm9 tpm.cerebellum, embryo E11, biol_rep2 (E11R2).CNhs13002.10126-102F9.mm9 tpm.cerebellum, embryo E11, biol_rep3 (E11R3).CNhs13014.10138-102H3.mm9 tpm.cerebellum, embryo E12, biol_rep1 (E12R1).CNhs12957.10115-102E7.mm9 tpm.cerebellum, embryo E12, biol_rep2 (E12R2).CNhs13003.10127-102G1.mm9 tpm.cerebellum, embryo E12, biol_rep3 (E12R3).CNhs13015.10139-102H4.mm9 tpm.cerebellum, embryo E13, biol_rep1 (E13R1).CNhs12958.10116-102E8.mm9 tpm.cerebellum, embryo E13, biol_rep2 (E13R2).CNhs13004.10128-102G2.mm9 tpm.cerebellum, embryo E13, biol_rep3 (E13R3).CNhs13016.10140-102H5.mm9 tpm.cerebellum, embryo E14, biol_rep1 (E14R1).CNhs12960.10117-102E9.mm9 tpm.cerebellum, embryo E14, biol_rep2 (E14R2).CNhs13005.10129-102G3.mm9 tpm.cerebellum, embryo E14, biol_rep3 (E14R3).CNhs13017.10141-102H6.mm9 tpm.cerebellum, embryo E15, biol_rep1 (E15R1).CNhs12961.10118-102F1.mm9 tpm.cerebellum, embryo E15, biol_rep2 (E15R2).CNhs13006.10130-102G4.mm9 tpm.cerebellum, embryo E15, biol_rep3 (E15R3).CNhs13018.10142-102H7.mm9 tpm.cerebellum, embryo E16, biol_rep1 (E16R1).CNhs13000.10119-102F2.mm9 tpm.cerebellum, embryo E16, biol_rep2 (E16R2).CNhs13007.10131-102G5.mm9
RNA	tpm.Clontech Human Universal Reference Total RNA, pool1.CNhs10608.10000-101A1.hg19	tpm.Clontech Mouse Universal Reference Total RNA, pool1.CNhs10609.10001-101A3.mm9
eye	tpm.eye, fetal, donor1.CNhs11762.10054-101G9.hg19 tpm.eye - muscle inferior rectus, donor1.CNhs13444.10272-104E2.hg19 tpm.eye - muscle lateral, donor2.CNhs13442.10298-104H1.hg19 tpm.eye - muscle medial, donor2.CNhs13443.10299-104H2.hg19 tpm.eye - muscle superior, donor2.CNhs13441.10297-104G9.hg19 tpm.eye - vitreous humor, donor1.CNhs13440.10268-104D7.hg19	tpm.eyeball, embryo E14.CNhs10521.399-16E2.mm9 tpm.eyeball, embryo E15.CNhs10593.426-16C9.mm9 tpm.eyeball, embryo E17.CNhs11023.1261-18D4.mm9 tpm.eyeball, neonate N00.CNhs11207.633-15C6.mm9 tpm.eyeball, neonate N01.CNhs11140.1532-43E7.mm9 tpm.eyeball, neonate N02.CNhs11205.1551-44G8.mm9 tpm.eyeball, neonate N16.CNhs11188.777-19A2.mm9 tpm.eyeball, adult.CNhs10484.31-12G4.mm9 tpm.eyeball, embryo E12.CNhs11016.345-16C6.mm9
RNA	tpm.SABiosciences XpressRef Human Universal Total RNA, pool1.CNhs10610.10002-101A5.hg19	tpm.SABiosciences XpressRef Mouse Universal Total RNA, pool1.CNhs10611.10003-101A7.mm9
epididymis	tpm.epididymis, adult.CNhs12847.10197-103E8.hg19	tpm.epididymis, adult.CNhs10490.58-23B2.mm9 tpm.epididymis and seminiferous tubule, neonate N30.CNhs11199.1387-42A2.mm9 tpm.epididymis and seminiferous tubule, neonate N00.CNhs11218.1310-23B1.mm9

Table S2 (b)

Cluster name	Human	Mouse
Cluster 1, subcluster various mouse tissues - nervous, reproductive and digestive system	-	tpm stomach− embryo E12−mm9 tpm intestine− embryo E12−mm9 tpm forelimb− embryo E11−mm9 tpm forelimb− embryo E13−mm9 tpm forelimb− embryo E12−mm9 tpm lung− embryo E12−mm9 tpm lung− embryo E14−mm9 tpm intestine− embryo E13−mm9 tpm gonad− embryo E13−mm9 tpm testis− embryo E13−mm9 tpm pituitary gland− embryo E12−mm9 tpm pituitary gland− embryo E13−mm9 tpm pituitary gland− embryo E14−mm9 tpm cerebellum− biol_rep2 −mm9 tpm cerebellum− biol_rep1 −mm9 tpm cerebellum− biol_rep3 −mm9 tpm cerebellum− biol_rep1 −mm9 tpm whole body− embryo E11−mm9 tpm cerebellum− biol_rep3 −mm9 tpm cerebellum− biol_rep2 −mm9 tpm eyeball− embryo E12−mm9 tpm whole body− embryo E12−mm9 tpm kidney− embryo E17−mm9 tpm kidney− embryo E18−mm9 tpm kidney− embryo E16−mm9 tpm kidney− neonate N00−mm9 tpm intestine− embryo E15−mm9 tpm stomach− embryo E15−mm9 tpm stomach− embryo E16−mm9 tpm intestine− embryo E16−mm9 tpm forelimb− embryo E14−mm9 tpm forelimb− embryo E15−mm9 tpm ovary− embryo E18−mm9 tpm ovary− neonate N00−mm9 tpm epididymis and seminiferous tubule− neonate N00−mm9 tpm testis− embryo E17−mm9 tpm testis− embryo E16−mm9 tpm testis− embryo E18−mm9 tpm testis− embryo E15−mm9 tpm testis− neonate N00−mm9 tpm testis− neonate N07−mm9 tpm testis− neonate N10−mm9 tpm pancreas− embryo E15−mm9 tpm cerebellum− biol_rep1 −mm9 tpm cerebellum− biol_rep3 −mm9 tpm cerebellum− biol_rep2 −mm9 tpm cerebellum− biol_rep3 −mm9 tpm cerebellum− biol_rep3 −mm9 tpm cerebellum− biol_rep2 −mm9 tpm cerebellum− biol_rep2 −mm9 tpm cerebellum− biol_rep1 −mm9 tpm cerebellum− biol_rep1 −mm9 tpm cerebellum− biol_rep1 −mm9 tpm cerebellum− biol_rep2 −mm9 tpm cerebellum− biol_rep3 −mm9 tpm corpus striatum− neonateN00−mm9 tpm cerebellum− biol_rep2 −mm9 tpm cerebellum− biol_rep2 −mm9 tpm cerebellum− biol_rep3 −mm9 tpm cerebellum− biol_rep3 −mm9 tpm cerebellum− biol_rep2 −mm9

		tpm cerebellum− biol_rep3 −mm9 tpm cerebellum− biol_rep1 −mm9 tpm cerebellum− biol_rep1 −mm9 tpm cerebellum− biol_rep1 −mm9 tpm cerebellum− biol_rep1 −mm9 tpm cerebellum− biol_rep2 −mm9 tpm cerebellum− biol_rep2 −mm9 tpm cerebellum− biol_rep3 −mm9 tpm cerebellum− biol_rep1 −mm9 tpm cerebellum− biol_rep2 −mm9 tpm cerebellum− biol_rep3 −mm9 tpm cerebellum− biol_rep1 −mm9 tpm cerebellum− biol_rep3 −mm9 tpm hippocampus− neonate N00−mm9 tpm pituitary gland− embryo E16−mm9 tpm pituitary gland− embryo E15−mm9 tpm adrenal gland− neonate N00−mm9 tpm adrenal gland− embryo E18−mm9 tpm adrenal gland− embryo E16−mm9 tpm adrenal gland− embryo E17−mm9 tpm adrenal gland− neonate N25−mm9 tpm adrenal gland− adult−mm9 tpm visual cortex-mm9 (various samples) tpm cortex− neonate N30−mm9 tpm cortex− adult−mm9 tpm eyeball− adult−mm9 pm hippocampus− adult−mm9 tpm diencephalon− adult−mm9 tpm corpora quadrigemina− adult−mm9 tpm diencephalon− neonate N30−mm9 tpm corpus striatum− adult−mm9 tpm medulla oblongata− adult−mm9 tpm spinal cord− adult−mm9 tpm medulla oblongata− neonate N30−mm9 tpm oviduct− adult pregnant day01−mm9 tpm uterus− adult−mm9 tpm ovary− adult−mm9 tpm urinary bladder− adult−mm9 tpm stomach− embryo E17−mm9 tpm stomach− embryo E18−mm9 tpm stomach− neonate N03−mm9 tpm stomach− neonate N07−mm9 pm kidney− neonate N25−mm9 tpm kidney− neonate N20−mm9 tpm kidney− neonate N30−mm9 tpm uterus− adult pregnant day19−mm9
Cluster 1, subcluster human newborn and fetal brain, reproductive tissues, lung and some outliers.	pm medial temporal gyrus− newborn−hg19 tpm occipital cortex− newborn−hg19 tpm hippocampus− newborn−hg19 tpm amygdala− newborn−hg19 tpm caudate nucleus− newborn−hg19 tpm thalamus− newborn−hg19 tpm medial frontal gyrus− newborn−hg19 tpm temporal lobe− fetal−hg19 tpm occipital lobe− fetal−hg19 tpm parietal lobe− fetal−hg19 tpm brain− fetal−hg19 tpm duodenum− fetal−hg19 tpm adipose− donor3.CNhs13974.10186.103D6.hg19−hg19 tpm adipose− donor2.CNhs13973.10185.103D5.hg19−hg19 tpm adipose− donor4.CNhs13975.10187.103D7.hg19−hg19 tpm adipose− donor1.CNhs13972.10184.103D4.hg19−hg19 tpm appendix− adult.CNhs12842.10189.103D9.hg19−hg19	

	tpm vein− adult.CNhs12844.10191.103E2.hg19−hg19 tpm lymph node− adult−hg19 tpm spleen− fetal−hg19 tpm spleen− adult−hg19 tpm dura mater− adult−hg19 tpm cruciate ligament− donor2.CNhs13439.10295.104G7.hg19−hg19 tpm achilles tendon− donor2.CNhs13435.10292.104G4.hg19−hg19 tpm eye vitreous humor− donor1.CNhs13440.10268.104D7.hg19−hg19 tpm kidney− fetal−hg19 tpm Clontech Human Universal Reference Total RNA− pool1.CNhs10608.10000.101A tpm adipose tissue− adult−hg19 tpm breast− adult−hg19 tpm bone marrow− adult.CNhs12845.10192.103E3.hg19−hg19 tpm lung− adult−hg19 tpm lung− right lower lobe−hg19 tpm lung− fetal−hg19 tpm prostate− adult−hg19 tpm uterus− adult−hg19 tpm ovary− adult−hg19 tpm cervix− adult−hg19 tpm epididymis− adult.CNhs12847.10197.103E8.hg19−hg19 tpm aorta− adult−hg19 tpm Urethra− donor2.CNhs13464.10319.105A4.hg19−hg19 tpm gall bladder− adult.CNhs12848.10198.103E9.hg19−hg19 tpm bladder− adult−hg19 tpm smooth muscle− adult−hg19 tpm colon− adult−hg19 tpm colon− fetal−hg19 tpm vagina− adult.CNhs12854.10204.103F6.hg19−hg19 tpm placenta− adult−hg19 tpm adrenal gland− adult−hg19 tpm trachea− adult−hg19 tpm tongue epidermis 28fungiform papillae 29− donor1.CNhs13460.10288.104F9.hg1 tpm tonsil− adult−hg19 tpm esophagus− adult−hg19 tpm Skin palm− donor1.CNhs13458.10286.104F7.hg19−hg19 tpm ductus deferens− adult.CNhs12846.10196.103E7.hg19−hg19 tpm seminal vesicle− adult.CNhs12851.10201.103F3.hg19−hg19	
Cluster1, mixed subcluster thymus, skin and some human fetal samples	tpm thymus− fetal−hg19 tpm thymus− adult−hg19 tpm rectum− fetal−hg19 tpm uterus− fetal−hg19 tpm umbilical cord− fetal−hg19 tpm skin− fetal−hg19 tpm skin− adult−hg19 tpm throat− fetal−hg19 tpm trachea− fetal−hg19 tpm eye− fetal−hg19 tpm stomach− fetal−hg19 t	ttpm lung− embryo E15−mm9 tpm lung− embryo E16−mm9 tpm kidney− embryo E15−mm9 tpm pancreas− embryo E14−mm9 tpm kidney− embryo E14−mm9 tpm thymus− embryo E14−mm9 tpm thymus− embryo E15−mm9 tpm thymus− embryo E16−mm9 tpm thymus− embryo E17−mm9 tpm thymus− neonate N03−mm9 tpm thymus− neonate N07−mm9 tpm thymus− neonate N02−mm9 tpm thymus− neonate N06−mm9 tpm thymus− neonate N10−mm9 tpm thymus− embryo E18−mm9 tpm thymus− neonate N20−mm9 tpm thymus− neonate N25−mm9

		tpm thymus− neonate N30−mm9 tpm thymus− adult−mm9 tpm accessory axillary lymph node− adult−mm9 tpm skin− neonate N03−mm9 tpm skin− neonate N00−mm9 tpm forelimb− embryo E17−mm9 tpm forelimb− embryo E18−mm9 tpm skin− neonate N06−mm9 tpm skin− neonate N10−mm9 tpm skin− adult−mm9
Cluster 1, mixed subcluster - heart	tpm heart− adult−hg19 tpm heart− adult−hg19 tpm left ventricle− adult−hg19 tpm heart pulmonic valve− adult.CNhs12856.10206.103F8.hg19−hg19 tpm heart− adult−hg19 tpm heart− fetal−hg19 tpm heart tricuspid valve− adult.CNhs12857.10207.103F9.hg19−hg19 tpm heart mitral valve− adult.CNhs12855.10205.103F7.hg19−hg19 tpm left atrium− adult−hg19	tpm heart− embryo E16−mm9 tpm heart− embryo E17−mm9 tpm heart− embryo E18−mm9 tpm heart− neonate N00−mm9 tpm heart− embryo E14−mm9 tpm heart− embryo E15−mm9 tpm heart− neonate N10−mm9 tpm heart− neonate N16−mm9 tpm heart− neonate N03−mm9 tpm heart− embryo E12−mm9 tpm heart− embryo E11−mm9 tpm heart− embryo E13−mm9
Cluster 1, mixed subcluster tongue, intestine + outliers	tpm colon− adult−hg19 tpm small intestine− adult−hg19 tpm skeletal muscle− fetal−hg19 tpm diaphragm− fetal−hg19 tpm tongue− fetal−hg19 tpm tongue− adult.CNhs12853.10203.103F5.hg19−hg19 tpm skeletal muscle− adult−hg19 tpm artery−adult.CNhs12843.10190.103E1.hg19−hg19 tpm cerebrospinal fluid− donor2.CNhs13437.10294.104G6.hg19−hg19 tpm penis− adult.CNhs12850.10200.103F2.hg19−hg19 tpm skeletal muscle soleus muscle− donor1.CNhs13454.10282.104F3.hg19−hg19 tpm throat− adult.CNhs12858.10209.103G2.hg19−hg19	tpm Follicle Associated Epithelium− pool3−mm9 tpm intestine− neonate N01−mm9 tpm intestine− adult−mm9 tpm intestine− neovnate N06−mm9 tpm intestine− neonate N10−mm9 tpm intestine− neonate N07−mm9 tpm intestine− embryo E17−mm9 tpm intestine− embryo E18−mm9 tpm intestine− neonate N25−mm9 tpm Ileum epithelium− pool1−mm9 tpm cecum− adult−mm9 tpm stomach− neonate N30−mm9 tpm whole body− neonate N06−mm9 tpm whole body− neonate N10−mm9 tpm bone 28os femoris 29− neonate N02−mm9 tpm whole body− neonate N01−mm9 tpm muscle 28biceps femoris 29− neonate N30−mm9 tpm tongue− adult−mm9 tpm eyeball− embryo E14−mm9 tpm eyeball− embryo E15−mm9 tpm eyeball− embryo E17−mm9 tpm eyeball− neonate N01−mm9 tpm eyeball− neonate N02−mm9 tpm eyeball− neonate N00−mm9 tpm eyeball− neonate N16−mm9 tpm testis− neonate N20−mm9 tpm testis− neonate N30−mm9 tpm testis− adult−mm9
Cluster 2, subcluster human brain	tpm paracentral gyrus− adult−hg19 tpm parietal lobe− adult−hg19 tpm nucleus accumbens− adult−hg19 tpm insula− adult−hg19 tpm frontal lobe− adult−hg19 tpm postcentral gyrus− adult−hg19 tpm occipital pole− adult−hg19 tpm temporal lobe− adult−hg19 tpm brain− adult−hg19 tpm occipital lobe− adult−hg19 tpm brain− adult−hg19 tpm medial temporal gyrus− adult−hg19 tpm parietal lobe− adult−hg19 tpm middle temporal gyrus− donor10252.CNhs12316.10156.103A3.hg19−hg19 tpm parietal lobe adult− donor10196.CNhs13797.10171.103B9.hg19−hg19	-

	tpm hippocampus− adult−hg19 tpm substantia nigra− adult−hg19 tpm thalamus− adult−hg19 tpm spinal cord− adult−hg19 tpm thalamus adult− donor10196.CNhs13794.10168.103B6.hg19−hg19 tpm globus pallidus adult− donor10196.CNhs13801.10175.103C4.hg19−hg19 tpm spinal cord adult− donor10196.CNhs13807.10181.103D1.hg19−hg19 tpm locus coeruleus adult− donor10196.CNhs13808.10182.103D2.hg19−hg19 tpm occipital cortex− adult−hg19 tpm diencephalon− adult.CNhs12610.10193.103E4.hg19−hg19 tpm pons− adult−hg19 tpm globus pallidus− newborn−hg19 tpm thalamus− adult−hg19 tpm substantia nigra− adult−hg19 tpm globus pallidus− adult−hg19 tpm locus coeruleus− adult−hg19 tpm spinal cord− adult−hg19 tpm medulla oblongata− adult−hg19 tpm corpus callosum− adult−hg19 tpm optic nerve− donor1.CNhs13449.10277.104E7.hg19−hg19 tpm substantia nigra adult− donor10196.CNhs13803.10178.103C7.hg19−hg19 tpm spinal cord− fetal−hg19 tpm medulla oblongata− newborn−hg19 tpm locus coeruleus− newborn−hg19 tpm substantia nigra− newborn−hg19 tpm spinal cord− newborn−hg19 tpm putamen− newborn−hg19 tpm kidney− adult−hg19 tpm cerebral meninges− adult.CNhs12840.10188.103D8.hg19−hg19 tpm retina− adult−hg19 tpm pineal gland− adult−hg19 tpm pineal gland adult− donor10196.CNhs13804.10179.103C8.hg19−hg19 tpm medulla oblongata− adult−hg19 tpm medulla oblongata adult− donor10196.CNhs13800.10174.103C3.hg19−hg1	
Cluster 2, mixed subcluster RNA and liver	tpm SABiosciences XpressRef Human Universal Total RNA− pool1.CNhs10610.10002 tpm Universal RNA Human Normal Tissues Biochain− pool1.CNhs10612.10007.101B tpm liver− adult−hg19 tpm liver− fetal−hg19	tpm liver− neonate N25−mm9 tpm liver− neonate N30−mm9 tpm liver− neonate N20−mm9 tpm liver− adult pregnant day01−mm9 tpm Universal RNA Mouse Normal Tissues Biochain− pool1−mm9 tpm liver− neonate N07−mm9 tpm liver− neonate N10−mm9 tpm liver− neonate N06−mm9 tpm liver− neonate N00−mm9 tpm liver− embryo E18−mm9 tpm liver− neonate N03−mm9 tpm whole body− embryo E18−mm9 tpm whole body− neonate N00−mm9 tpm SABiosciences XpressRef Mouse Universal Total RNA− pool1−mm9 tpm amnion− adult pregnant day17−mm9
Cluster 2, subcluster mouse embryo liver, spleen, lung, bone etc.	tpm blood− adult−hg19	spleen− neonate N20−mm9 tpm spleen− neonate N10−mm9 tpm spleen− adult−mm9 tpm spleen− neonate N25−mm9 tpm spleen− embryo E18−mm9 tpm liver− embryo E13−mm9 tpm liver− embryo E14−mm9

		tpm liver− embryo E15−mm9 tpm liver− embryo E12−mm9 tpm bone 28os femoris 29− adult−mm9 tpm epididymis and seminiferous tubule− neonate N30−mm9 tpm heart− neonate N30−mm9 tpm heart− neonate N25−mm9 tpm heart− neonate N20−mm9 tpm adrenal gland− embryo E14−mm9 tpm whole body− embryo E13−mm9 tpm whole body− embryo E14−mm9 tpm spleen− embryo E16−mm9 tpm lung− embryo E17−mm9 tpm lung− embryo E18−mm9 tpm lung− neonate N00−mm9 tpm bone 28os femoris 29− neonate N20−mm9 tpm bone 28os femoris 29− neonate N16−mm9 tpm whole body− embryo E17−mm9 tpm whole body− embryo E16−mm9 tpm whole body− embryo E14−mm9 tpm whole body− embryo E17−mm9 tpm liver− embryo E16−mm9 tpm liver− embryo E17−mm9 tpm liver− embryo E17−mm9 tpm lung− neonate N07−mm9 tpm lung− neonate N06−mm9 tpm lung− neonate N10−mm9 tpm lung− neonate N20−mm9 tpm lung− neonate N25−mm9 tpm lung− neonate N30−mm9 tpm Clontech Mouse Universal Reference Total RNA−pool1−mm9
Cluster 3, mixed endocrine glands, pancreas, digestive system of mouse	tpm duodenum− fetal−hg19 tpm temporal lobe− fetal−hg19 tpm pancreas− adult−hg19 tpm pituitary gland− adult−hg19 tpm pituitary gland adult−donor10196.CNhs13805.10180.103C9.hg19−hg19 tpm submaxillary gland−adult.CNhs12852.10202.103F4.hg19−hg19 tpm salivary gland− adult−hg19	tpm intestine− neonate N00−mm9 tpm small intestine− neonate N16−mm9 tpm intestine− neonate N30−mm9 tpm intestinal mucosa− adult−mm9 tpm colon− adult−mm9 tpm pancreas− adult−mm9 tpm pancreas− neonate N30−mm9 tpm pancreas− neonate N25−mm9 tpm pancreas− neonate N16−mm9 tpm pancreas− embryo E16−mm9 tpm pancreas− embryo E17−mm9 tpm pancreas− embryo E18−mm9 tpm pancreas− neonate N02−mm9 tpm pancreas− neonate N01−mm9 tpm pancreas− neonate N00−mm9 tpm stomach− neonate N25−mm9 tpm stomach− adult−mm9 tpm placenta− adult pregnant day10−mm9 tpm placenta− adult pregnant day17−mm9 tpm pituitary gland− embryo E17−mm9 tpm pituitary gland− neonate N00−mm9 tpm pituitary gland− adult−mm9 tpm submandibular gland− adult−mm9

Table S8

esophagus, adult, pool1.CNhs10620.10015.101C6.hg19 Tetrapoda		
gene	average expression	name
NM_002274	13082.2	keratin 13
NM_153490	13082.2	keratin 13
NM_002272	11030.4	keratin 4
NM_000424	6259.86	keratin 5
NM_005554	4055.68	keratin 6A
NM_000700	3702.54	annexin A1
NM_001199893	2896.67	actin, gamma 2, smooth muscle, enteric
NM_001615	2896.67	actin, gamma 2, smooth muscle, enteric
NM_001613	1913.05	actin, alpha 2, smooth muscle, aorta
NM_002275	1681.03	keratin 15
adipose, donor1.CNhs13972.10184.103D4.hg19 HUMAN		
NM_003542	3140.93	histone cluster 1, H4c
NM_003545	2515.18	histone cluster 1, H4e
NM_003537	1922.87	histone cluster 1, H3b
NM_003539	1719.11	histone cluster 1, H4d
NM_003544	1652.23	histone cluster 1, H4b
NM_003533	1608.02	histone cluster 1, H3i
NM_003546	1493.81	histone cluster 1, H4l
NM_003540	1022.51	histone cluster 1, H4f
NM_021018	704.817	histone cluster 1, H3f
NM_003532	704.251	histone cluster 1, H3e
parotid gland, adult.CNhs12849.10199.103F1.hg19 Homo/Pan/Gorilla		
NM_002723	136988	proline-rich protein BstNI subfamily 4
NM_000200	126071	histatin 3
NM_006249	47975.3	proline-rich protein BstNI subfamily 3
NM_006685	38292.5	submaxillary gland androgen regulated protein 3B

Table S8

NM_002159	25146.6	histatin 1
NM_002568	1033.51	poly(A) binding protein, cytoplasmic 1
NM_003299	206.46	heat shock protein 90kDa beta (Grp94), member 1
NM_012423	149.031	ribosomal protein L13a
NM_001014	134.32	ribosomal protein S10
NM_001203245	134.32	ribosomal protein S10
salivary gland, adult, pool1.CNhs11677.10093.102C3.hg19 Homo/Pan/Gorilla		
NM_006685	295980	submaxillary gland androgen regulated protein 3B
NM_000200	25866.1	histatin 3
NM_002159	24816.8	histatin 1
NM_001322	16457	cystatin SA
NM_002568	693.334	poly(A) binding protein, cytoplasmic 1
NM_001898	575.298	cystatin SN
NM_012390	229.766	submaxillary gland androgen regulated protein 3A
NM_001203245	108.578	ribosomal protein S10
NM_001014	108.452	ribosomal protein S10
NM_001204091	108.452	ribosomal protein S10
parotid gland, adult.CNhs12849.10199.103F1.hg19 Catarrhini		
NM_002723	136988	proline-rich protein BstNI subfamily 4
NM_006250	57348.8	proline-rich protein HaeIII subfamily 1
NM_006249	47975.3	proline-rich protein BstNI subfamily 3
NM_001110213	31692.8	proline-rich protein HaeIII subfamily 2
NM_005042	31692.8	proline-rich protein HaeIII subfamily 2
NM_001900	10157.6	cystatin D
NM_000099	1494.35	cystatin C

Table S8

NM_001004	1105.09	ribosomal protein, large, P2
NM_001098538	512.105	proline rich 4 (lacrimal)
NM_007244	512.105	proline rich 4 (lacrimal)
salivary gland, adult, pool1.CNhs11677.10093.102C3.hg19 Catarrhini		
NM_001322	16457	cystatin SA
NM_006250	15336.8	proline-rich protein HaeIII subfamily 1
NM_001900	8931.88	cystatin D
NM_001110213	6711.33	proline-rich protein HaeIII subfamily 2
NM_005042	6711.33	proline-rich protein HaeIII subfamily 2
NM_001098538	6034.26	proline rich 4 (lacrimal)
NM_007244	6034.26	proline rich 4 (lacrimal)
NM_000099	2302.08	cystatin C
NM_001004	859.543	ribosomal protein, large, P2
NM_001898	575.298	cystatin SN
vagina, adult.CNhs12854.10204.103F6.hg19 HUMAN		
NM_005345	19049.3	heat shock 70kDa protein 1A
NM_005346	11243.1	heat shock 70kDa protein 1B
NM_003542	288.354	histone cluster 1, H4c
NM_003544	145.209	histone cluster 1, H4b
NM_006164	139.704	nuclear factor (erythroid-derived 2)-like 2
NM_005526	116.993	heat shock transcription factor 1
NM_003543	114.241	histone cluster 1, H4h
NM_003545	99.7885	histone cluster 1, H4e
NM_017971	86.0246	mitochondrial ribosomal protein L20
NM_005406	80.519	Rho-associated, coiled-coil containing protein kinase 1
placenta, adult, pool1.CNhs10627.10021.101D3.hg19 Homo/Pan/Gorilla		

Table S8

NM_021016	5474.12	pregnancy specific beta-1-glycoprotein 3
NM_000518	3718.3	hemoglobin, beta
NM_002784	1765.17	pregnancy specific beta-1-glycoprotein 9
NM_001184825	1693.14	pregnancy specific beta-1-glycoprotein 1
NM_001184826	1693.14	pregnancy specific beta-1-glycoprotein 1
NM_006905	1693.14	pregnancy specific beta-1-glycoprotein 1
NM_001632	1430.24	alkaline phosphatase, placental
NM_001031850	1212.55	pregnancy specific beta-1-glycoprotein 6
NM_002782	1212.55	pregnancy specific beta-1-glycoprotein 6
NM_003299	1189.73	heat shock protein 90kDa beta (Grp94), member 1
seminal vesicle, adult.CNhs12851.10201.103F3.hg19 Catarrhini		
NM_003007	70653.1	semenogelin I
NM_003008	21241.3	semenogelin II
NM_013230	1660.22	CD24 molecule
NM_001540	1436.72	heat shock 27kDa protein 1
NM_001004	792.435	ribosomal protein, large, P2
NM_184041	329.578	aldolase A, fructose-bisphosphate
NM_000099	328.991	cystatin C
NM_005022	197.473	profilin 1
NM_007278	161.658	GABA(A) receptor-associated protein
NM_005953	158.918	metallothionein 2A
testis, adult, pool2.CNhs12998.10096.102C6.hg19 Eutheria		
NM_170610	7779.16	histone cluster 1, H2ba
NM_170745	4616.21	histone cluster 1, H2aa
NM_005323	1436.98	histone cluster 1, H1t
NM_000099	1093.46	cystatin C

Table S8

NM_003529	1029.76	histone cluster 1, H3a
NM_001004	783.309	ribosomal protein, large, P2
NM_002568	774.761	poly(A) binding protein, cytoplasmic 1
NM_005319	718.593	histone cluster 1, H1c
NM_018955	660.592	ubiquitin B
NM_006082	656.726	tubulin, alpha 1b
uterus, fetal, donor1.CNhs11763.10055.101H1.hg19 Eutheria		
NM_002274	4112.03	keratin 13
NM_153490	4112.03	keratin 13
NM_003295	3509.84	tumor protein, translationally-controlled 1
NM_005554	3223.21	keratin 6A
NM_001097589	2454.6	small proline-rich protein 3
NM_005416	2454.6	small proline-rich protein 3
NM_001004	2421.19	ribosomal protein, large, P2
NM_001028	1780.75	ribosomal protein S25
NM_003125	1493.34	small proline-rich protein 1B
NM_000978	1463.44	ribosomal protein L23
putamen, adult, donor10258.CNhs14225.10372.105G3.hg19 HUMAN		
NM_003537	1631.66	histone cluster 1, H3b
NM_003542	1507.45	histone cluster 1, H4c
NM_003535	834.907	histone cluster 1, H3j
NM_003533	464.921	histone cluster 1, H3i
NM_002295	453.387	ribosomal protein SA
NM_003539	431.206	histone cluster 1, H4d
NM_003536	365.549	histone cluster 1, H3h
NM_003545	342.48	histone cluster 1, H4e
NM_002266	316.75	karyopherin alpha 2 (RAG cohort 1, importin alpha 1)
NM_003495	238.672	histone cluster 1, H4i
parietal lobe, fetal, donor1.CNhs11782.10072.101I9.hg19 HUMAN		

Table S8

NM_003537	727.108	histone cluster 1, H3b
NM_003533	436.071	histone cluster 1, H3i
NM_003542	423.15	histone cluster 1, H4c
NM_003545	419.92	histone cluster 1, H4e
NM_003535	274.24	histone cluster 1, H3j
NM_003531	272.625	histone cluster 1, H3c
NM_021018	270.687	histone cluster 1, H3f
NM_003530	254.698	histone cluster 1, H3d
NM_003539	175.074	histone cluster 1, H4d
NM_003546	167.968	histone cluster 1, H4l
putamen, adult, donor10258.CNhs14225.10372.105G3.hg19 HUMAN		
NM_003537	1631.66	histone cluster 1, H3b
NM_003542	1507.45	histone cluster 1, H4c
NM_003535	834.907	histone cluster 1, H3j
NM_003533	464.921	histone cluster 1, H3i
NM_002295	453.387	ribosomal protein SA
NM_003539	431.206	histone cluster 1, H4d
NM_003536	365.549	histone cluster 1, H3h
NM_003545	342.48	histone cluster 1, H4e
NM_002266	316.75	karyopherin alpha 2 (RAG cohort 1, importin alpha 1)
NM_003495	238.672	histone cluster 1, H4i
parietal lobe, fetal, donor1.CNhs11782.10072.101I9.hg19 HUMAN		
NM_003537	727.108	histone cluster 1, H3b
NM_003533	436.071	histone cluster 1, H3i
NM_003542	423.15	histone cluster 1, H4c
NM_003545	419.92	histone cluster 1, H4e
NM_003535	274.24	histone cluster 1, H3j
NM_003531	272.625	histone cluster 1, H3c
NM_021018	270.687	histone cluster 1, H3f
NM_003530	254.698	histone cluster 1, H3d
NM_003539	175.074	histone cluster 1, H4d
NM_003546	167.968	histone cluster 1, H4l

Table S8

dura mater, adult, donor1.CNhs10648.10041.101F5.hg19 Catarrhini		
NM_005953	7672.17	metallothionein 2A
NM_021034	2825.61	interferon induced transmembrane protein 3
NM_175617	2239.11	metallothionein 1E
NM_005514	1775.07	major histocompatibility complex, class I, B
NM_006435	1698.99	interferon induced transmembrane protein 2
NM_000099	1672.46	cystatin C
NM_001004	1605.27	ribosomal protein, large, P2
NM_005952	1461.66	metallothionein 1X
NM_033554	1436.79	major histocompatibility complex, class II, DP alpha 1
NM_021103	1241.36	thymosin beta 10